

Manuscript Number: LITHOS5623R1

Title: Upper Paleozoic mafic and intermediate volcanic rocks associated with the Sn-W deposit of the Mount Pleasant caldera in southwestern New Brunswick (Canada): Petrogenesis and metallogenic implications

Article Type: Regular Article

Keywords: bimodal volcanic rocks; Sn-W deposit; petrogenesis; crustal contamination; Devonian

Corresponding Author: Dr. Jaroslav Dostal, PhD

Corresponding Author's Institution: Saint Mary's University

First Author: Jaroslav Dostal, PhD

Order of Authors: Jaroslav Dostal, PhD

Abstract: Upper Paleozoic (~365 Ma) mafic and intermediate volcanic rocks of the Piskahegan Group constitute a subordinate part of the Mount Pleasant caldera, which is associated with a significant polymetallic deposit (tungsten-molybdenum-bismuth zones ~ 33 Mt ore with 0.21% W, 0.1% Mo and 0.08% Bi and tin-indium zones ~ 4.8 Mt with 0.82% Sn and 129 g/t In) in southwestern New Brunswick (Canada). The epicontinental caldera complex formed during the opening of the late Paleozoic Maritimes Basin in the northern Appalachians. The mafic and intermediate rocks make up two compositionally distinct associations. The first association includes evolved rift-related continental tholeiitic basalts, and the second association comprises calc-alkaline andesites, although both associations were emplaced penecontemporaneously. The basalts have low Mg# ~ 0.34-0.40, smooth chondrite-normalized REE patterns with (La/Yb)_n ~ 5-6, primitive mantle-normalized trace element patterns without noticeable negative Nb-Ta anomalies, and their $\epsilon_{\text{Nd}}(\text{T})$ ranges from +2.5 to +2.2. The basalts were generated by partial melting of a transition zone between spinel and garnet mantle peridotite at a depth of ~70-90 km. The calc-alkaline andesites of the second association have chondrite-normalized REE patterns that are more fractionated, with (La/Yb)_n ~ 7-8.5, but without significant negative Eu anomalies. Compared to the basaltic rocks, they have lower $\epsilon_{\text{Nd}}(\text{T})$ values, ranging from +0.5 to +1.9, and their mantle-normalized trace element plots show negative Nb-Ta anomalies. The $\epsilon_{\text{Nd}}(\text{T})$ values display negative correlations with indicators of crustal contamination, such as Th/La, Th/Nb and SiO₂. The andesitic rocks are interpreted to have formed by assimilation-fractional crystallization processes, which resulted in the contamination of a precursor basaltic magma with crustal material. The parent basaltic magma for both suites underwent a different evolution. The tholeiitic basalts experienced shallow-seated fractional crystallization and evolved along a tholeiitic trend of "early iron" enrichment (non-oxic conditions). The contaminated magma of the second association followed a calc-alkaline fractionation trend of "no iron" enrichment (oxidizing conditions) characterized by a high P(H₂O) and P(O₂) environment at the mid-crust levels. The Piskahegan Group, which is associated with an important polymetallic mineral deposit, differs from the numerous non-mineralized

rift-related volcanic suites of the regional Upper Devonian to Lower Carboniferous successions in the Maritimes Basin by the presence of a significant amount of coeval calc-alkaline andesite, which may be an indicator of potential mineralization.

Dear Editor:

Attached is a copy of our manuscript entitled “Upper Paleozoic mafic and intermediate volcanic rocks of the Mount Pleasant caldera associated with the Sn-W deposit in southwestern New Brunswick (Canada): Petrogenesis and metallogenic implications” by Dostal and Jutras for your consideration for publication in *Lithos*.

Major and trace elements, whole-rock Nd isotopes together with field work and petrography are used to characterize Upper Paleozoic basalts and andesites associated with the polymetallic deposit (Sn-W). The basalts are continental tholeiites while the andesites are calc-alkaline types, although both were emplaced penecontemporaneously. Compared to mantle-derived basalts, the calc-alkaline andesites are interpreted to have formed by assimilation-fractional crystallization processes, which resulted in the contamination of a precursor basaltic magma with crustal material. The volcanic package, which is related to an important polymetallic mineralization, differs from the numerous non-mineralized rift-related volcanic suites of the regional Upper Devonian to Lower Carboniferous successions by the presence of a significant amount of coeval calc-alkaline andesites. These rocks may be indicators of a fertile environment. The subcontinental lithospheric mantle of the Avalon and Gander terranes of the Northern Appalachians in Atlantic Canada had an isotopically similar composition during the Late Devonian and Early Carboniferous.

The research presented in this paper is new and not under consideration for publication anywhere else nor will be under consideration anywhere else unless the paper is rejected. If you have further questions regarding this manuscript, please do not hesitate to contact me.

Sincerely,

Jaroslav Dostal

Department of Geology
Saint Mary's University
Halifax, Nova Scotia B3H 3C3
Canada
e-mail: jdostal@smu.ca

Dear Dr. Eby:

We have revised the manuscript entitled “Upper Paleozoic mafic and intermediate volcanic rocks associated with Sn-W deposits of the Mount Pleasant caldera in southwestern New Brunswick (Canada): Petrogenesis and metallogenic implications (LITHOS5623)” according to the reviewers’ comments. The reviewers’ comments helped us to significantly improve the manuscript. In addition, we made some modifications in style and grammar. The marked original manuscript is attached.

I hope you will find the manuscript satisfactory.

Regards,

J. Dostal

email: jdostal@smu.ca

Revisions:

A. Comments of the reviewer #1:

We have modified the manuscript according to the comments of this reviewer marked on an annotated pdf. The changes were mainly of style and grammar so most of them are not enumerated below.

1. L. 60 references rearranged
2. L. 67 corrected
3. L. 89-90 references re-arranged
4. L. 98 corrected
5. L. 100 corrected
6. L. 302 corrected

B. Comments of the reviewer #2 (John Greenough)

Specific Comments:

1. L. 46 corrected
2. L. 46 added
3. p. 5 L. 121 corrected
4. p. 5 L. 126
5. p.9 L. 251 corrected; the same done on l. 221, 222, 251, 252, 269, 309.
6. p. 11 L. 300 corrected
7. p. 13, L. 355 modified
8. p. 13, L. 360 references added
9. p. 14, L. 378 reworded as suggested
10. p. 14-15 the problem clarified; we have added that the reason for a comparison is that the rocks are ~ 30 My younger.
11. Table 3. Info added

12. Caption to Figure 1B- references added
13. Noted in the text
14. Caption to Figure 14 – modified

C. Comments of the reviewer #3:

1. L. 22 the size of the deposit quantified
2. L. 29 “linear” replaced by “smooth” as suggested
3. L. 45 difficult to quantified in the abstract- done in the text
4. L. 46 corrected
5. L. 48 “fertile” replaced by “mineralization” as suggested
6. L. 100 text modified
7. L. 127 “volcanics” replaced by “volcanic rocks”
8. L. 129 the exact proportions of various rock-types are not known, however, we have added reference to Figure 2 from which they can be estimated
9. L. 139 dated moly samples by Thorne et al. described better
10. L. 145 all units have now acronyms
11. L. 179 the name of the analytical package added
12. L. 238 corrected
13. l. 251 “graph” replaced by “diagram”
14. L. 259 The sentence moved to discussion.
15. L. 278-280. We would like to keep this sentence here for sake of better understanding and following the text
16. L. 288 modified as suggested
17. L. 290 modified as suggested
18. L. 293-296 Moved to Discussion
19. L. 300 depleted model ages added to this section
20. L. 359-360 references added
21. L. 380+388. We added a section called “6.2. Contaminant and metallogenic province” to explain this.
22. L. 426 explanation is in the new section 6.2.
23. L. 438-442. Sentence modified
24. L. 442+462 explanation is in the new section 6.2.
25. Figure 2 and Caption to Figure 2 corrected and modified
26. Like in most papers in Lithos, we prefer to keep both chondrite- and primitive mantle normalized plots.
27. Caption to Figure 10 modified; gives an explanation for bars. Due to data overlaps, plotting of individual samples is not reader friendly
28. Table 1; average is defined in the footnote; raw data are given in Appendix 1
29. Table 2; note that the major element oxides are not recalculated given in the footnote; additional data are in Appendix 2.

Upper Paleozoic (~365 Ma) mafic and intermediate volcanic rocks of the Piskahegan Group constitute a subordinate part of the Mount Pleasant caldera, which is associated with a significant polymetallic deposit (tungsten-molybdenum-bismuth zones ~ 33 Mt ore with 0.21% W, 0.1% Mo and 0.08% Bi and tin-indium zones ~ 4.8 Mt with 0.82% Sn and 129 g/t In) in southwestern New Brunswick (Canada). The epicontinental caldera complex formed during the opening of the late Paleozoic Maritimes Basin in the northern Appalachians. The mafic and intermediate rocks make up two compositionally distinct associations. The first association includes evolved rift-related continental tholeiitic basalts, and the second association comprises calc-alkaline andesites, although both associations were emplaced penecontemporaneously. The basalts have low Mg# ~ 0.34-0.40, smooth chondrite-normalized REE patterns with $(La/Yb)_n \sim 5-6$, primitive mantle-normalized trace element patterns without noticeable negative Nb-Ta anomalies, and their $\epsilon_{Nd(T)}$ ranges from +2.5 to +2.2. The basalts were generated by partial melting of a transition zone between spinel and garnet mantle peridotite at a depth of ~70-90 km. The calc-alkaline andesites of the second association have chondrite-normalized REE patterns that are more fractionated, with $(La/Yb)_n \sim 7-8.5$, but without significant negative Eu anomalies. Compared to the basaltic rocks, they have lower $\epsilon_{Nd(T)}$ values, ranging from +0.5 to +1.9, and their mantle-normalized trace element plots show negative Nb-Ta anomalies. The $\epsilon_{Nd(T)}$ values display negative correlations with indicators of crustal contamination, such as Th/La, Th/Nb and SiO_2 . The andesitic rocks are interpreted to have formed by assimilation-fractional crystallization processes, which resulted in the contamination of a precursor basaltic magma with crustal material. The parent basaltic magma for both suites underwent a different evolution. The tholeiitic basalts experienced shallow-seated fractional crystallization and evolved along a tholeiitic trend of "early iron" enrichment (non-oxic conditions). The contaminated magma of the second association followed a calc-alkaline fractionation trend of "no iron" enrichment (oxidizing conditions) characterized by a high $P_{(H_2O)}$ and $P_{(O_2)}$ environment at the mid-crust levels. The Piskahegan Group, which is associated with an important polymetallic mineral deposit, differs from the numerous non-mineralized rift-related volcanic suites of the regional Upper Devonian to Lower Carboniferous successions in the Maritimes Basin by the presence of a significant amount of coeval calc-alkaline andesite, which may be an indicator of potential mineralization.

365 Ma basalts and andesites are part of a bimodal suite of the Mount Pleasant caldera which hosts a polymetallic (Sn-W) deposit

Rift-related continental tholeiites were formed by melting of a subcontinental lithospheric mantle at the spinel-garnet transition

Calc-alkaline andesites were formed by crustal contamination of basaltic magma

The suite differs from the non-mineralized rift-related volcanic sequences in the region by the presence of coeval calc-alkaline andesite

1 **Upper Paleozoic mafic and intermediate volcanic rocks associated with the Sn-W deposit of**
2 **the Mount Pleasant caldera in southwestern New Brunswick (Canada): Petrogenesis and**
3 **metallogenic implications**

4

5

6

7

8

9

10

11 Jaroslav Dostal^{1a} and Pierre Jutras¹

12

13

14 1. Department of Geology, Saint Mary's University, Halifax, Nova Scotia B3H, Canada

15 a. Corresponding author: e-mail: jdostal@smu.ca; phone: 902-420-5747

16

17

18

19

20

21 **Abstract**

22 Upper Paleozoic (~365 Ma) mafic and intermediate volcanic rocks of the Piskahegan Group
23 constitute a subordinate part of the Mount Pleasant caldera, which is associated with a significant
24 polymetallic deposit (tungsten-molybdenum-bismuth zones ~ 33 Mt ore with 0.21% W, 0.1%
25 Mo and 0.08% Bi and tin-indium zones ~ 4.8 Mt with 0.82% Sn and 129 g/t In) in southwestern
26 New Brunswick (Canada). The epicontinental caldera complex formed during the opening of the
27 late Paleozoic Maritimes Basin in the northern Appalachians. The mafic and intermediate rocks
28 make up two compositionally distinct associations. The first association includes evolved rift-
29 related continental tholeiitic basalts, and the second association comprises calc-alkaline
30 andesites, although both associations were emplaced penecontemporaneously. The basalts have
31 low Mg# ~ 0.34-0.40, smooth chondrite-normalized REE patterns with $(La/Yb)_n \sim 5-6$, primitive
32 mantle-normalized trace element patterns without noticeable negative Nb-Ta anomalies, and
33 their $\epsilon_{Nd(T)}$ ranges from +2.5 to +2.2. The basalts were generated by partial melting of a transition
34 zone between spinel and garnet mantle peridotite at a depth of ~70-90 km. The calc-alkaline
35 andesites of the second association have chondrite-normalized REE patterns that are more
36 fractionated, with $(La/Yb)_n \sim 7-8.5$, but without significant negative Eu anomalies. Compared to
37 the basaltic rocks, they have lower $\epsilon_{Nd(T)}$ values, ranging from +0.5 to +1.9, and their mantle-
38 normalized trace element plots show negative Nb-Ta anomalies. The $\epsilon_{Nd(T)}$ values display
39 negative correlations with indicators of crustal contamination, such as Th/La, Th/Nb and SiO₂.
40 The andesitic rocks are interpreted to have formed by assimilation-fractional crystallization
41 processes, which resulted in the contamination of a precursor basaltic magma with crustal
42 material. The parent basaltic magma for both suites underwent a different evolution. The
43 tholeiitic basalts experienced shallow-seated fractional crystallization and evolved along a
44 tholeiitic trend of “early iron” enrichment (non-oxic conditions). The contaminated magma of
45 the second association followed a calc-alkaline fractionation trend of “no iron” enrichment
46 (oxidizing conditions) characterized by a high P_{H2O} and P_{O2} environment at the mid-crust levels.
47 The Piskahegan Group, which is associated with an important polymetallic mineral deposit,
48 differs from the numerous non-mineralized rift-related volcanic suites of the regional Upper
49 Devonian to Lower Carboniferous successions in the Maritimes Basin by the presence of a

50 significant amount of coeval calc-alkaline andesite, which may be an indicator of potential
51 mineralization.

52

53 **1. Introduction**

54 Felsic rocks of continental rift-related magmatic settings have been the focus of extensive
55 investigation and numerous publications in part because they may host rare metal mineralization,
56 which in some cases are of economic significance (e.g., Richardson and Birkett, 1996; Cerny et
57 al. 2005; Linnen and Cuney, 2005). These rocks are commonly associated with a
58 compositionally diverse variety of mafic and intermediate rocks (e.g., Nekvasil et al., 2000).
59 Much is still unknown about the processes that lead to the diversity of magmas within such
60 bimodal series and about the global diversity of intraplate magmatics. In mineralized bimodal
61 complexes where felsic rocks are dominant, the subordinate mafic and intermediate rocks are
62 commonly only poorly known, although they might provide important information on the
63 tectonic environment of such bimodal associations, as well as on the origin of the felsic rocks
64 and their mineralization, thus providing clues for the exploration for rare metal deposits. One
65 such suite is the upper Paleozoic Piskahegan Group of southwestern New Brunswick (Canada).
66 The latter group forms a volcanic caldera complex (e.g., McCutcheon, 1990; McCutcheon et al.,
67 1997; Thorne et al., 2013) that is spatially and genetically associated with the Mount Pleasant
68 polymetallic deposit (tungsten-molybdenum-bismuth zones containing ~ 33 Mt ore with 0.21%
69 W, 0.1% Mo and 0.08% Bi and tin-indium zones ~ 4.8 Mt with 0.82% Sn and 129 g/t In). The
70 deposit is recognized as the world's largest known undeveloped resource of indium (Sinclair et
71 al., 2006; Thorne et al., 2013). To contribute to the debate on the origin of these bimodal suites,
72 we have investigated mafic and intermediate volcanic rocks of the Mount Pleasant caldera (Figs.
73 1 and 2). Major and trace elements in these rocks, as well as neodymium isotopes, may provide
74 information related not only to the origin of the bimodal suite and its mineralization, but also on
75 the nature of the mantle source (e.g., DePaolo, 1988). Such data are also useful to evaluate the
76 composition of the subcontinental lithospheric mantle (SCLM).

77 The purpose of this paper is: (1) to present geochemical data on the mafic and
78 intermediate volcanic rocks of the Mount Pleasant caldera, including major and trace elements

79 and Nd isotopic ratios, (2) to constrain the origin of the rocks in the caldera, (3) to investigate the
80 differences between mineralized and barren Devonian to Carboniferous bimodal volcanic suites
81 in this part of the Northern Appalachians, (4) to evaluate the nature of the SCLM, and (5) to
82 compare this information with data from time equivalent basaltic rocks of New Brunswick and
83 Nova Scotia, which belong to the peri-Gondwanan Gander and Avalon terranes of the North
84 American Appalachians. The comparison of SCLM properties in two neighboring exotic terranes
85 could reveal whether or not both terranes were underlain by the same SCLM during the
86 Paleozoic and thus contribute to the Ganderian controversy (i.e. whether or not the Gander and
87 Avalon zones represent distinct terranes; e.g., van Staal and Barr, 2012; Dostal et al., 2016a).

88

89 **2. Geological setting**

90 Volcanic rocks of the Piskahegan Group occur along the western margin of the Maritimes
91 Basin in southwestern New Brunswick (Fig. 1). The Maritimes Basin is a major late Paleozoic
92 successor basin (Gibling et al., 2008) that was initiated after the Early to Middle Devonian
93 Acadian Orogeny (~400 Ma) in the Canadian Appalachians. This composite basin first
94 developed as a series of pull-apart sub-basins along the Minas Fault Zone, a large east- trending
95 dextral strike-slip system that juxtaposed the Meguma and Avalon terranes during the Late
96 Devonian and the Carboniferous (Murphy et al., 2011a). Associated with these pull-apart
97 structures are large bimodal plutons, as well as a series of NW-trending mafic dykes. Closely
98 spaced U-Pb dates for peak Acadian metamorphism and for the emplacement and exhumation of
99 post-Acadian plutons along the Minas Fault Zone suggest that the transition from orogenic
100 compression to transtension along this fault system was very rapid (Dostal et al., 2006). Also
101 associated with this transtensional magmatic event are widely distributed bimodal volcanic
102 suites, one of which is the Piskahegan Group and its associated polymetallic deposit (Kooiman et
103 al., 1986; McCutcheon et al., 1997; Thorne et al., 2013). The complex, referred to as the Mount
104 Pleasant caldera, is a northeast-trending elliptical feature that is defined by geophysical data
105 (regional gravimetric and magnetic studies) as about 13 km wide and 34 km long (McLeod and
106 Smith, 2010). However, the northern part of the complex is overlain by middle Mississippian
107 (Visean) and Pennsylvanian strata of the Maritimes Basin in such a way that the exposed length
108 is restrained to about 17 km. This epicontinental caldera, which was emplaced in a transtensional

109 setting (Fyffe et al., 2011), is associated with high-level subvolcanic granitic intrusions and has
110 been interpreted to have formed by roof collapse in an epizonal magma chamber. The
111 Piskahegan Group (Figs. 1 and 2) disconformably overlies deformed Ordovician to Silurian
112 turbiditic metasedimentary rocks of the Gander Terrane. These rocks bound the caldera to the
113 east and west. The caldera is in turn paraconformably overlain by Visean clastic rocks formerly
114 mapped as the Shin Redbeds by van de Poll (1967) and recently assigned the Shin Member of
115 the Hopewell Cape Formation (Jutras et al., 2015), which confine the caldera to the north (Fig.
116 1). Late Silurian to Devonian granitic rocks of the Saint George Batholith represent the southern
117 boundary of the complex (McLeod, 1990). Both the batholith and the caldera complex lie within
118 the boundaries of the Gander Terrane.

119 The Piskahegan Group (Fig. 2) has been subdivided into three volcanic facies (in the
120 sense of Fisher and Schmincke, 1984) in order to reflect their depositional setting in relation to
121 the volcanic architecture: (1) exocaldera, (2) intracaldera and (3) late caldera-fill sequences
122 (McCutcheon, 1990; McCutcheon et al., 1997; Thorne et al., 2013). The caldera is composed
123 mainly of felsic volcanic and volcanoclastic rocks and associated sedimentary rocks, which are
124 intruded by subvolcanic granitic bodies (McCutcheon et al., 1997). All three volcanic facies
125 contain subordinate amounts of mafic and intermediate volcanic rocks (Fig. 2).

126 The Piskahegan Group was emplaced during the initial stages of basin development.
127 Paleontological records and radiometric dating show that most of the caldera is Fammenian
128 (Upper Devonian) in age and coincides with the emplacement of voluminous granitic intrusions.
129 Anderson (1992) obtained a whole-rock Rb-Sr isochron age of 368 ± 5 Ma for the Piskahegan
130 Group. The Carrow Formation (CF) of the exocaldera sequence yielded a U-Pb zircon age of
131 363.8 ± 2.2 Ma (Tucker et al., 1998), whereas a spore assemblage recovered from drill core
132 above the zircon sample yielded a late Famennian age (McGregor and McCutcheon, 1988). More
133 recently, Thorne et al. (2013) reported Re-Os ages of 369.7 ± 1.6 Ma and 370.1 ± 1.7 Ma from
134 molybdenite samples associated with W-Mo-Bi mineralization. There are also several $^{40}\text{Ar}/^{39}\text{Ar}$
135 ages of ca. 360 Ma on the granitic rocks (Sinclair et al., 1988), and the youngest phase of the
136 neighbouring Saint George Batholith, which is probably related to them, gave a U-Pb zircon age
137 of 367 ± 1 Ma (Bevier 1988). Hence, all available data in the Piskahegan Group and associated
138 plutonic rocks range within the Fammenian (*sensu* Richards, 2013).

139 The exocaldera sequence includes three units that also contain mafic or intermediate
140 volcanic rocks. In ascending stratigraphic order, they are the Hoyt Station Basalt (HSB), the
141 South Oromocto Andesite (SOA) and the Carrow Formation (CF). HSB is the basal unit of the
142 exocaldera sequence (McCutcheon et al., 1997) and it consists mainly of a basalt flow unit that is
143 about 20 m thick. The basalt is underlain by rhyolitic volcanoclastic rocks. The SOA unit is an up
144 to 130 m thick succession of lava flows that is conformably overlain by the CF. The latter is
145 composed mainly of clastic sediments, but also contains an aphyric basalt flow (< 20 m thick)
146 near the top of the formation.

147 At the base, the intracaldera sequence includes the Scoullar Mountain Formation (SMF),
148 which lies along the periphery of the caldera complex at the contact with pre-caldera rocks. This
149 unit, the thickness of which ranges between 225 and 450 m, is composed predominantly of
150 clastic sedimentary rocks and interbedded andesitic lava flows and felsic volcanoclastic rocks.
151 The upper part of the late caldera-fill sequence contains the Kleef Formation (KF), which
152 consists of conglomeratic redbeds (40-75 m thick), basalts (70-80 m), and volcanoclastic rocks (>
153 4 m).

154 The polymetallic deposit is located near the southwestern margin of the caldera complex
155 (McCutcheon et al., 1997). It consists of mineralized stockworks and quartz veinlets, breccia
156 infill and lode mineralization. Its formation is associated with the emplacement of the
157 subvolcanic granitic rocks that host it. Thorne et al. (2013) inferred that the mineralization was
158 associated with caldera collapse, which was marked by the emplacement of a series of
159 subvolcanic granitic intrusions (Fig. 2).

160

161 **3. Analytical methods**

162 Mineral compositions (Table 1; Appendix 1) were determined using a JEOL Superprobe
163 733 equipped with four wave-length-dispersive spectrometers and one energy-dispersive
164 spectrometer, and operated with a beam current of 15 kV at 5 nA at the Department of Earth
165 Sciences of Dalhousie University, Halifax, Nova Scotia (Canada).

166 Major and several trace element analyses of whole rocks (Table 2; Appendix 2) were
167 performed on fused glass disks using a Philips PW2400 X-ray fluorescence spectrometer at the
168 University of Ottawa, Ontario (Canada). Duplicate analyses of the samples yielded total errors of

169 $\pm 3\%$ (1σ). Trace element analysis was done using lithium metaborate-tetraborate fusion and a
170 Perkin Elmer Optima 3000 ICP mass spectrometer at Activation Laboratories, Ancaster, Ontario
171 (Canada). Replicate analyses of the reference standard rocks indicate that the errors were
172 between 2 and 8 % of the values cited. The detection limits and other information on the trace
173 element analyses (analytical package 4B2) are available at the Activation Laboratories web site
174 (www.actlabs.com).

175 Nd isotope ratios (Table 3) were determined by isotope dilution mass spectrometry at the
176 Department of Earth Sciences of the Memorial University of Newfoundland (St. John's,
177 Newfoundland, Canada). Concentration data are standard ICP-MS analyses and are precise to
178 $\pm 5\%$ (2σ). Ratios of $^{147}\text{Sm}/^{144}\text{Nd}$ (except samples 38A and 69) were measured directly by high-
179 precision ICP-MS with an estimated precision of $\pm 0.5\%$ (2σ). The isotopic ratios of $^{143}\text{Nd}/^{144}\text{Nd}$
180 were determined using a multicollector Finnigan MAT 262V thermal ionization mass
181 spectrometer operated in a static mode. Measured $^{143}\text{Nd}/^{144}\text{Nd}$ values were normalized to a
182 $^{146}\text{Nd}/^{144}\text{Nd}$ ratio of 0.7219. Replicate analyses of the LaJolla standard, which was analyzed
183 repeatedly throughout, gave an average value for $^{143}\text{Nd}/^{144}\text{Nd}=0.511849 \pm 9$. The 2σ values for
184 all samples are less than or equal to 0.000008 for $^{143}\text{Nd}/^{144}\text{Nd}$ and are given in Table 3. Values
185 for $\epsilon_{\text{Nd}(T)}$ were calculated with respect to CHUR using present-day $^{143}\text{Nd}/^{144}\text{Nd}$ and $^{147}\text{Sm}/^{144}\text{Nd}$
186 ratios of respectively 0.512638 and 0.196593, and subsequently age-corrected. A $T_{\text{DM}1}$ model
187 age was calculated using a linear evolution for a mantle that separated from CHUR at 4.55 Ga,
188 and that has a present day ϵ value of +10. The $T_{\text{DM}2}$ model age was calculated according to the
189 model of DePaolo (1988).

190

191 **4. Petrography and mineral chemistry**

192 Basalts and andesites of the Piskahegan Group vary from massive to amygdaloidal.
193 Amygdales occur particularly in the upper part of the flows and are commonly filled by
194 carbonates or silica. Although rocks of the caldera are not significantly deformed and contain
195 unstrained quartz with primary glass inclusions (Gray et al., 2011), the amygdaloidal rocks are
196 altered. Igneous textures are mostly preserved, but the primary magmatic minerals are frequently
197 replaced by secondary phases. The rocks exhibit greenschist grade metamorphism that produced
198 chlorite, epidote and actinolite. Textures range from aphyric to coarse subophitic and ophitic, as

199 well as porphyritic and glomeroporphyritic. The basalts are composed predominantly of
200 plagioclase and clinopyroxene, which are variably altered and occur both as phenocrysts and as
201 the main components of the groundmass. The rocks also contain minor Fe-Ti oxides and
202 accessory apatite. No orthopyroxene was observed. When fresh, the plagioclase phenocrysts
203 show zoning with labradorite-bytownite cores and andesine rims. However, plagioclase is mostly
204 albitized or altered to sericite and calcite. Some plagioclase phenocrysts contain zones of sieve
205 texture. The intermediate rocks contain relics of dark brownish-green amphibole replaced mainly
206 by chlorite and epidote. In these rocks, subhedral amphibole crystallized together with
207 plagioclase, Fe-Ti oxide, and apatite after the crystallization of clinopyroxene (Anderson, 1992).
208 Amphibole may contain a core of clinopyroxene. The clinopyroxene phenocrysts show zoning,
209 but are partially replaced by chlorite and epidote. Clinopyroxenes typically form subhedral
210 phenocrysts and microphenocrysts or occur in a subophitic to ophitic groundmass of the mafic
211 rocks. Relics of fresh clinopyroxene in the mafic and intermediate rocks are typically augite
212 (Anderson, 1992; Table 1; Appendix 1). On tectonic discrimination diagrams for pyroxene
213 (Leterrier et al., 1982), clinopyroxenes of the basalts plot in the “non-orogenic” field (Anderson,
214 1992; McCutcheon et al., 1997). Clinopyroxenes from the intermediate rocks (Table 1) also plot
215 in the “non-orogenic” field (Fig. 3) of Leterrier et al. (1982). The rarity of phenocrysts in some
216 samples of evolved rocks may be caused by the separation of early fractionated phases from the
217 melt on the way to the surface.

218

219 **5. Whole-rock geochemistry**

220 *5.1. Alteration*

221 Alteration and metamorphic processes have affected the rocks. Petrographic evidence
222 includes the saussuritization, sericitization, and albitization of feldspar, the chloritization of
223 clinopyroxene as well as the accumulation of silica and calcite in amygdales. Although the
224 original abundances of mobile elements such as Ca, Na and K might have been modified, the
225 concentrations and ratios of high-field strength elements (HFSE) and rare earth elements (REE)
226 show well-defined trends indicating that these elements were immobile during alteration. This is
227 also supported by many other studies (e.g., Winchester and Floyd, 1977) indicating that HFSE
228 and REE retain their distribution during alteration. Furthermore, an investigation of melt

229 inclusions in quartz of associated rhyolitic rocks (Gray et al., 2011) showed that post-magmatic
230 processes did not modify the whole-rock composition. Similarly, it is typically inferred that the
231 Sm and Nd isotope characteristics of a rock are resistant to geological disturbances (e.g.,
232 DePaolo, 1988).

233

234 *5.2. Major and trace elements*

235 All the major oxide compositions were recalculated to 100% on a volatile free basis for
236 plotting on geochemical diagrams. According to their major element compositions (Fig. 4), the
237 mafic and intermediate volcanic rocks of the Piskahegan Group can be subdivided into two
238 associations: Association 1 includes basalts of the KF and CF formations, which are
239 characterized by low SiO₂ (48-52 wt.%), and high TiO₂ (> 2.5 wt.%) and FeO_(t) (~ 13-15 wt.%),
240 whereas Association 2 comprises intermediate rocks of the SOA and SMF, with SiO₂ > 54 wt.%,
241 TiO₂ < 2 wt.%, and FeO_(t) < 9 wt.%. The division is also shown in the Zr/TiO₂ versus Nb/Y
242 diagram (Fig. 5), in which Association 1 rocks plot in the basaltic field, whereas rocks of
243 Association 2 plot mainly in the andesitic field.

244 According to the conventional AFM [(K₂O+Na₂O)-FeO_(t)-MgO] diagram (Fig. 6),
245 Association 1 rocks are tholeiites. They have characteristics of differentiated tholeiitic basalts
246 with low MgO, Ni and Cr, as well as high Fe, Ti and P. Their chondrite-normalized REE patterns
247 show a negative slope, resulting from an enrichment of light REE (LREE) with (La/Yb)_n ~5-6,
248 but without Eu anomalies (Fig.7). The primitive mantle-normalized incompatible element plots
249 of Association 1 rocks do not display noticeably negative Nb-Ta anomalies (Fig. 8). The patterns
250 show distinct negative anomalies for Ti and Sr, which together with low Ni and Cr indicate that
251 the rocks underwent fractional crystallization dominated by plagioclase and clinopyroxene. Both
252 patterns (Figs. 7 and 8) resemble those of rift-related continental tholeiites or transitional basalts
253 (e.g., Dostal and Dupuy, 1984; Pegram, 1990; Dostal et al., 1992; Peate and Hawkesworth,
254 1996). In comparison with arc mafic rocks, the basalts have high Ti/V (70-100) and Zr/Y (6-8),
255 and their primitive mantle-normalized trace element patterns do not exhibit pronounced negative
256 Nb-Ta anomalies (Fig. 8). In addition, on geochemical discrimination diagrams, they plot in the
257 field of rift-related basalts (Fig. 9).

258 Compared to those of Association 1, rocks of Association 2 have calc-alkaline
259 characteristics (e.g., Fig. 6), although they were emplaced penecontemporaneously and in the
260 same tectonic and geographic settings. With increasing SiO₂, the andesites show a decrease in
261 Fe, Ti, Mg# (MgO/[MgO+FeO_(t)]) and Ni, but also an increase in alkalis and in the Al₂O₃/CaO
262 and La/Yb ratios (Fig. 4), indicating the crystallization of clinopyroxene, plagioclase and Fe-Ti
263 oxide. The fractionation of Fe-Ti oxides, which is implied by a decrease of FeO_(t), TiO₂, and V
264 with increasing SiO₂ in the calc-alkaline suite, suggests high P_{H₂O} and P_{O₂} conditions. The
265 difference between tholeiitic and calc-alkaline suites can be partially due to the depth of
266 fractional crystallization (e.g., Grove and Kinzler, 1986). Crystallization of the calc-alkaline
267 magmas at mid-crustal depth may have differed from that of tholeiitic magma, which could have
268 taken place at lower P_{tot} and lower P_{O₂} conditions (i.e., within a shallow upper crustal magma
269 chamber).

270 There are subtle differences between the SOA and SMF rocks. The SOA have SiO₂ ~55-
271 58 wt.%, TiO₂ < 2 wt.% and FeO_(t) ~ 8 wt.%. The SMF rocks are more fractionated, although
272 there is some overlap in composition. They have typically higher SiO₂ (59-66 wt.%), lower TiO₂
273 < 1.5 wt.% and lower FeO_(t) < 8 wt.% (Table 2).

274 In addition to the differences in major element compositions between associations 1 and
275 2, the andesites have more fractionated REE patterns, with (La/Yb)_n ~ 7-8.5, but also without
276 significant Eu anomalies. Their light REE (LREE) abundances are similar to those of the first
277 association, but they have lower heavy REE (HREE) contents. The primitive mantle-normalized
278 incompatible element plots of Association 2 show distinct negative Nb-Ta anomalies, which are
279 indicative of either subduction or crustal assimilation.

280 5.3. Nd isotopic ratios

281 The Sm-Nd isotopic signatures of the basaltic and andesitic rocks are given in Table 3, in
282 which they are all age-corrected to 365 Ma. The ε_{Nd(T)} values of the basalts range from +2.5 to +
283 2.2, and ¹⁴⁷Sm/¹⁴⁴Nd ratios vary from 0.13 to 0.14 (Table 3). The values are in good agreement
284 with the data of Anderson (1992) for mafic rocks of the caldera. The data plot within the range
285 reported for the Devonian to Carboniferous basaltic rocks of the Maritimes Basin in New
286 Brunswick and Nova Scotia (Fig. 10). They are also similar to those from rift-related basalts,
287 continental flood basalts and xenoliths from the subcontinental lithosphere (Faure and Mensing,

288 2005). These $\epsilon_{\text{Nd}(T)}$ values are considerably lower than values expected for juvenile magmas from
289 a depleted mantle source (Fig. 10), although the positive $\epsilon_{\text{Nd}(T)}$ values preclude a significant
290 contribution from substantially older continental crust or sedimentary rocks derived from it. The
291 Piskahegan basaltic rocks plot in the field of Avalonian and peri-Rodinian lithosphere (Fig. 10),
292 and their $\epsilon_{\text{Nd}(T)}$ values are consistent with derivation from a SCLM.

293 Neodymium depleted-mantle model ages of DePaolo (1988) for these rocks range
294 between 800 and 900 Ma (Table 3) and are similar to those determined for the Devonian to
295 Carboniferous basaltic rocks above the Avalon and Gander terranes in the Maritimes Basin
296 (Keppie et al., 1997; Pe-Piper and Piper, 1998). These similarities suggest that the model ages
297 represent a bulk weighted average of the source composition.

298 The andesites have lower $\epsilon_{\text{Nd}(T)}$ than the basalts (Table 3), but they still plot in the field of
299 Avalonian and Ganderian lithosphere (Fig. 10). The negative Nb-Ta anomalies and the lower
300 $\epsilon_{\text{Nd}(T)}$ values (+0.5 to +1.9) of these rocks are consistent with an inferred involvement of
301 continental lithosphere in their evolution, most probably through crustal contamination.

302

303 **6. Discussion**

304 *6. 1. Petrogenesis*

305 Although all volcanic rocks of the Piskahegan Group are spatially and temporarily
306 associated, the Association 1 basalts are not related to the Association 2 andesites through simple
307 crystal-liquid equilibria processes. The absence of smooth variation trends when various
308 elements and element ratios are plotted against a differentiation index, such as SiO_2 (Fig. 4),
309 suggests that the Association 2 andesites did not simply result from the fractional crystallization
310 of Association 1 basalts.

311 The Association 1 rocks are evolved tholeiites that were emplaced in an epicontinental
312 rift-related setting. Compared to primitive basalts that have Mg# values of ~ 0.70 (Hanson and
313 Langmuir, 1978), the Piskahegan basalts (Table 2) have significantly lower values (0.34-0.40),
314 suggesting that they have undergone high degrees of fractional crystallization. The fractional
315 crystallization was dominated by crystallization of clinopyroxene and plagioclase. On the Th/Yb
316 versus Nb/Yb diagram (Fig. 11), which has been used for the evaluation of lithospheric inputs in
317 basalts (Pearce, 2008), the averages of N-type MORB, E-type MORB and OIB form a diagonal

318 mantle array (Fig. 11). Magmas that were modified by an interaction with continental crust or
319 that involved material with a subduction history are displaced to higher Th/Yb values. The
320 basaltic rocks of the Piskahegan Group straddle the boundary of the mantle array, implying that
321 crustal contamination and subduction imprints were insignificant. This is also consistent with the
322 lack of a discernible negative Nb-Ta anomaly on the spider plots (Fig. 8). Thus, the composition
323 of the basalts mostly reflects the original characteristics of the mantle source and, together with
324 positive $\epsilon_{Nd(T)}$ values, indicate that they were derived from a relatively uncontaminated and
325 moderately enriched mantle, similar to an ocean island basalt (OIB)-type source (Faure and
326 Mensing, 2005).

327 On the Tb/Yb versus La/Sm graph (Fig.12), the basaltic samples straddle the spinel
328 peridotite-garnet peridotite boundary, suggesting that they were formed in a spinel-garnet
329 transition zone, at a depth of ~70-90 km (Wang et al., 2002). Whereas Tb/Yb ratios are related to
330 the pressure conditions and depth at which melting occurred, La/Sm ratios correlate with the
331 degree of partial melting and tend to decrease with an increase of mantle peridotite melting.
332 Ratios for the CF and KF basalts are overlapping, which indicates that they were generated at the
333 same depth by similar degrees of partial melting from a similar mantle source.

334 The andesites of the Piskahegan Group underwent fractional crystallization dominated by
335 plagioclase, clinopyroxene and Fe-Ti oxide, as indicated by the variation trends of several
336 elements and element ratios when plotted against SiO₂ (Fig. 4). The compositional characteristics
337 of the Association 2 rocks, including negative Nb-Ta anomalies and their position on the Th/Yb
338 versus Nb/Yb diagram (Fig. 11), suggest that the rocks record an additional process to fractional
339 crystallization. The SOA and SMF andesites are displaced toward higher Th/Yb ratios relative to
340 the mantle array, implying crustal contamination or inputs from a subcontinental mantle that had
341 previously been affected by subduction fluids.

342 Correlation of element and isotopic ratios suggests that the andesites were significantly
343 changed by crustal contamination as discussed below. Trace element ratios, which are not
344 modified by the fractional crystallization of major rock forming minerals and which have
345 significantly different values for oceanic basalts (OIB, MORB) and continental crust (e.g.,
346 Th/La, Th/Nb, Th/Ta, Nb/U), are typically used as indicators for crustal contamination (e.g.,
347 Jochum et al., 1991; D'Antonio et al., 2007). The SOA andesites have higher Th/La (~0.15-

348 0.16), Th/Nb (0.3-0.45) and Th/Ta (5-7) ratios than the basalts (Th/La~0.08-0.1, Th/Nb ~0.11-
349 0.19, and Th/Ta~1-3), indicating crustal input. The same applies for the SMF andesites, which
350 have even higher Th/La (~0.20-0.25), Th/Nb (>0.5) and Th/Ta (8-11) ratios. These ratios, which
351 are sensitive indicators of crustal contamination, correlate with SiO₂ (Fig. 4) and are consistent
352 with an origin of the intermediate rocks by the crustal contamination of basalts accompanied by
353 fractional crystallization. Such a process is also supported by mixing trends on the Nb/Th versus
354 Th/Yb diagram (Fig. 13), in which the andesitic rocks plot along the mixing line between typical
355 mantle-derived tholeiites and crustal material. A similar trend is also shown on Figure 9. Due to
356 the absence of geochemical analyses from the underlying basement/continental crust, we have
357 used the average continental crust composition of Taylor and McLennan (1985) as a reference
358 contaminant for these graphs. Likewise, the plots involving Nd isotopes and contamination-
359 sensitive trace element ratios or SiO₂ suggest a mixing between the basaltic melts derived from
360 the SCLM and crustal material. The rocks show a general trend of lower $\epsilon_{Nd(T)}$ with higher Th on
361 the $\epsilon_{Nd(T)}$ versus Th/La graph (Fig. 14), confirming the involvement of continental crust in the
362 rocks with lower $\epsilon_{Nd(T)}$.

363 The highly fractionated nature of the basalts as well as the observed gap between basalts
364 and intermediate rocks indicate that the original magmas of each association had to undergo a
365 separate evolution, although they may have had comparable parent magma. The Association 1
366 basalts underwent fractional crystallization during their rise to the surface, whereas the
367 Association 2 andesites were modified by crustal contamination through assimilation-fractional
368 crystallization (AFC) processes, probably at mid-crust levels. As the andesitic rocks contain
369 hornblende indicative of mid-crust crystallization and show a calc-alkaline fractionation trend
370 that is typical of high $P_{(tot)}$ and P_{H_2O} conditions, the contamination had to take place at a deeper
371 crustal level (e.g., Osborn, 1959; Zimmer et al., 2010). In addition to amphibole, the calc-
372 alkaline rocks also contain clinopyroxene phenocrysts, which, like those of the basalts, are
373 typical of within plate, “non-orogenic” rocks (Fig. 3). The wet and/or oxidizing environment is
374 also consistent with the lack of distinct negative Eu anomalies in most of the andesitic rocks
375 (Fig. 7) which could be because the magmatic water content was high (Moore and Carmichael,
376 1998) and/or because the magmatic oxidation state was high, in which case most of the Eu would

377 have been present as Eu^{3+} and would not have been incorporated into the crystallizing
378 plagioclase (e.g., Sisson and Grove, 1993).

379 Crustal contamination led to a change from a non-oxic environment, typical of tholeiitic
380 rocks, to the oxidizing environment that is typical of calc-alkaline rocks (e.g., Osborn, 1959;
381 Zimmer et al., 2010). In the case of the tholeiitic basalts, the original magma fractionated along a
382 tholeiitic trend of “early iron” enrichment (non-oxic conditions). The magma which mixed with
383 continental crust material followed a calc-alkaline fractionation trend of “no iron” enrichment
384 (oxidizing conditions).

385

386 *6.2. Crustal contamination in a metallogenic province*

387 In the near vicinity of the Mount Pleasant caldera, there are several small Late Devonian
388 plutons composed of Li-F-rich granites (e.g., Taylor, 1992; Whalen et al., 1996). These plutons
389 as well as the Mount Pleasant complex are a part of a large tin belt described by Schuiling (1967)
390 and Strong (1980), among others, which extends from North America to Europe. This belt,
391 characterised by the occurrences of the mineralized Devono-Carboniferous Li-F- rich
392 peraluminous leucogranites with broadly contemporaneous S-W-(U) mineralization, can be
393 followed along the late Paleozoic fold belts of the Canadian Appalachians and the Hercynian
394 Orogen of western and central Europe, from New Brunswick (Mount Pleasant complex) and
395 Nova Scotia (South Mountain Batholith at East Kemptville), to Newfoundland (Ackley Pluton),
396 and across the Atlantic Ocean to southwestern England (Cornwall), France (Armorican Massif
397 and Massif Central), Germany (Altenberg, Erzgebirge) and the Czech Republic (Zinnwald,
398 Erzgebirge). The belt has a long mining history of Sn, W and U dating back to the Romans.
399 Numerous studies (e.g., Dostal and Chatterjee, 1995; Haapala, 1997; Cuney et al., 2002; Dostal
400 et al., 2004; Cerny et al., 2005) inferred that the magmatic and hydrothermal mineralizing events
401 were essentially synchronous and that the uncommon chemical characteristics of the Li-F-rich
402 leucogranites require an uncommon source material. It has been inferred that the parental
403 magmas of the leucogranites, including those around the Mount Pleasant caldera, were derived
404 from similar source reservoirs (Romer and Kroner, 2014), probably phlogopite/biotite-rich mid-
405 crustal metasedimentary rocks (e.g., Dostal et al., 2004). Similar fluid-rich rocks could have
406 acted as a crustal contaminant.

407
408
409
410
411
412
413
414
415
416
417
418
419
420
421
422
423
424
425
426
427
428
429
430
431
432
433
434
435
436

6. 3. Comparable rock suites and possible mantle sources

Comparable Upper Devonian to Lower Carboniferous bimodal volcanic suites occur within the Maritimes Basin in Nova Scotia (western Cape Breton Island, Antigonish Highlands and Cobequid Highlands) and southern New Brunswick (e.g., Dostal et al., 1983; Keppie and Dostal, 1980; Keppie et al., 1997; Pe-Piper and Piper, 1998). The basaltic rocks are rift-related, mainly fractionated continental tholeiites. In these basaltic rocks, $\epsilon_{Nd(T)}$ values are variable, ranging from +2.2 to +5.2 (Keppie et al., 1997; Pe-Piper and Piper, 1998). The basalts are considered to be derived from the SCLM (Pe-Piper and Piper, 1998).

To evaluate lithospheric mantle sources in the area, as well as the changes that they underwent during the Carboniferous, we have also determined the Nd isotopic ratios of the Carboniferous trachytes (~335 Ma old) from the Cumberland Hill Formation (Gander Terrane) of southern New Brunswick as these rocks are younger by about 30 M.y. than the bulk of the Devonian-Carboniferous magmatism. These rocks were interpreted to be derived from an alkali basaltic magma by extensive fractional crystallization without being affected by crustal contamination (Gray et al., 2010). Such an origin is also in an agreement with their primitive mantle-normalized plots, in which the rocks do not show any negative Nb-Ta anomalies (Gray et al., 2010). These rocks have higher $\epsilon_{Nd(T)}$ values (+4.3 to + 3.3) than the basaltic rocks of the Piskahegan Group, but have younger model ages (~0.6 Ga; Table 3).

Model ages, variation ranges of $\epsilon_{Nd(T)}$, and chemical compositions of the basaltic rocks of the Piskahegan Group, which are similar to those recorded in penecontemporaneous mafic lavas in both Avalonia and Ganderia, can be accounted for by derivation from a subcontinental lithospheric mantle that was locally modified by the upward invasion of enriched (OIB) asthenospheric magma (e.g., Pe-Piper and Piper, 1998). The basaltic magmas extruded due to rapid lithospheric thinning and an associated steepening of the geothermal gradient (e.g., Lynch and Tremblay, 1994; Pe-Piper and Piper, 1998). There does not appear to be a systematic difference between the Avalon and Gander terranes in the isotopic composition of the SCLM during the Late Devonian and the Early Carboniferous, and composition of the SCLM could therefore have been similar beneath both terranes in this part of the Appalachians.

437 *6. 4. Possible link between mineralization and the development of a subordinate calc-alkaline*
438 *suite*

439 The Upper Devonian to Lower Carboniferous rift-related volcanic suites that onlap the
440 Avalon and Gander terranes along the margin of the Maritimes Basin are mostly bimodal
441 continental tholeiite - rhyolite associations. The Piskahegan Group, which is associated with a
442 significant polymetallic mineralization, differs from the rest of them by the presence of a
443 significant amount of coeval calc-alkaline intermediate rocks. This calc-alkaline suite is
444 interpreted to be the result of AFC processes involving the crustal contamination of a basaltic
445 magma precursor, and of a change from non-oxic to oxidizing conditions accompanied by a
446 relatively high content of magmatic water. The basalts also display an iron enrichment trend that
447 is typical of low P shallow-seated fractionation that occurs in a non-oxic environment (Osborn,
448 1959; Zimmer et al., 2010). The calc-alkaline suite had a relatively high magmatic water content
449 and/or high oxidation state, which are considered to be an indication of fertility for many
450 polymetallic ore-bearing felsic and intermediate units (Candela, 1992; Richards, 2011). As
451 rhyolites of the Piskahegan Group are also related to the andesitic rocks (Anderson, 1992;
452 McCutcheon et al., 1997; Dostal et al., 2016b), it can be suggested that the evolution of these
453 felsic rocks differed from those of other Upper Devonian to Lower Carboniferous bimodal
454 volcanic suites. The presence of a significant amount of calc-alkaline volcanic rocks in such
455 bimodal suites could be an indicator of potential mineralization.

456

457 **7. Conclusions**

458 Mafic and intermediate rocks of the Piskahegan Group constitute two distinct
459 associations that are spatially and temporarily related within a Late Paleozoic caldera complex
460 that hosts a significant polymetallic deposit of tin, tungsten, molybdenum, indium and bismuth.
461 The first association includes basalts of the Kleef and Carrow formations, whereas the second
462 association encompasses andesites of the South Oromocto Andesite and Scoullar Mountain
463 formations. The basalts of the first association are fractionated, rift-related continental tholeiites
464 with high contents of Fe, Ti, P and V, but low Mg, Mg#, Ni and Cr. They display tholeiitic
465 fractionation trends of Fe and Ti enrichment that are characteristic of dry and non-oxic
466 environments. They underwent the main pulse of fractional crystallization at a relatively shallow

467 depth, although the parent magma was generated in the transition zone between spinel and garnet
468 peridotite at a depth of ~70-90 km. The mantle- normalized patterns of the basalts do not show
469 distinct negative Nb-Ta anomalies, and their geochemical characteristics mainly reflect a mantle
470 source without noticeable signs of significant crustal contamination. Rocks of the second
471 association display a typical calc-alkaline fractionation trend that is characterized by a gradual
472 depletion of Fe and Ti with increasing differentiation, which is indicative of a wet and oxidizing
473 environment. This is also consistent with the absence of a negative Eu anomaly in the REE
474 patterns of these rocks, and with the presence of hornblende in their modal composition. The
475 rocks resulted from the mixing of continental crust material (probably phlogopite/biotite-rich
476 metasedimentary rocks) with primitive basaltic melt, probably at mid-crust level. Although the
477 parent basaltic magmas of both suites could have been derived from the same SCLM source,
478 they underwent separate and different evolution pathways. The Piskahegan Group, which is
479 associated with the Mount Pleasant polymetallic deposit, differs from penecontemporaneous,
480 non-mineralized bimodal suites that occur along the margins of the Maritimes Basin through
481 New Brunswick and Nova Scotia by the presence of a significant amount of coeval calc-alkaline
482 intermediate rocks. As such rocks evolve in water- and oxygen-rich magmatic environments,
483 their presence may be considered to be an indicator of potential mineralization.

484

485 **Acknowledgements**

486 This study was supported by the New Brunswick Department of Energy and Mines,
487 Geological Surveys Branch and the Natural Sciences and Engineering Research Council of
488 Canada (Discovery grant to J.D.). We thank Malcom McLeod for the initiation of this project
489 and Randy Corney for technical assistance. Constructive reviews by Drs. John Greenough,
490 Nelson Eby and two anonymous referees improved the manuscript.

491

492

493

494

495

496 **References**

- 497 Anderson, H.E. 1992. A chemical and isotopic study of the age, petrogenesis and magmatic
498 evolution of the Mount Pleasant caldera complex, New Brunswick. Unpublished Ph.D.
499 thesis, Carleton University, Ottawa, Ontario. 203 p.
- 500 Bevier, M.L., 1988. U-Pb geochronologic studies of igneous rocks in N.B. In: Abbott, S.A. (Ed.)
501 Thirteenth Annual Review of Activities, Project Résumés. New Brunswick Department of
502 Natural Resources and Energy, Minerals and Energy Division, Information Circular 88-2,
503 pp. 134-140.
- 504 Candela, P.A., 1992. Controls on ore metal ratios in granite-related ore systems: An experimental
505 and computational approach. Transactions of the Royal Society of Edinburgh, Earth
506 Sciences 83, 317-326.
- 507 Cerny, P., Blevin, P.L., Cuney M., London, D., 2005. Granite-related ore deposits. Economic
508 Geology 100, 337-370.
- 509 Cuney, M., Alexandrov, P., LeCarlier de Veslud, C., Cheilletz, A., Raimbault, L., Ruffet, G.,
510 Scaillet S., 2002. The timing of W–Sn-rare metals mineral deposit formation in the Western
511 Variscan chain in their orogenic setting: the case of the Limousin area (Massif Central,
512 France). Geological Society of London Special Publication 204, 213-228.
- 513 D'Antonio, M., Tonarini, S., Arienzo, I., Covetta, L., Di Renzo, V., 2007. Components and
514 processes in the magma genesis of the Phlegrean Volcanic District, southern Italy.
515 Geological Society of America Special Papers 418, 203-220.
- 516 DePaolo, D.J., 1988. Neodymium Isotope Geochemistry: An Introduction. Springer Verlag, New
517 York, 187 p.
- 518 Dostal, J., Dupuy, C., 1984. Geochemistry of the North Mountain basalts, Nova Scotia,
519 Canada. Chemical Geology 45, 245-261.
- 520 Dostal, J., Chatterjee, A.K. 1995. Origin of topaz-bearing and related peraluminous granites of
521 late Devonian Davis Lake pluton, Nova Scotia, Canada. Chemical Geology 123, 67-88.
- 522 Dostal, J., Chatterjee, A.K., Kontak, D.J. 2004. Chemical and isotopic (Pb, Sr) zonation in a
523 peraluminous granite pluton: role of fluid fractionation. Contributions to Mineralogy and
524 Petrology 147,74-90.
- 525 Dostal, J., Dupuy, C., Nicollet, C., Cantagrel, J.M., 1992. Geochemistry and petrogenesis of

526 southern Malagasy. *Chemical Geology* 97, 199-218.

527 Dostal, J., Keppie, J. D., Dupuy, C., 1983. Petrology and geochemistry of Devonian-Carboniferous
528 volcanic rocks in Nova Scotia. *Maritime Sediments and Atlantic Geology* 19, 59-71.

529 Dostal, J., Keppie, J.D., Jutras, P., Miller, B.V., Murphy, J.B., 2006. Evidence of the granulite-
530 granite connection: Penecontemporaneous high-grade metamorphism, granitic magmatism
531 and core complex development in the Liscomb Complex, Nova Scotia, Canada. *Lithos* 86,
532 77-90.

533 Dostal, J., Keppie, J.D., Wilson, R. A., 2016a. Nd isotopic and trace element constraints on the
534 source of Silurian–Devonian mafic lavas in the Chaleur Bay Synclinorium of New
535 Brunswick (Canada): Tectonic implications. *Tectonophysics* 681, 364-375.

536 Dostal, J., van Hengstum, T.R., Shellnutt, J.G., Hanley, J.J. 2016b. Petrogenetic evolution of
537 Late Paleozoic rhyolites of the Harvey Group, southwestern New Brunswick (Canada)
538 hosting uranium mineralization. *Contributions to Mineralogy and Petrology* 171: DOI
539 10.1007/s00410-016-1270-8.

540 Faure, G., Mensing, T. M., 2005. *Isotopes: Principles and Applications*. John Wiley and Sons,
541 Hoboken, New Jersey, 3rd edition, 897 p.

542 Fisher, R.V., Schmincke, H.U., 1984. *Pyroclastic rocks*. Springer-Verlag, New York, 472 pp.

543 Fyffe, L.R., Johnson, S.C., van Staal, C.R., 2011. A review of Proterozoic to Early Paleozoic
544 lithotectonic terranes in the northeastern Appalachian orogen of New Brunswick, Canada,
545 and their tectonic evolution during Penobscot, Taconic, Salinic, and Acadian orogenesis.
546 *Atlantic Geology* 47, 211-248.

547 Gibling, M.R., Culshaw, N., Rygel, M.C., Pascucci, V., 2008. The Maritimes Basin of Atlantic
548 Canada: Basin Creation and Destruction in the Collisional Zone of Pangea. In: Miall, A.D.
549 (Ed.) *Sedimentary Basins of the World*, Vol. 5, pp. 211-244. Elsevier, Amsterdam.

550 Gray, T.R., Dostal, J., McLeod, M., Keppie, J.D., Zhang, Y.Y., 2010. Geochemistry of Late
551 Paleozoic peralkaline felsic volcanic rocks, central New Brunswick. *Atlantic Geology* 46,
552 173-184.

553 Gray, T.R., Hanley, J.J., Dostal, J., Guillong, M., 2011. Magmatic enrichment of uranium,
554 thorium and rare earth elements in late Paleozoic rhyolites of southern New Brunswick,
555 Canada: evidence from silicate melt inclusions. *Economic Geology* 106, 127-143.

556 Grove, T.L., Kinzler, R.J., 1986. Petrogenesis of andesites. *Annual Review of Earth and*
557 *Planetary Sciences* 14, 417-454.

558 Haapala, I., 1997. Magmatic and postmagmatic processes in tin mineralized granites: topaz-
559 bearing leucogranite in the Eurajoki Rapakivi granite stock, Finland. *Journal of Petrology*
560 38, 1645-1659.

561 Hanson, G.N., Langmuir, C.H., 1978. Modelling of major elements in mantle-melt systems using
562 trace element approaches. *Geochimica et Cosmochimica Acta* 42, 725 -742.

563 Irvine, T. N., Baragar, W. R. A., 1971. A guide to the chemical classification of the common
564 volcanic rocks. *Canadian Journal of Earth Sciences* 8, 523-548.

565 Jochum, K.P., Arndt, N.T., Hofmann, A.W., 1991. Nb-Th-La in komatiites and basalts:
566 constraints on komatiite petrogenesis and mantle evolution. *Earth and Planetary Science*
567 *Letters* 107, 272-291.

568 Jutras, P., McLeod, J., MacRae, R.A., Utting, J., 2015. Complex, interplay of faulting,
569 glacioeustatic variations and halokinesis during deposition of upper Viséan units over thick
570 salt in the western Cumberland Basin of Atlantic Canada. *Basin Research* 2015, 1-24.

571 Keppie, J. D., Dostal, J., 1980. Palaeozoic volcanic rocks of Nova Scotia. *International*
572 *Geological Correlation Programme Project 27: Caledonide Orogen. Proceedings of Virginia*
573 *Polytechnic Institute and State University Memoir* 2, 249-256.

574 Keppie, J. D., Dostal, J., Murphy, J. B., Cousens, B. L., 1997. Palaeozoic within-plate volcanic
575 rocks in Nova Scotia (Canada) reinterpretation: isotopic constraints on magmatic source
576 and palaeocontinental reconstructions. *Geological Magazine* 134, 425-447.

577 Keppie, J.D., Murphy, J.B., Nance, R.D., Dostal, J., 2012. Mesoproterozoic Oaxaquia-type
578 basement in peri-Gondwanan terranes of Mexico, the Appalachians and Europe: TDM age
579 constraints on extent and significance. *International Geology Review* 54, 313-324.

580 Kooiman, G.J.A., McLeod, M.J., Sinclair, W.D., 1986. Porphyry tungsten-molybdenum ore
581 bodies, polymetallic veins and replacement bodies, and tin-bearing greisen zones in the Fire
582 Tower Zone, Mount Pleasant, New Brunswick. *Economic Geology* 81, 1356-1373.

583 Leterrier, J., Maury, R.C., Thoron, P., Girard, D., Marchal, M., 1982. Clinopyroxene
584 composition as a method of identification of the magmatic affinities of paleo-volcanic series.
585 *Earth and Planetary Science Letters* 59, 139-154.

586 Linnen, R.L., Cuney, M., 2005. Granite-related rare-element deposits and experimental
587 constraints on Ta-Nb-W-Sn-Zr-Hf mineralization. In: Linnen, R.L., Samson, I.M. (Eds.)
588 Rare-element geochemistry and mineral deposits: Geological Association of Canada Short
589 Course Notes, v. 17, p. 45-68.

590 Lynch, G., Tremblay, C., 1994. Late Devonian-Carboniferous detachment faulting and
591 extensional tectonics in western Cape Breton Island, Nova Scotia, Canada. *Tectonophysics*
592 238, 55-69.

593 McCutcheon, S.R., 1990. The Late Devonian Mount Pleasant Caldera complex stratigraphy,
594 mineralogy, geochemistry and geological setting of a Sn-W deposit in southwestern New
595 Brunswick. Unpublished Ph.D. thesis, Dalhousie University, Halifax, Nova Scotia, 609 p.

596 McCutcheon, S.R., Anderson, H.E., Robinson, P.T., 1997. Stratigraphy and eruptive history of
597 the Late Devonian Mount Pleasant Caldera Complex, Canadian Appalachians. *Geological*
598 *Magazine* 134, 17-36.

599 McCutcheon, S.R., Sinclair, W.D., McLeod, M.J., Boyd, T., Kooiman, G.J.A., 2010. Mount
600 Pleasant Sn-W-Mo-Bi-In deposit. In: Fyffe, L.R., Thorne, K.G. (Eds.) *Polymetallic Deposits*
601 *of Sisson Brook and Mount Pleasant, New Brunswick, Canada*. New Brunswick Department
602 of Natural Resources; Lands, Minerals and Petroleum Division, Field Guide No. 3, p. 37-68.

603 McGregor, D.C., McCutcheon, S.R. 1988. Implications of spore evidence for Late Devonian
604 age of the Piskahegan Group, southwestern New Brunswick. *Canadian Journal of Earth*
605 *Sciences* 25, 1349-1364.

606 McLeod, M.J., 1990. *Geology, Geochemistry, and Related Mineral Deposits of the Saint George*
607 *Batholith; Charlotte, Queens, and Kings Counties, New Brunswick*. New Brunswick
608 Department of Natural Resources and Energy, Mineral Resources, Mineral Resource Report
609 5, 169 p.

610 McLeod, M. J., Smith, E.A., 2010. Uranium. New Brunswick Department of Natural Resources;
611 Lands, Minerals and Petroleum Division, Mineral Commodity Profile No. 6, 7 p.

612 Moore, G.M., Carmichael, I.S.E., 1998. The hydrous phase equilibria (to 3 kbar) of an andesite
613 and basaltic andesite from western Mexico: constraints on water content and conditions of
614 phenocryst growth. *Contributions to Mineralogy and Petrology* 130, 304-319.

615 Murphy, J.B., Dostal, J., Keppie, J.D., 2008. Neoproterozoic–Early Devonian magmatism

616 in the Antigonish Highlands, Avalon terrane, Nova Scotia: tracking the evolution of the
617 mantle and crustal sources during the evolution of the Rheic Ocean. *Tectonophysics*
618 461, 181-201.

619 Murphy, J.B., Waldron, J.W.F, Kontak, D.J., Pe-Piper, G.P., Piper, D. J.W., 2011a. Minas fault
620 zone; late Paleozoic history of an intra-continental orogenic transform fault in the Canadian
621 Appalachians. *Journal of Structural Geology* 33, 312-328.

622 Murphy, J.B., Dostal, J., Gutierrez-Alonso, G., Keppie, J.D., 2011b. Early Jurassic magmatism
623 on the northern margin of CAMP: derivation from a Proterozoic sub-continental lithospheric
624 mantle. *Lithos* 123, 158-164.

625 Nekvasil, H., Simon, A., Lindsley, D. H., 2000. Crystal fractionation and the evolution of intra-
626 plate hy-normative igneous suites: insights from their feldspars. *Journal of Petrology* 41,
627 1743-1757.

628 Osborn, E. F., 1959. Role of oxygen pressure in the crystallization and differentiation of basaltic
629 magma. *American Journal of Science* 257, 609-647.

630 Pe-Piper, G., Piper, D.J.W., 1998. Geochemical evolution of Devonian-Carboniferous igneous
631 rocks of the Maritimes Basin, Eastern Canada: Pb-and Nd-isotope evidence for mantle and
632 lower crustal sources. *Canadian Journal of Earth Science* 35, 201-221.

633 Pearce, J.A., 2008. Geochemical fingerprinting of oceanic basalts with applications to ophiolite
634 search for Archean oceanic crust. *Lithos* 100, 14-48.

635 Peate, D.W., Hawkesworth, C.J., 1996. Lithosphere to asthenosphere transition in low-Ti
636 from southern Paraná, Brazil. *Chemical Geology* 127, 1-24.

637 Pegram, W.J., 1990. Development of continental lithospheric mantle as reflected in the
638 Appalachian tholeiites. *Earth and Planetary Science Letters* 97, 316-331.

639 Richards, B.C., 2013. Current status of the International Carboniferous Time Scale. In: Lucas, S.
640 G., et al., (Eds.) *The Carboniferous-Permian Transition*. New Mexico Museum of Natural
641 History and Science, Bulletin 60, 348-353.

642 Richards, J.P., 2011. High Sr/Y magmas and porphyry Cu ± Mo ± Au deposits: Just add water.
643 *Economic Geology* 106, 1075-1081.

644 Richardson, D.G., Birkett, T.C., 1996. Peralkaline rock-associated rare metals. In: *The Geology*
645 *of North America*, Geological Society of America, v. P-1, p. 523-540.

646 Romer, R.L., Kroner, U., 2014. Magmatic tin-tungsten deposits within the Acadian-Variscan-
647 Alleghanian orogen: from the Gondwana source to the mineralization. Gondwana 15
648 Conference, Madrid, Abstract Book, p. 151.

649 Schuiling, R. D., 1967. Tin belts on the continents around the Atlantic Ocean. *Economic*
650 *Geology* 62, 540-550. Sinclair, W.D., Kooiman, G.J.A., Martin, D.A., 1988. Geological
651 setting of granites and related tin deposits in the North Zone, Mount Pleasant, New
652 Brunswick. In: *Current Research, Part B, Geological Survey of Canada, Paper 88-1B*, pp.
653 201–208.

654 Sinclair, W.D., Kooiman, G.J.A., Martin, D.A., Kjarsgaard, I.M., 2006. Geology, geochemistry
655 and mineralogy of indium resources at Mount Pleasant, New Brunswick, Canada. *Ore*
656 *Geology Reviews* 28, 123-145.

657 Sisson, T.W., Grove, T.L., 1993. Experimental investigations of the role of H₂O in calc-alkaline
658 differentiation and subduction zone magmatism. *Contributions to Mineralogy and Petrology*
659 113, 143–166.

660 Smith, E., 2006. Bedrock geology of southwestern New Brunswick (NTS 21 g, part of 21 B).
661 New Brunswick Department of Natural Resources, Minerals, Policy and Planning Division,
662 Plate NR-5 2nd edition, scale 1:250 000.

663 Smith, E., Fyffe, L.R., 2006. Bedrock geology of central New Brunswick (NTS 21J). New
664 Brunswick Department of Natural Resources, Minerals, Policy, and Planning Division, Plate
665 NR-4 2nd edition, scale 1: 250 000.

666 Strong, D.F., 1980. Granitoid rocks and associated mineral deposits of eastern Canada and
667 western Europe. In: D.W. Strangway, D. W. (Ed.) *The Continental Crust and its Mineral*
668 *Deposits. Geological Association of Canada Special Paper* 20, 742-769.

669 Sun, S. S., McDonough, W. F., 1989. Chemical and isotopic systematics of oceanic basalts:
670 implications for mantle composition and processes. In: Saunders, A.D., Norry, M.J. (Eds.)
671 *Magmatism in the Ocean Basins: Geological Society London Special Publication* 42, 313-
672 345.

673 Taylor, R.P., 1992. Petrological and geochemical characteristics of the Pleasant Ridge
674 zinwaldite-topaz granite, southern New Brunswick, and comparison with other topaz-
675 bearing felsic rocks. *Canadian Mineralogist* 30, 895-921.

676 Taylor, S.R., McLennan, S.M., 1985. The continental crust: Its composition and evolution: An
677 examination of the geochemical record preserved in sedimentary rocks. Blackwell Scientific,
678 Oxford, United Kingdom, 312 p.

679 Thorne, K. G., Fyffe, L.R. Creaser, R.A., 2013. Re-Os geochronological constraints on the
680 mineralizing events within the Mount Pleasant Caldera: implications for the timing of
681 subvolcanic magmatism. *Atlantic Geology* 49, 131-150.

682 Tucker, R.D., Bradley, D.C., Ver Straeten, C.A., Harris, A.G., Ebert, J.R., McCutcheon,
683 S.R., 1998. New U-Pb zircon ages and the duration and division of Devonian time: Earth
684 and Planetary Science Letters 158, 175-186.

685 van de Poll, H. W., 1967. Carboniferous volcanic and sedimentary rocks of the Mount Pleasant
686 area, New Brunswick. New Brunswick Department of Natural Resources and Energy,
687 Mineral Resources Branch, Report of Investigations 3. 52 pp.

688 van Staal, C.R., Barr, S.M., 2012. Lithospheric architecture and tectonic evolution of the
689 Canadian Appalachians and associated Atlantic margin. Chapter 2. In: Percival, J.A.,
690 Cook, F.A., Clowes, R.M. (Eds.), *Tectonic Styles in Canada: the LITHOPROBE*
691 *Perspective*. Geological Association of Canada, Special Paper 49, pp. 41–95.

692 Wang, K., Plank, T., Walker, J.D., Smith, E.I., 2002. A mantle melting profile across the Basin
693 and Range. SW USA. *Journal of Geophysical Research* 107(B1): ECV 5-1–ECV 5-21.

694 Whalen J.B., Fyffe, L.R., Longstaffe, F.J., Jenner, G.A., 1996. The position and nature of the
695 Gander-Avalon boundary, southern New Brunswick, based on geochemical and isotopic
696 data from granitoid rocks. *Canadian Journal of Earth Sciences* 33, 129-139.

697 Winchester, J.A., Floyd, P.A., 1977. Geochemical discrimination of different magma series and
698 their differentiation products using immobile elements. *Chemical Geology* 20, 325-343.

699 Wood, D. A., 1980. The application of a Th-Hf-Ta diagram to problems of tectomagmatic
700 classification and to establishing the nature of crustal contamination of basaltic lavas of the
701 British Tertiary Volcanic Province. *Earth and Planetary Science Letters* 50, 11-30,

702 Zimmer, M.M., Plank, T., Hauri, E.H., Yogodzinski, G.M., Stealing, P., Larsen, J., Singer, B.,
703 Jicha, B., Mandeville, C., Nye, C., 2010. The role of water in generating the calc-alkaline
704 trend: new volatile data for Aleutian magmas and a new tholeiitic index. *Journal of*
705 *Petrology* 51, 2411-2444.

706

707 **Captions to Figures**

708 Figure 1. A - Map of a part of Atlantic Canada that shows the western boundary of the Maritimes
709 Basin and the location of the Harvey and Piskahegan groups (black fields). B - Simplified
710 geological map of the southwestern part of the Marysville sub-basin and its surroundings
711 (modified from Smith, 2006, and Smith and Fyffe, 2006) showing the location of Figure 2.
712 The insert (map of Canada) shows the location of Figure 1A.

713 Figure 2. Geology of the Mount Pleasant Caldera Complex and its surroundings (modified from
714 McCutcheon et al. 2010, and Thorne et al., 2013). Late Devonian caldera complex includes
715 Late caldera-fill sequence, Subvolcanic intrusive rocks, Intracaldera and Exocaldera
716 sequences while the Piskahegan Group encompasses Late caldera-fill, Intracaldera and
717 Exocaldera sequences.

718 Figure 3. (Ti + Cr) versus Ca (number of cations per six oxygens) discrimination diagram of
719 Leterrier et al. (1982) comparing the composition of clinopyroxenes from the intermediate
720 rocks of the Piskahegan Group with compositional fields for clinopyroxenes from
721 nonorogenic and orogenic rocks. Each value (Table 1) is an average composition of a
722 number of analyzed crystals, and composition of each crystal is an average of 4 analyses
723 (Table 1).

724 Figure 4. Variations of $\text{FeO}_{(\text{tot})}$, TiO_2 (wt.%) and various element ratios versus SiO_2 (wt.%) in the
725 basaltic and andesitic rocks of the Piskahegan Group. Association 1 - basalt: Carrow
726 Formation (CF), Kleef Formation (KF); Association 2 - andesite: South Oromocto Andesite
727 Formation (SOA); Scoullar Mountain Formation (SMF). In A and B, the vectors show calc-
728 alkaline and tholeiitic trends whereas E and F show vectors for crustal contamination (cc)
729 and fractional crystallization (fc).

730 Figure 5. Zr/TiO_2 versus Nb/Y discrimination diagram of Winchester and Floyd (1977) for mafic
731 and intermediate rocks of the Piskahegan Group. Alk-Bas - alkali basalt; TrachAnd -
732 trachyandesite. Association 1 - basalt: Carrow Formation (CF), Kleef Formation (KF);
733 Association 2 - andesite: South Oromocto Andesite (SOA); Scoullar Mountain Formation
734 (SMF).

735 Figure 6. AFM diagram ($A = \text{Na}_2\text{O} + \text{K}_2\text{O}$, $F = \text{total Fe as FeO}$, $M = \text{MgO}$) for analyzed

736 mafic and intermediate volcanic rocks from the Piskahegan Group. The solid line is the
737 boundary between tholeiitic and calc-alkaline fields after Irvine and Baragar (1971);
738 Association 1 (basalts): Carrow Formation (CF), Kleef Formation (KF); Association 2
739 (andesites): South Oromocto Andesites (SOA), Scoullar Mountain Formation (SMF).

740 Figure 7. Chondrite-normalized REE patterns for basaltic and andesitic rocks of the Piskahegan
741 Group. A- Range of basalts from the Carrow Formation; B - Range of basalts from the Kleef
742 Formation; C - Range of andesites from the South Oromocto Andesite Formation; D - range
743 of andesites from the Scoullar Mountain Formation. Normalizing values are after Sun and
744 McDonough (1989).

745 Figure 8. Primitive mantle-normalized multielement patterns in basaltic and andesitic rocks of
746 the Piskahegan Group. A - Basalts of the Carrow Formation; B - basalts of the Kleef
747 Formation; C- andesites of the South Oromocto Andesite Formation; D- andesites of the
748 Scoullar Mountain Formation. Normalizing values are after Sun and McDonough (1989).

749 Figure 9. Th-Hf-Ta tectonic discrimination diagram of Wood (1980) for mafic and intermediate
750 volcanic rocks of the Piskahegan Group. Fields: N-MORB - normal, depleted mid-ocean
751 ridge basalt; E-MORB/WPT - enriched mid-ocean ridge basalt and within-plate tholeiite;
752 Alk WPB - alkaline within-plate basalt; CAB - calc-alkaline volcanic arc basalts; ATB -
753 volcanic arc tholeiites; CC (star) - average continental crust composition of Taylor and
754 McLennan (1985). Note that the trend of the Piskahegan rocks is suggestive of a mixing
755 between basaltic magma and crustal material.

756 Figure 10. $\epsilon_{Nd(t)}$ versus time plot comparing Sm-Nd isotopic data of the Piskahegan basalts and
757 andesites and the Carboniferous Cumberland Hill trachytes with a compilation of Sm-Nd
758 isotopic data for the Upper Devonian-Lower Carboniferous volcanic rocks of the Maritimes
759 Basin and the Avalon Terrane (Keppie et al., 1997, Pe-Piper and Piper, 1998). The shaded
760 area is the Avalonian basement and the SCLM (after Murphy et al., 2011b, Dostal et al.,
761 2016a). The field for Mesoproterozoic rocks is from Murphy et al. (2008). Bars show a
762 range of samples.

763 Figure 11. Th/Yb versus Nb/Yb diagram of Pearce (2008) for Piskahegan basalts and andesites.
764 Vectors indicate the influence of a subduction component (S), within-plate enrichment (W),
765 crustal contamination (C), and fractional crystallization (FC); N-MORB- N-type mid-ocean

766 ridge basalt; E-MORB- enriched mid-ocean ridge basalt; OIB-ocean island basalt (after Sun
767 and McDonough, 1989). The star (CC) is the average of continental crust (Taylor and
768 McLennan, 1985).

769 Figure 12. $(Tb/Yb)_n$ versus $(La/Sm)_n$ diagram for the Piskahegan basalts and andesites. The
770 values are normalized to the primitive mantle after Sun and McDonough (1989). The solid
771 line separating the range of magmas formed by the melting of spinel peridotite mantle from
772 that of magmas formed by the melting of garnet peridotite mantle is after Wang et al. (2002).
773 Vector D indicates an increase of melting depth whereas the vector M depicts an increase in
774 the degree of partial melting. The limited range of $(Tb/Yb)_n$ values for the basalts indicates a
775 similar mantle source. The higher $(La/Sm)_n$ ratios of the calc-alkaline rocks is more
776 suggestive of crustal contamination than of changes in the magma source region. The E-
777 MORB (enriched mid-ocean ridge basalt) and OIB (ocean island basalt) are after Sun and
778 McDonough (1989).

779 Figure 13. $(Nb/Th)_n$ versus $(Th/Yb)_n$ diagram for the Piskahegan basalts and andesites. The ratios
780 are normalized to the primitive mantle values of Sun and McDonough (1989). N-MORB and
781 E-MORB compositions are from Sun and McDonough (1989). CC (star) - average
782 continental crust (Taylor and McLennan, 1985). Note that the very distinct trend (the solid
783 curve is a mixing curve) of the Piskahegan rocks is suggestive of a mixing between parental
784 basaltic magmas and crustal material, indicating that the andesitic magma assimilated
785 significant amounts of crustal material prior to its emplacement.

786 Figure 14. Th/La versus $\epsilon_{Nd(T)}$ plot for the Piskahegan basalts and andesites. An increase of the
787 Th/La ratio accompanied by a decrease of $\epsilon_{Nd(T)}$ is indicative of a crustal contamination of
788 the basaltic magmas. CC (star) - average continental crust composition (Taylor and
789 McLennan, 1985). The solid triangles are data from Anderson (1992) for the Piskahegan
790 basaltic and andesitic rocks.

791
792
793
794
795

796 **Tables**

797 Table 1. Chemical composition and structural formulas of clinopyroxene in andesites of the
798 Piskahegan Group

799 Table 2. Major and trace element compositions in the mafic and intermediate rocks of the
800 Piskahegan Group

801 Table 3. Sm-Nd isotopic data for volcanic rocks of the Piskahegan Group and Cumberland Hill
802 Formation

803

804 Appendix 1. Composition of clinopyroxenes from andesites of the Piskahegan Group

805 Appendix 2. Major and trace element compositions of andesitic rocks of the Piskahegan Group

806

1 | Upper Paleozoic mafic and intermediate volcanic rocks associated with the Sn-W deposit of
2 | the Mount Pleasant caldera ~~associated with the Sn-W deposit~~ in southwestern New
3 | Brunswick (Canada): Petrogenesis and metallogenic implications
4 |
5 |
6 |
7 |
8 |
9 |
10 |

11 | Jaroslav Dostal^{1a} and Pierre Jutras¹
12 |
13 |

14 | 1. Department of Geology, Saint Mary's University, Halifax, Nova Scotia B3H, Canada

15 | a. Corresponding author: e-mail: jdostal@smu.ca; phone: 902-420-5747
16 |
17 |
18 |
19 |
20 |

21 Abstract

22 Upper Paleozoic (~365 Ma) mafic and intermediate volcanic rocks of the Piskahegan Group
23 constitute a subordinate part of the Mount Pleasant caldera, which is ~~associated with~~related to a
24 significant polymetallic deposit (~~tin, tungsten, molybdenum, bismuth zones ~ 33 Mt ore with~~
25 0.21% W, 0.1% Mo and 0.08% Bi and tin-indium zones ~ 4.8 Mt with 0.82% Sn and 129 g/t In,
26 zinc, indium and bismuth) in southwestern New Brunswick (Canada). The epicontinental caldera
27 complex formed during the opening of the late Paleozoic Maritimes Basin ~~of in~~ the ~~Northern~~
28 northern Appalachians. The mafic and intermediate rocks make up two compositionally distinct
29 associations. The first association includes evolved rift-related continental tholeiitic basalts, and
30 the second association ~~comprises~~encompasses calc-alkaline andesites, although both associations
31 were emplaced penecontemporaneously. The basalts have low Mg# ~ 0.34-0.40, ~~smooth~~linear
32 chondrite-normalized REE patterns with $(La/Yb)_n \sim 5-6$, primitive mantle-normalized trace
33 element patterns without noticeable negative Nb-Ta anomalies, and their $\epsilon_{Nd(T)}$ ranges ~~s~~
34 to +2.2. The basalts were generated by partial melting of a transition zone between spinel and
35 garnet mantle peridotite at a depth of (~~~70-90 km depth~~). The calc-alkaline andesites of the
36 second association have chondrite-normalized REE patterns that are more fractionated, with
37 $(La/Yb)_n \sim 7-8.5$, but without significant negative Eu anomalies. Compared to the basaltic rocks,
38 they have lower $\epsilon_{Nd(T)}$ values, ranging from +0.5 to +1.9, and their mantle-normalized trace
39 element plots show negative Nb-Ta anomalies. The $\epsilon_{Nd(T)}$ values display negative correlations
40 with indicators of crustal contamination, such as Th/La, Th/Nb, and SiO₂. The andesitic rocks are
41 interpreted to have formed by assimilation-fractional crystallization processes, which resulted in
42 the contamination of a precursor basaltic magma with crustal material. The parent basaltic
43 magma for both suites underwent a different evolution. The tholeiitic basalts experienced
44 shallow-seated fractional crystallization and evolved along a tholeiitic trend of “early iron”
45 enrichment (non-oxic conditions). The contaminated magma of the second association followed
46 a calc-alkaline fractionation trend of “no iron” enrichment (oxidizing conditions) characterized
47 by a high P_{H2O} and P_{O2} environment at the mid-crust levels. The Piskahegan Group, which is
48 ~~with~~to an important polymetallic mineral deposit~~ization~~, differs from the
49 numerous non-mineralized rift-related volcanic suites of the regional Upper Devonian to Lower
50 Carboniferous successions ~~of in~~ the Maritimes Basin by the presence of a significant amount of

51 coeval calc-alkaline andesite, which may be an indicator of potential mineralization. ~~These~~
52 ~~rocks may be indicators of a mineralization~~ fertile environment. The subcontinental lithospheric
53 ~~mantle of the Avalon and Gander terranes of the Northern Appalachians in Atlantic Canada had~~
54 ~~an isotopically similar composition during the Late Devonian and Early Carboniferous.~~

55

56

57

58 1. Introduction

59 Felsic rocks of continental rift-related magmatic ~~settings~~ regimes have been the focus of
60 extensive investigation and numerous publications in part because they may host rare metal
61 mineralizations, which in some cases ~~is~~ are of economic significance (e.g., [Richardson and](#)
62 [Birkett, 1996](#); Cerny et al. 2005; Linnen and Cuney, 2005; ~~Richardson and Birkett, 1996~~). These
63 ~~rocks granites and rhyolites~~ are commonly associated with a compositionally diverse variety of
64 mafic and intermediate rocks (e.g., Nekvasil et al., 2000). Much is still unknown about the
65 processes that lead to the diversity of magmas within such ~~bimodal series~~ bimodal suites ~~or and~~
66 ~~about~~ the global diversity of intraplate ~~magmatic suites~~ suite types. In mineralized bimodal
67 complexes where felsic rocks are dominant, the ~~subordinate~~ mafic and intermediate rocks are
68 commonly only poorly known, although they might provide important information on the
69 tectonic environment of ~~such bimodal complex~~ the bimodal associations, as well as on the origin
70 of the felsic rocks and their mineralization, thus providing clues for the exploration for rare metal
71 deposits. One ~~of~~ such ~~bimodal suites~~ suite is the upper Paleozoic Piskahegan Group ~~in~~ of
72 southwestern New Brunswick (Canada). The latter group forms a volcanic caldera complex (e.g.,
73 McCutcheon, 1990; McCutcheon et al., 1997; Thorne et al., 2013) that is spatially and
74 genetically associated with the Mount Pleasant polymetallic deposit (~~tin, tungsten, molybdenum,~~
75 ~~bismuth zones containing ~ 33 Mt ore with 0.21% W, 0.1% Mo and 0.08% Bi and tin-indium~~
76 ~~zones ~ 4.8 Mt with 0.82% Sn and 129 g/t In), molybdenum, zinc, indium, and bismuth). The~~
77 deposit is recognized as the world's largest known undeveloped resource of indium (Sinclair et
78 al., 2006; Thorne et al., 2013). To contribute to the debate on the origin of these bimodal suites,
79 we have investigated mafic and intermediate volcanic rocks of the Mount Pleasant caldera (Figs.

80 | 1 and 2). ~~Whole rock major~~ Major and trace elements in these rocks, as well as neodymium
81 | ~~isotopic isotopes ratios of these rocks~~, may provide information related not only to the origin of
82 | the bimodal suite and its mineralization, but also on the nature of the mantle source (e.g.,
83 | DePaolo, 1988). Such data are also useful to evaluate the composition of the subcontinental
84 | lithospheric mantle (SCLM).

85 | The purpose of this paper is: (1) to present geochemical data on the mafic and
86 | intermediate volcanic rocks of the Mount Pleasant caldera, including major and trace elements
87 | and Nd isotopic ratios, (2) to constrain the origin of the rocks in the caldera, (3) to investigate the
88 | differences between mineralized and barren Devonian to Carboniferous bimodal volcanic suites
89 | in this part of the Northern Appalachians, (4) to evaluate the nature of the SCLM, and (5) to
90 | compare this information with data from time equivalent basaltic rocks of New Brunswick and
91 | Nova Scotia, which belong to the peri-Gondwanan Gander and Avalon terranes of the North
92 | American Appalachians ~~of eastern North America~~. The comparison of SCLM properties in two
93 | neighboring exotic terranes could reveal whether or not both terranes were underlain by the same
94 | SCLM during the Paleozoic and thus contribute to the Ganderian controversy (i.e. whether or not
95 | ~~the~~ Gander and Avalon zones represent distinct terranes; e.g., van Staal and Barr, 2012; ~~van Staal~~
96 | ~~et al., 2009~~; Dostal et al., 2016a5).

98 | 2. Geological setting

99 | Volcanic rocks of the Piskahegan Group occur along the western margin of the Maritimes
100 | Basin in southwestern New Brunswick (Fig. 1). The Maritimes Basin ~~of the Northern~~
101 | ~~Appalachians~~ is a major Late-late Paleozoic successor basin (Gibling et al., 2008) that was
102 | initiated after the Early to Middle Devonian Acadian Orogeny (~400 Ma) in the Canadian
103 | Appalachians. ~~The This~~ composite ~~Maritimes Basin basin~~ first developed as a series of pull-apart
104 | sub-basins along the Minas Fault Zone, a large east-~~west~~ trending dextral strike-slip system that
105 | juxtaposed the Meguma and Avalon terranes during the Late Devonian and the Carboniferous
106 | (Murphy et al., 2011a**b**). Associated with these pull-apart structures are large felsic, intermediate
107 | and mafic plutons bimodal plutons, as well as is a series of NW-~~SE~~ trending mafic dykes, ~~as well~~
108 | ~~as large felsic, intermediate, and mafic plutons~~. Closely spaced U-Pb dates for peak Acadian
109 | metamorphism and for the emplacement and exhumation of post-Acadian plutons along the

110 Minas Fault Zone suggest that the transition from orogenic compression to transtension along
111 this fault system was very rapid (Dostal et al., 2006). Also associated with this transtensional
112 magmatic event are widely distributed bimodal volcanic suites, one of which is the Piskahegan
113 Group. ~~This group forms a volcanic caldera complex that is spatially, temporarily, and~~
114 ~~genetically and its~~ associated ~~with the Mount Pleasant~~ polymetallic deposit (Kooiman et al.,
115 1986; McCutcheon et al., 1997; Thorne et al., 2013). The complex, ~~referred to as~~ the
116 Mount Pleasant caldera, is a northeast-trending elliptical feature that is defined by geophysical
117 data (regional gravimetric and magnetic studies) as about 13 km wide and 34 km long (McLeod
118 and Smith, 2010). ~~However,~~ the northern part of the complex is overlain by middle
119 Mississippian (Visean) and Pennsylvanian strata of the Maritimes Basin in such a way that the
120 exposed length is restrained to about 17 km. This epicontinental caldera, which was emplaced in
121 a trans-tensional setting (Fyffe et al., 2011), is associated with high-level subvolcanic granitic
122 intrusions and has been interpreted to have formed by roof collapse in an epizonal magma
123 chamber. The Piskahegan Group (Figs. 1 and 2) disconformably overlies ~~poly~~deformed
124 Ordovician to Silurian turbiditic metasedimentary rocks of the Gander Terrane. These rocks
125 bound the caldera to the east and west. The caldera is in turn paraconformably overlain by
126 Visean (~~mid-Mississippian~~) clastic rocks formerly mapped as the Shin Redbeds by van de Poll
127 (1967), ~~which were and~~ recently assigned the Shin Member of the Hopewell Cape Formation
128 (Jutras et al., 2015), ~~and~~ which confine the caldera to the north (Fig. 1). Late Silurian to
129 Devonian granitic rocks of the Saint George Batholith represents the southern boundary of the
130 complex (McLeod, 1990). Both the batholith and the caldera complex lie within the boundaries
131 of the Gander Terrane.

132 The Piskahegan Group (Fig. 2) has been subdivided into three volcanic facies (in the
133 sense of Fisher and Schmincke, 1984) in order to reflect their depositional setting in relation to
134 the volcanic architecture: (1) exocaldera, (2) intracaldera and (3) late caldera-fill sequences
135 (McCutcheon, 1990; McCutcheon et al., 1997; Thorne et al., 2013). ~~The caldera is composed~~
136 mainly of felsic volcanic ~~ands,~~ volcanoclastic rocks and associated sedimentary rocks, ~~which are~~
137 ~~and it is~~ intruded by subvolcanic granitic bodies (McCutcheon et al., 1997). All three volcanic
138 facies contain subordinate amounts of mafic and intermediate volcanic rocks (Fig. 2).

139 | The Piskahegan Group was emplaced during the initial stages of basin development. ~~The~~
140 | ~~p~~Paleontological records, ~~as well as and~~ radiometric dating, show that most of the caldera is
141 | Fammenian (Upper Devonian) in age and coincides with the emplacement of voluminous
142 | granitic intrusions. Anderson (1992) obtained a whole-rock Rb-Sr isochron age of 368 ± 5 Ma for
143 | the Piskahegan Group. The Carrow Formation (CF) of the exocaldera sequence yielded a U-Pb
144 | zircon age of 363.8 ± 2.2 Ma (Tucker et al., 1998), whereas a spore assemblage recovered from
145 | drill core above the zircon sample yielded a late Famennian age (McGregor and McCutcheon,
146 | 1988). More recently, Thorne et al. (2013) reported Re-Os ages of 369.7 ± 1.6 Ma and $370.1 \pm$
147 | 1.7 Ma from molybdenite samples associated with W-Mo-Bi mineralization. There are also
148 | several $^{40}\text{Ar}/^{39}\text{Ar}$ ages of ca. 360 Ma on the granitic rocks (Sinclair et al., 1988), and ~~the~~
149 | youngest phase of the neighbouring Saint George Batholith, which is probably related to them,
150 | gave a U-Pb zircon age of 367 ± 1 Ma (Bevier 1988). Hence, all available data in the Piskahegan
151 | Group and associated plutonic rocks range within the Fammenian (*sensu* Richards, 2013).

152 | The exocaldera sequence includes three units that also contain mafic or intermediate
153 | volcanic rocks. In ascending stratigraphic order, they are the Hoyt Station Basalt (HSB), the
154 | South Oromocto Andesite (SOA) and the Carrow Formation (CF). ~~HSB~~The Hoyt Station Basalt
155 | is the basal unit of the exocaldera sequence (McCutcheon et al., 1997) and it consists mainly of a
156 | basalt flow unit that is about 20 m thick. The basalt is underlain by rhyolitic volcanoclastic rocks.
157 | The SOA unit is an up to 130 m thick succession of lava flows that is conformably overlain by
158 | the CF. The latter is composed mainly of clastic sediments, but also contains an aphyric basalt
159 | flow (< 20 m thick) near the top of the formation.

160 | At the base, the intracaldera sequence includes the Scoullar Mountain Formation (SMF),
161 | which lies along the periphery of the caldera complex at the contact with pre-caldera rocks. This
162 | unit, the thickness of which ranges between 225 and 450 m, is composed predominantly of
163 | clastic sedimentary rocks and interbedded andesitic lava flows and felsic volcanoclastic rocks.
164 | The upper part of the late caldera-fill sequence contains the Kleef Formation (KF), which
165 | consists of conglomeratic redbeds (40-75 m thick), basalts (70-80 m), and volcanoclastic rocks (>
166 | 4 m).

167 | The polymetallic deposit ~~is~~ located near the southwestern margin of the caldera
168 | complex (McCutcheon et al., 1997). ~~It~~ consists of mineralized stockworks and quartz veinlets,

169 breccia infill and lode mineralization, ~~and its, its~~ formation is associated with the emplacement
170 of the subvolcanic granitic rocks that host it. Thorne et al. (2013) inferred that the mineralization
171 was associated with caldera collapse, which was marked by the emplacement of a series of
172 subvolcanic [granitic intrusions \(Fig. 2 McDougall Brook and Mount Pleasant granitic suites; e.g.,](#)
173 [Yang et al., 2003](#)).
174

175

176

176 3. Analytical methods

177 Mineral compositions (Table 1; [Appendix 1](#)) were determined using a JEOL Superprobe
178 733 equipped with four wave-length-dispersive spectrometers and one energy-dispersive
179 spectrometer, and operated with a beam current of 15 kV at 5 nA at the Department of Earth
180 Sciences of Dalhousie University, Halifax, Nova Scotia (Canada).

181 Major and several trace element analyses of whole rocks (Table 2; [Appendix 2+\)](#) were
182 performed on fused glass disks using a Philips PW2400 X-ray fluorescence spectrometer at the
183 University of Ottawa, Ontario (Canada). Duplicate analyses of the samples yielded total errors of
184 $\pm 3\%$ (1σ). ~~Trace element analysis was done using lithium metaborate-tetraborate fusion and a~~
185 Perkin Elmer Optima 3000 ICP mass spectrometer at Activation Laboratories, Ancaster, Ontario
186 (Canada). Replicate analyses of the reference standard rocks indicate that the errors were
187 between 2 and 8 % of the values cited. The detection limits and other information on the trace
188 element analyses ([analytical package 4B2](#)) are available at the Activation Laboratories web site
189 ([www.actlabs.com](#)).

190 Nd isotope ratios (Table 3) were determined by isotope dilution mass spectrometry at the
191 Department of Earth Sciences of the Memorial University of Newfoundland (St. John's,
192 Newfoundland, Canada). Concentration data are standard ICP-MS analyses and are precise to
193 $\pm 5\%$ (2σ). Ratios of $^{147}\text{Sm}/^{144}\text{Nd}$ (except samples 38A and 69) were measured directly by high-
194 precision ICP-MS with an estimated precision of $\pm 0.5\%$ (2σ). The isotopic ratios of $^{143}\text{Nd}/^{144}\text{Nd}$
195 were determined using a multicollector Finnigan MAT 262V thermal ionization mass
196 spectrometer operated in a static mode. Measured $^{143}\text{Nd}/^{144}\text{Nd}$ values were normalized to a
197 $^{146}\text{Nd}/^{144}\text{Nd}$ ratio of 0.7219. Replicate analyses of the LaJolla standard, which was analyzed

198 repeatedly throughout, gave an average value for $^{143}\text{Nd}/^{144}\text{Nd}=0.511849 \pm 9$. The 2σ values for
199 all samples are less than or equal to 0.000008 for $^{143}\text{Nd}/^{144}\text{Nd}$ and are given in Table 3. Values
200 for $\epsilon_{\text{Nd}}(T)$ were calculated with respect to CHUR using present-day $^{143}\text{Nd}/^{144}\text{Nd}$ and $^{147}\text{Sm}/^{144}\text{Nd}$
201 ratios of respectively 0.512638 and 0.196593, and subsequently age-corrected. A T_{DM1} model
202 age was calculated using a linear evolution for a mantle that separated from CHUR at 4.55 Ga,
203 and that has having a present day ϵ value of +10. The T_{DM2} model age was calculated according
204 to the model of DePaolo (1988).

205
206

Formatted: Indent: First line: 0 cm

207 4. Petrography and mineral chemistry

208 Basalts and andesites ~~The mafic and intermediate rocks~~ of the Piskahegan Group include
209 ~~basalts and andesites. The rocks~~ vary from massive to amygdaloidal. Amygdales occur
210 particularly in the upper part of the flows and are commonly filled by carbonates or silica.
211 Although rocks of the caldera are not significantly deformed and contain unstrained quartz with
212 primary glass inclusions (Gray et al., 2011), the amygdaloidal ~~Amygdaloidal~~ rocks are
213 extensively altered, ~~although the rocks of the caldera are not significantly deformed, and felsic~~
214 ~~rocks contain unstrained quartz with primary glass inclusions (Gray et al., 2011).~~ Igneous
215 textures are mostly preserved, but the primary magmatic minerals are frequently replaced by
216 secondary phases. The rocks exhibit greenschist grade metamorphism that produced chlorite,
217 epidote and actinolite. Textures range from aphyric to coarse subophitic and ophitic, as well as
218 porphyritic and glomeroporphyritic. The basalts are composed predominantly of plagioclase and
219 clinopyroxene, which are variably altered and occur both as phenocrysts and as the main
220 components of the groundmass. The rocks also contain minor Fe-Ti oxides and accessory apatite.
221 No orthopyroxene was observed. When fresh, the plagioclase phenocrysts show zoning with
222 labradorite-bytownite cores and andesine rims. However, plagioclase is mostly albitized or
223 altered to sericite and calcite. Some plagioclase phenocrysts contain zones of sieve texture. The
224 intermediate rocks contain relics of dark brownish-green amphibole replaced mainly by chlorite
225 and epidote. In these rocks, subhedral amphibole crystallized together with plagioclase, Fe-Ti
226 oxide, and apatite after the crystallization of clinopyroxene (Anderson, 1992). Amphibole may
227 contain a core of clinopyroxene. The clinopyroxene phenocrysts show zoning, but are partially

228 replaced by chlorite and epidote. Clinopyroxene_s typically form_s subhedral phenocrysts and
229 microphenocrysts or occur_s in a subophitic to ophitic groundmass of the mafic rocks. ~~The r~~Relics
230 of fresh clinopyroxene in the mafic and intermediate rocks are typically augite (Anderson,
231 1992; Table 1; [Appendix 1](#)). On tectonic discrimination diagrams for pyroxene (Leterrier et al.,
232 1982), ~~the~~clinopyroxene_s of the basalts plot_s into the “non-orogenic” field (Anderson, 1992;
233 McCutcheon et al., 1997). ~~We have analyzed e~~Clinopyroxenes from the intermediate ~~rock units~~
234 (Table 1), ~~which~~ also plot into the “non-orogenic” field (Fig. 3) of Leterrier et al. (1982). The
235 rarity of phenocrysts in some samples of evolved rocks may be caused by the separation of early
236 fractionated phases from the melt on the way to the surface.

237
238

239 **5. Whole-rock geochemistry**

240 *5.1. -Alteration*

241 Alteration and metamorphic processes have affected the rocks. Petrographic evidence
242 includes the saussuritization, sericitization, and albitization of feldspar, the chloritization of
243 clinopyroxene as well as the accumulation of silica and calcite in amygdales. Although the
244 original abundances of mobile elements such as Ca, Na, and K might have been modified, the
245 concentrations and ratios of high-field strength elements (HFSE) and rare earth elements (REE)
246 show well-defined trends indicating that these elements were immobile during alteration. This is
247 also supported by many other studies (e.g., Winchester and Floyd, 1977) indicating that HFSE
248 and REE retain their distribution during alteration. Furthermore, an investigation of melt
249 inclusions in quartz of associated rhyolitic rocks (Gray et al., 2011) show~~eds~~ that post-magmatic
250 processes did not modify the whole-rock composition. Similarly, ~~it is typically inferred that the~~
251 ~~Sm and Nd isotope characteristics of a rock for the Nd isotopic ratios, the Sm-Nd isotopic pair is~~
252 ~~are~~ resistant to geological disturbances (e.g., DePaolo, 1988) ~~and it is typically inferred that the~~
253 ~~Nd isotope characteristics of rocks were not modified.~~

254

255 *5.2. -Major and trace elements*

256 All the major oxide compositions were recalculated to 100% on a volatile free basis for
257 plotting on geochemical diagrams. According to their major element compositions (Fig. 4), the

258 mafic and intermediate volcanic rocks of the Piskahegan Group can be subdivided into two
259 associations: Association 1 includes basalts of the KF and CF formations, which are
260 characterized by low SiO₂ ~~~50 wt.%~~ (48-52 wt.%), and high TiO₂ (> 2.5 wt.%) and FeO_(t) (~ 13-
261 15 wt.%), whereas Association 2 comprises intermediate rocks of the SOA and ~~SMF~~, with SiO₂
262 > 54 wt.%, TiO₂ < 2 wt.%, and FeO_(t) < 9 wt.%. The division is also shown in ~~a the~~ Zr/TiO₂
263 versus Nb/Y ~~diagram~~ graph (Fig. 5), in which Association 1 rocks plot ~~into~~ the basaltic field,
264 whereas rocks of Association 2 plot mainly ~~into~~ the andesitic field.

265 According to the conventional AFM [(K₂O+Na₂O)-FeO_(t)-MgO] diagram (Fig. 6),
266 Association 1 rocks are tholeiites. They have characteristics of differentiated tholeiitic basalts
267 with low MgO, Ni, and Cr, as well as high Fe, Ti, and P. ~~Compared to primitive basalts that~~
268 ~~have Mg# (MgO/[MgO+FeO_(t)]) values of ~0.70 (Hanson and Langmuir, 1978), the Piskahegan~~
269 ~~basalts (Table 2) have significantly lower values (0.34-0.40), suggesting that they have~~
270 ~~undergone high degrees of fractional crystallization.~~ Their chondrite-normalized REE patterns
271 show a negative slope, resulting from an enrichment of light REE (LREE) with (La/Yb)_n ~5-6,
272 but without Eu anomalies (Fig. 7). ~~The primitive mantle-normalized incompatible element plots~~
273 ~~of Association 1 rocks do not display noticeable show distinct significant~~ negative Nb-Ta
274 anomalies (Fig. 8). The patterns show distinct negative anomalies for Ti and Sr, which together
275 with low Ni and Cr indicate that the rocks underwent fractional crystallization dominated by ~~that~~
276 ~~of~~ plagioclase and clinopyroxene. Both patterns (Figs. 7 and 8) resemble those of rift-related
277 continental tholeiites or transitional basalts (e.g., Dostal and Dupuy, 1984; Pegram, 1990; Dostal
278 et al., 1992; Peate and Hawkesworth, 1996). In comparison with arc mafic rocks, the basalts have
279 high Ti/V (70-100) and Zr/Y (6-8), and their primitive mantle-normalized trace element patterns
280 do not exhibit ~~pronounced distinct significant~~ negative Nb-Ta anomalies (Fig. 8). In addition, on
281 geochemical discrimination diagrams, they ~~also~~ plot ~~into~~ the field of rift-related basalts (Fig. 9).

282 Compared to those of Association 1, rocks of Association 2 have calc-alkaline
283 characteristics (e.g., Fig. 6), although they were emplaced penecontemporaneously and in the
284 same tectonic and geographic settings. ~~With increasing SiO₂, the andesites show a decrease in~~
285 ~~Fe, Ti, Mg# (MgO/[MgO+FeO_(t)]), and Ni, but also an increase of in alkalis and of in the~~
286 ~~Al₂O₃/CaO and La/Yb ratios (Fig. 4), indicating the crystallization of clinopyroxene, plagioclase~~
287 ~~and Fe-Ti oxide. The fractionation of Fe-Ti oxides, which is implied by a decrease of FeO_(t),~~

288 | TiO₂ and V with increasing SiO₂ in the calc-alkaline suite, suggests high P_{H2O} and P_{O2}
289 | conditions. The difference between tholeiitic and calc-alkaline suites can be partially due to the
290 | depth of fractional crystallization (e.g., Grove and Kinzler, 1986). Crystallization of the calc-
291 | alkaline magmas at mid-crustal depth may have differed from that of tholeiitic magma, which
292 | could have taken place at lower P_{tot} and lower P_{O2} conditions (i.e., within a shallow upper crustal
293 | magma chamber).

294 | There are subtle differences between the SOA and SMF rocks. The SOA have SiO₂ ~55-
295 | 58 wt.%, TiO₂ < 2 wt.% and FeO_(t) ~ 8 wt.%. The SMF rocks are more fractionated, although
296 | there is some overlap in composition. They have typically higher SiO₂ (59-66 wt.%), lower
297 | TiO₂ < 1.5 wt.% and lower FeO_(t) < 8 wt.% (Table 2).

298 | In addition to the differences in major element compositions between associations 1 and
299 | 2, the andesites have more fractionated REE patterns, with (La/Yb)_n ~ 7-8.5, but also without
300 | significant Eu anomalies. Their light REE (LREE) abundances are similar to those of the first
301 | association, but they have lower heavy REE (HREE) contents. The primitive mantle-
302 | normalized incompatible element plots of Association 2 show distinct negative Nb-Ta
303 | anomalies, which are indicative of either a subduction or crustal assimilation imprint. The
304 | absence of significant negative Eu anomalies in most of the andesitic rocks (Fig. 7) suggests that
305 | fractionation of plagioclase was not significant in these magmas (Eu²⁺ can substitute for Ca²⁺ in
306 | plagioclase). This could be because the magmatic water content was high (Moore and
307 | Carmichael, 1998) and/or because the magmatic oxidation state was high, in which case most of
308 | the Eu would have been present as Eu³⁺ and would not have been incorporated into crystallizing
309 | plagioclase (e.g., Sisson and Grove, 1993).

310 |

311 | 5.-3. -Nd isotopic ratios

312 | The Sm-Nd isotopic signatures of the basaltic and andesitic rocks are given in Table 3, in
313 | which they are all age-corrected to 365 Ma. The ε_{Nd(T)} values of the basalts range from +2.5 to
314 | + 2.2, and ¹⁴⁷Sm/¹⁴⁴Nd ratios vary from 0.13 to 0.14 (Table 3). The values are in show a good
315 | agreement with the data of Anderson (1992) for mafic rocks of the caldera. The data plot within
316 | the range reported for the Devonian to Carboniferous basaltic rocks of the Maritimes Basin in
317 | New Brunswick and Nova Scotia (Fig. 10). They are also similar to those from rift-related

318 basalts, continental flood basalts and xenoliths from the subcontinental lithosphere (Faure and
319 Mensing, 2005). These $\epsilon_{Nd(T)}$ values are considerably lower than values expected for juvenile
320 magmas from a depleted mantle source (Fig. 10), although the positive $\epsilon_{Nd(T)}$ values
321 ~~preclude~~ a significant contribution from substantially older continental crust or
322 sedimentary rocks derived from it. The Piskahegan basaltic rocks plot into the field of Avalonian
323 and peri-Rodanian lithosphere (Fig. 10), and their $\epsilon_{Nd(T)}$ values are consistent with derivation
324 from a SCLM.

325 ~~Based on DePaolo (1988), depleted-mantle-Næodymium depleted-mantle model ages of~~
326 ~~DePaolo (1988) for these rocks range between 800 and 900 Ma (Table 3) and are similar to those~~
327 ~~determined for the Devonian to Carboniferous basaltic rocks above the Avalon and Gander~~
328 ~~terranes in the Maritimes Basin (Keppie et al., 1997; Pe-Piper and Piper, 1998).~~
329 ~~The similarities of the model ages for the Devonian to Carboniferous basaltic rocks above the~~
330 ~~Avalon and Gander terranes in the Maritimes Basin (Keppie et al., 1997; Pe Piper and Piper,~~
331 ~~1998).~~ ~~These similarities~~ suggest that the model ages represent a bulk weighted average of the
332 source composition.

333 The andesites have lower $\epsilon_{Nd(T)}$ (~~Table 3~~) than the basalts (~~Table 3~~), but they still plot in
334 the field of Avalonian and Ganderian lithosphere (Fig. 10).- The negative Nb-Ta anomalies ~~along~~
335 ~~with and~~ the lower $\epsilon_{Nd(T)}$ values (+0.5 to +1.9) of these rocks are consistent with an ~~inferred~~
336 involvement of continental lithosphere in their evolution, most probably through crustal
337 contamination.

338

339 6. Discussion

340 6. 1. Petrogenesis

341 Although all volcanic rocks of the Piskahegan Group are spatially and temporarily
342 associated, the ~~Association 1~~ basaltic rocks are not related to the Association 2 andesitic rocks
343 through simple crystal-liquid equilibria processes. The absence of smooth variation trends when
344 various elements and element ratios are plotted against a differentiation index, such as SiO_2 (Fig.
345 4), suggests that the Association 2 andesites did not simply result from the fractional
346 crystallization of Association 1 basalts.

Formatted: Indent: First line: 0 cm

347 The Association 1 rocks are evolved tholeiites that were emplaced in an epicontinental
348 rift-related setting. Compared to primitive basalts that have Mg# values of ~ 0.70 (Hanson and
349 Langmuir, 1978), the Piskahegan basalts (Table 2) have significantly lower values (0.34-0.40),
350 suggesting that they have undergone high degrees of fractional crystallization. ~~The y~~ underwent
351 ~~extensive~~ fractional crystallization was dominated by crystallization ~~that~~ of clinopyroxene and
352 plagioclase. On the Th/Yb versus Nb/Yb diagram (Fig. 11), which has been used for the
353 evaluation of lithospheric inputs in basalts (Pearce, 2008), the averages of N-type MORB, E-type
354 MORB, and OIB form a diagonal mantle array (Fig. 11). Magmas that were modified by an
355 interaction with continental crust or that involved material with a subduction history are
356 displaced to higher Th/Yb values. The basaltic rocks of the Piskahegan Group straddle the
357 boundary of the mantle array, implying that crustal contamination and subduction imprints were
358 insignificant. This is also consistent with the lack of a discernible negative Nb-Ta anomaly on
359 the spider plots (Fig. 8). Thus, the composition of the basalts mostly reflects the original
360 characteristics of the mantle source, and together with positive $\epsilon_{Nd(T)}$ values, indicate that they
361 were derived from a relatively uncontaminated and moderately enriched mantle, similar to an
362 ocean island basalt (OIB)-type source (Faure and Mensing, 2005).

363 On the Tb/Yb versus La/Sm graph (Fig. 12), the basaltic samples straddle the spinel
364 peridotite-garnet peridotite boundary, suggesting that they were formed in a spinel-garnet
365 transition zone, at a depth of ~70-90 km (Wang et al., 2002). Whereas ~~the~~ Tb/Yb ratios is-are
366 related to the pressure conditions and depth at which melting occurred, ~~the~~ La/Sm ratios
367 correlates with the degree of partial melting, and ~~it~~ tends to decrease with an increase of mantle
368 peridotite melting. Ratios for the CF and KF basalts are overlapping, which indicates that they
369 were generated at the same depth by similar degrees of partial melting from a similar mantle
370 source.

371 The andesites of the Piskahegan Group underwent fractional crystallization dominated by
372 ~~that of~~ plagioclase, clinopyroxene and Fe-Ti oxide, as indicated by the variation trends of
373 several elements and element ratios when plotted against SiO₂ (Fig. 4). The compositional
374 characteristics of the Association 2 rocks, including negative Nb-Ta anomalies and their position
375 on the Th/Yb versus Nb/Yb diagram (Fig. 11), suggest that the rocks record an additional
376 process in addition to fractional crystallization, ~~the rocks record an additional process~~. The SOA

377 and SMF andesites are displaced toward higher Th/Yb ratios relative to the mantle array,
378 implying crustal contamination or inputs from a subcontinental mantle that had previously been
379 affected by subduction fluids.

380 Correlation of element and isotopic ratios suggests that the andesites were significantly
381 changed by crustal contamination [as discussed below](#). Trace element ratios, which are not
382 modified by [the](#) fractional crystallization of major rock forming minerals, and which have
383 significantly different values for oceanic basalts (OIB, MORB) and continental crust (e.g.,
384 Th/La, Th/Nb, Th/Ta, Nb/U), are typically used as indicators for crustal contamination ([e.g.,](#)
385 [Jochum et al., 1991; D'Antonio et al., 2007](#)). The SOA andesites have higher Th/La (~0.15-
386 0.16), Th/Nb (0.3-0.45) and Th/Ta (5-7) ratios than the basalts (Th/La~0.08-0.1; Th/Nb ~0.11-
387 0.19; and Th/Ta~1-3), indicating crustal input. The same applies ~~to~~ for the SMF andesites,
388 which have even higher Th/La (~0.20-0.25), Th/Nb (>0.5) and Th/Ta (8-11) ratios. These ratios,
389 which are sensitive indicators of crustal contamination, correlate with SiO₂ (Fig. 4) and are
390 consistent with an origin of the intermediate rocks by the crustal contamination of basalts
391 accompanied by fractional crystallization. Such a process is also supported by mixing trends on
392 the Nb/Th versus Th/Yb diagram (Fig. 13), in which the andesitic rocks plot along the mixing
393 line between typical mantle-derived tholeiites and crustal material. A similar trend is also
394 shown on Figure 9. Due to the absence of geochemical analyses from the underlying
395 basement/continental crust, we have used ~~in these graphs~~ the average continental crust
396 composition of Taylor and McLennan (1985) as a reference contaminant [for these graphs](#).
397 Likewise, the plots involving Nd isotopes and contamination-sensitive trace element ratios or
398 SiO₂ suggest a mixing between the basaltic melts derived from the SCLM and crustal material.
399 The rocks show a general trend of lower $\epsilon_{Nd(T)}$ with higher Th on the $\epsilon_{Nd(T)}$ versus Th/La graph
400 (Fig. 14), ~~confirming the involvement~~ of continental crust in the rocks with lower $\epsilon_{Nd(T)}$.

401 The highly fractionated nature of the basalts as well as the observed gap between basalts
402 and intermediate rocks indicate that the original magmas of each association had to undergo a
403 separate evolution, although they ~~may have probably~~ had [a](#) comparable parent magma. The
404 Association 1 basalts underwent fractional crystallization during their rise to the surface, whereas
405 the Association 2 andesites were modified by crustal contamination through assimilation-
406 fractional crystallization (AFC) processes, probably at mid-crust levels. [As the andesitic rocks](#)

407 contain hornblende indicative of mid-crust crystallization and show a calc-alkaline fractionation
408 trend that is typical of high $P_{(tot)}$ and P_{H_2O} conditions, the contamination had to take place at a
409 deeper crustal level (e.g., Osborn, 1959; Zimmer et al., 2010). In addition to amphibole, the calc-
410 alkaline rocks also contain clinopyroxene phenocrysts, which, like those of the basalts, are
411 typical of within plate, “non-orogenic” rocks (Fig. 3). -The wet and/or oxidizing environment is
412 also consistent with the lack of distinct negative Eu anomalies in most of the andesitic rocks
413 (Fig. 7) which could be because the magmatic water content was high (Moore and Carmichael,
414 1998) and/or because the magmatic oxidation state was high, in which case most of the Eu would
415 have been present as Eu^{3+} and would not have been incorporated into the crystallizing
416 plagioclase (e.g., Sisson and Grove, 1993).

417 Crustal contamination lead to a change from a non-oxic environment, typical of tholeiitic
418 rocks, to the oxidizing environment that is of typical of calc-alkaline rocks (e.g., Osborn, 1959;
419 Zimmer et al., 2010). In the case of the tholeiitic basalts, the original magma fractionated along a
420 tholeiitic trend of “early iron” enrichment (non-oxic conditions). -The magma which mixed with
421 continental crust material followed a calc-alkaline fractionation trend of “no iron” enrichment
422 (oxidizing conditions).

424 6.2 Crustal contamination in a ~~Contaminant and~~ metallogenic province

425 In the near vicinity of the Mount Pleasant caldera, there are several small Late Devonian
426 plutons composed of Li-F-rich granites (e.g., Taylor, 1992; Whalen et al., 1996). These plutons
427 as well as the Mount Pleasant complex are a part of a large tin belt described by ~~the tin belt of~~
428 Schuiling (1967) and Strong (1980), among others, which extends ~~from one continent to another,~~
429 from North America to Europe. This belt, characterised by the occurrences of the mineralized
430 Devono-Carboniferous Li-F- rich peraluminous leucogranites with broadly contemporaneous S-
431 W-(U) mineralization, can be followed along the ~~L~~ate Paleozoic fold belts ~~in~~of the Canadians
432 Appalachians and ~~the Hercynian Orogen~~ of western and central Europe, from ~~-New Brunswick~~
433 (Mount Pleasant complex) to Nova Scotia (~~East Kemptville,~~ South Mountain ~~b~~Batholith at East
434 Kemptville), ~~New Brunswick (Mount Pleasant complex)~~ and Newfoundland (Ackley ~~p~~Pluton),
435 and across the Atlantic Ocean ~~-to~~ southwestern England (Cornwall), France (Armorican Massif
436 and ~~French~~ Massif Central), ~~-Germany~~ (Altenberg, Erzgebirge) and the Czech Republic

Formatted: Font: Italic

Formatted: Font: Italic

Formatted: Indent: First line: 1.27 cm

437 ~~(Zinnwald) Armorican Massif to (Czech Republic and Germany).~~ The belt has a long mining
438 ~~history of mining of Sn, W and U (mined already by dating back to the Romans).~~ Numerous
439 ~~studies (e.g., Dostal and Chatterjee, 1995; Haapala, 1997; Cuney et al., 2002; Dostal et al., 2004;~~
440 ~~Cerny et al., 2005) inferred that the magmatic and hydrothermal mineralizing events were~~
441 ~~essentially synchronous and that the uncommon chemical characteristics of the Li-F-rich~~
442 ~~leucogranites require an uncommon a distinct source material. It has been inferred that the~~
443 ~~parental magmas of the leucogranites, including those around the Mount Pleasant caldera, were~~
444 ~~derived from similar but uncommon source reservoirs (Romer and Kroner, 2014), probably~~
445 ~~phlogopite/biotite-rich mid-crustal metasedimentary rocks (e.g., Dostal et al., 2004). Similar~~
446 ~~fluid-rich rocks could have acted as been a crustal contaminant.~~

447
448
449 ~~In the near vicinity of the Mount Pleasant caldera, there are several small Late Devonian plutons~~
450 ~~composed of Li F rich granites (e.g., Taylor, 1992; Whalen et al., 1996). These plutons were~~
451 ~~probably derived from phlogopite/biotite bearing mid-crustal metasediments. Similar fluid rich~~
452 ~~rocks could have been a crustal contaminant.~~

454 6. ~~32.~~ *Comparable rock suites and possible mantle sources*

455 Comparable Upper Devonian to Lower Carboniferous bimodal volcanic suites occur
456 within the Maritimes Basin in Nova Scotia (western Cape Breton Island, Antigonish Highlands,
457 ~~and~~ Cobequid Highlands) ~~and~~ southern New Brunswick ~~and Magdalen Islands~~ (e.g., Dostal et
458 al., 1983; ~~Barr et al., 1985; Fyffe and Barr, 1986;~~ Keppie and Dostal, 1980; Keppie et al., 1997;
459 ~~LaFlèche et al., 1998;~~ Pe-Piper and Piper, 1998). The basaltic rocks are rift-related, mainly
460 fractionated continental tholeiites. ~~In these basaltic rocks, $\epsilon_{Nd(T)}$ values are variable, ranging~~
461 ~~from +2.2 to +5.2 (Keppie et al., 1997; Pe-Piper and Piper, 1998). The basalts are considered to~~
462 ~~be derived from the SCLM (Pe-Piper and Piper, 1998).~~

463 To evaluate lithospheric mantle sources in the area, as well as the changes that they
464 underwent during the Carboniferous, we have also determined the Nd isotopic ratios of the
465 Carboniferous trachytes (~335 Ma old) from the Cumberland Hill Formation (Gander Terrane)
466 of southern New Brunswick ~~as these rocks are younger (by about 30 M.y.) than the bulk of the~~

Formatted: Indent: First line: 1.27 cm

467 | [Devono-Carboniferous magmatism](#). These rocks were interpreted to be derived from an alkali
468 basaltic magma by extensive fractional crystallization without being affected by crustal
469 contamination (Gray et al., 2010). Such an origin is also in an agreement with their primitive
470 mantle-normalized plots, in which the rocks do not show any negative Nb-Ta anomalies (Gray et
471 al., 2010). These rocks have higher $\epsilon_{Nd(T)}$ values (+4.3 to + 3.3) than the basaltic rocks of the
472 Piskahegan Group, but have younger model ages (~0.6 Ga; Table 3).

473 Model ages, variation ranges of $\epsilon_{Nd(T)}$, and chemical compositions of the basaltic rocks of
474 the Piskahegan Group, which are similar to those recorded in penecontemporaneous mafic lavas
475 | in [both](#) Avalonia and Ganderia, can be accounted for by derivation from a subcontinental
476 lithospheric mantle that was locally modified by the upward invasion of enriched (OIB)
477 asthenospheric magma (e.g., Pe-Piper and Piper, 1998). The basaltic magmas extruded due to
478 | rapid lithospheric thinning and an associated steepening of the geothermal gradient (e.g., Lynch
479 and Tremblay, 1994; Pe-Piper and Piper, 1998). There does not appear to be a systematic
480 difference between the Avalon and Gander terranes in the isotopic composition of the SCLM
481 during the Late Devonian and the Early Carboniferous, and composition of the SCLM could
482 | therefore have been similar beneath [both terranes Avalonia and Ganderia](#) in this part of the
483 Appalachians.

484

485 | 6. ~~43~~. *[Possible link between mineralization and the development of a subordinate calc-alkaline](#)*
486 *[suite Relationship between mineralization and the mafic and intermediate rocks](#)*

487 The Upper Devonian to Lower Carboniferous rift-related volcanic suites that onlap the
488 Avalon and Gander terranes along the margin of the Maritimes Basin are [mostly](#) bimodal
489 continental tholeiite - rhyolite associations. ~~–~~ The Piskahegan Group, which is associated with a
490 significant polymetallic mineralization, differs from the rest of them by the presence of a
491 significant amount of coeval calc-alkaline intermediate rocks. ~~–~~ This calc-alkaline suite is
492 interpreted to be the result of AFC processes involving the crustal contamination of [a](#) basaltic
493 magma [precursor](#), and of a change from non-oxic to oxidizing conditions accompanied by a
494 relatively high content of magmatic water. ~~–~~ [As the andesitic rocks contain hornblende indicative](#)
495 [of mid-crust crystallization and show a calc-alkaline fractionation trend that is typical of high](#)
496 [P_{\(tot\)} and P_{H2O} conditions, the contamination had to take place at a deeper crustal level \(e.g.,](#)

497 ~~Osborn, 1959; Zimmer et al., 2010). In addition to amphibole, the calc-alkaline rocks also~~
498 ~~contain clinopyroxene phenocrysts, which, like those of the basalts, are typical of within plate~~
499 ~~("non-orogenic") rocks (Fig. 3).~~

500 The basalts also display an iron enrichment trend that is typical of low P shallow-seated
501 fractionation that occurs in a non-oxic environment (Osborn, 1959; Zimmer et al., 2010). The
502 calc-alkaline suite had a relatively high magmatic water content and/or high oxidation state,
503 which are considered to be an indication of fertility for many polymetallic ore-bearing felsic and
504 intermediate units (Candela, 1992; Richards, 2011). As rhyolites of the Piskahegan Group are
505 also related to the andesitic rocks (Anderson, 1992; McCutcheon et al., 1997; [Dostal et al.,](#)
506 [2016b](#)), it can be suggested that the evolution of ~~these these felsic~~ rocks differed from those of
507 other Upper Devonian to Lower Carboniferous bimodal volcanic suites, ~~although the isotopic~~
508 ~~composition of the underlying SCLM was similar~~. The presence of a significant amount of ~~the~~
509 calc-alkaline volcanic rocks in such [bimodal](#) suites could be an indicator of ~~fertility~~[potential](#)
510 [mineralization](#).

511

512 7. Conclusions

513 Mafic and intermediate rocks of the Piskahegan Group constitute two distinct
514 associations that are spatially and temporarily related within a Late Paleozoic caldera complex
515 ~~that, which~~ hosts a significant polymetallic deposit of tin, tungsten, molybdenum, ~~zinc~~, indium
516 and bismuth. The first association includes basalts of the ~~Kleef and Carrow KF and CF~~
517 formations, whereas the second association encompasses andesites of the ~~South Oromocto~~
518 ~~Andesite and Scoullar Mountain formations SOA and SMF~~. The basalts of the first association
519 are fractionated, rift-related continental tholeiites with high contents of Fe, Ti, P_2 and V, but low
520 Mg, Mg#, Ni and Cr. They display tholeiitic fractionation trends of Fe and Ti enrichment that are
521 characteristic of dry and non-oxic environments. They underwent the main pulse of fractional
522 crystallization at a relatively shallow depth, although the parent magma was generated in the
523 transition zone between spinel and garnet peridotite at a depth of ~70-90 km. The mantle-
524 normalized patterns of the basalts do not show distinct negative Nb-Ta anomalies, and their
525 geochemical characteristics mainly reflect a mantle source without noticeable signs of significant
526 crustal contamination. Rocks of the second association display a typical calc-alkaline

527 fractionation trend that is characterized by a gradual depletion of Fe and Ti with increasing
528 differentiation, which is indicative of a wet and oxidizing environment. This is also consistent
529 with the absence of a negative Eu anomaly in the REE patterns of these rocks, and with the
530 presence of hornblende in their modal composition. The rocks resulted from the mixing of
531 continental crust material (probably [phlogopite/biotite-rich water-bearing metasedimentary](#)
532 [rockss](#)) with primitive basaltic melt, probably at mid-crust level. Although the parent basaltic
533 magmas of both suites could have been derived from the same SCLM source, they underwent
534 separate and different evolution pathways. The Piskahegan Group, which is associated with the
535 Mount Pleasant polymetallic deposit, differs from ~~other~~ penecontemporaneous, non-mineralized
536 bimodal suites that occur along the margins of the Maritimes Basin through New Brunswick and
537 Nova Scotia by the presence of a significant amount of coeval calc-alkaline intermediate rocks.
538 ~~As such rocks evolve in water- and oxygen-rich magmatic environments, their~~ ~~Their~~ presence
539 may be considered to be an indicator of [potential mineralization fertility](#). ~~The isotopic~~
540 ~~composition of the SCLM beneath the Avalon and Gander terranes of the Northern Appalachians~~
541 ~~in Atlantic Canada did not show significant differences during the Late Devonian and the Early~~
542 ~~Carboniferous.~~

544 **Acknowledgements**

545 This study was supported by the New Brunswick Department of Energy and Mines,
546 Geological Surveys Branch and the Natural Sciences and Engineering Research Council of
547 Canada (Discovery grant to J.D.). We thank Malcom McLeod for the initiation of this project
548 and Randy Corney for technical assistance. [Constructive reviews by Drs. John Greenough,](#)
549 [Nelson Eby and two anonymous referees improved the manuscript.](#)

550

551

552 **References**

553 Anderson, H.E. 1992. A chemical and isotopic study of the age, petrogenesis and magmatic
554 evolution of the Mount Pleasant caldera complex, New Brunswick. Unpublished Ph.D.
555 thesis, Carleton University, Ottawa, Ontario. 203 p.

556 ~~Barr, S.M., Brisebois, D., MacDonald, A.S., 1985. Carboniferous volcanic rocks of the~~
557 ~~Magdalen Islands, Gulf of St. Lawrence. Canadian Journal of Earth Sciences 22, 1679-1688.~~
558 Bevier, M.L., 1988. U-Pb geochronologic studies of igneous rocks in N.B. In: Abbott, S.A. (Ed.)
559 Thirteenth Annual Review of Activities, Project Résumés. New Brunswick Department of
560 Natural Resources and Energy, Minerals and Energy Division, Information Circular 88-2,
561 pp. 134-140.
562 Candela, P.A., 1992. Controls on ore metal ratios in granite-related ore systems: An experimental
563 and computational approach. Transactions of the Royal Society of Edinburgh, Earth
564 Sciences 83, 317-326.
565 Cerny, P., Blevin, P.L., Cuney M., London, D., 2005. Granite-related ore deposits. Economic
566 Geology 100, 337-370.
567 [Cuney, M., Alexandrov, P., LeCarlier de Veslud, C., Cheilletz, A., Raimbault, L., Ruffet, G.,](#)
568 [Scaillet S., 2002. The timing of W-Sn-rare metals mineral deposit formation in the Western](#)
569 [Variscan chain in their orogenic setting: the case of the Limousin area \(Massif Central,](#)
570 [France\). Geological Society of London Special Publication 204, 213-228.](#)
571 [D'Antonio, M., Tonarini, S., Arienzo, I., Covetta, L., Di Renzo, V., 2007. Components and](#)
572 [processes in the magma genesis of the Phlegrean Volcanic District, southern Italy.](#)
573 [Geological Society of America Special Papers 418, 203-220.](#)
574
575 DePaolo, D.J., 1988. Neodymium Isotope Geochemistry: An Introduction. Springer Verlag, New
576 York, 187 p.
577 Dostal, J., Dupuy, C., 1984. Geochemistry of the North Mountain basalts, Nova Scotia,
578 Canada. Chemical Geology 45, 245-261.
579
580 [Dostal, J., Chatterjee, A.K. 1995. Origin of topaz-bearing and related peraluminous granites of](#) ← **Formatted: Indent: Hanging: 0.75**
581 [late Devonian Davis Lake pluton, Nova Scotia, Canada. Chemical Geology 123, 67-88.](#)
582 [Dostal, J., Chatterjee, A.K., Kontak, D.J. 2004. Chemical and isotopic \(Pb, Sr\) zonation in a](#)
583 [peraluminous granite pluton: role of fluid fractionation. Contributions to Mineralogy and](#)
584 [Petrology 147,74-90.](#) ← **Formatted: Indent: Hanging: 0.75**
585
586

587 Dostal, J., Dupuy, C., Nicollet, C., Cantagrel, J.M., 1992. Geochemistry and petrogenesis of
588 southern Malagasy. *Chemical Geology* 97, 199-218.

589 Dostal, J., Keppie, J. D., Dupuy, C., 1983. Petrology and geochemistry of Devonian-Carboniferous
590 volcanic rocks in Nova Scotia. *Maritime Sediments and Atlantic Geology* 19, 59-71.

591 Dostal, J., Keppie, J.D., Jutras, P., Miller, B.V., Murphy, J.B., 2006. Evidence of the granulite-
592 granite connection: Penecontemporaneous high-grade metamorphism, granitic magmatism
593 and core complex development in the Liscomb Complex, Nova Scotia, Canada. *Lithos* 86,
594 77-90.

595 Dostal, J., Keppie, J.D., Wilson, R. A., 2016a. Nd isotopic and trace element constraints on the
596 source of Silurian–Devonian mafic lavas in the Chaleur Bay Synclinorium of New
597 Brunswick (Canada): Tectonic implications. *Tectonophysics* 681, 364-375.
598 <http://dx.doi.org/10.1016/j.tecto.2015.10.002>

599 [Dostal, J., van Hengstum, T.R., Shellnutt, J.G., Hanley, J.J. 2016b. Petrogenetic evolution of
600 Late Paleozoic rhyolites of the Harvey Group, southwestern New Brunswick \(Canada\)
601 hosting uranium mineralization. *Contributions to Mineralogy and Petrology* 171: DOI
602 10.1007/s00410-016-1270-8.](#)

603 Faure, G., Mensing, T. M., 2005. *Isotopes: Principles and Applications*. John Wiley and Sons,
604 Hoboken, New Jersey, 3rd edition, 897 p.

605 Fisher, R.V., Schmincke, H.U., 1984. *Pyroclastic rocks*. Springer-Verlag, New York, 472 pp.

606 Fyffe, L.R., Johnson, S.C., van Staal, C.R., 2011. A review of Proterozoic to Early Paleozoic
607 lithotectonic terranes in the northeastern Appalachian orogen of New Brunswick, Canada,
608 and their tectonic evolution during Penobscot, Taconic, Salinic, and Acadian orogenesis.
609 *Atlantic Geology* 47, 211-248.

610 Gibling, M.R., Culshaw, N., Rygel, M.C., Pascucci, V., 2008. The Maritimes Basin of Atlantic
611 Canada: Basin Creation and Destruction in the Collisional Zone of Pangea. In: Miall, A.D.
612 (Ed.) *Sedimentary Basins of the World*, Vol. 5, pp. 211-244. Elsevier, Amsterdam.

613 Gray, T.R., Dostal, J., McLeod, M., Keppie, J.D., Zhang, Y.Y., 2010. Geochemistry of Late
614 Paleozoic peralkaline felsic volcanic rocks, central New Brunswick. *Atlantic Geology* 46,
615 173-184.

- 616 Gray, T.R., Hanley, J.J., Dostal, J., Guillong, M., 2011. Magmatic enrichment of uranium,
617 thorium and rare earth elements in late Paleozoic rhyolites of southern New Brunswick,
618 Canada: evidence from silicate melt inclusions. *Economic Geology* 106, 127-143.
- 619 Grove, T.L., Kinzler, R.J., 1986. Petrogenesis of andesites. *Annual Review of Earth and*
620 *Planetary Sciences* 14, 417-454.
- 621 [Haapala, I., 1997. Magmatic and postmagmatic processes in tin mineralized granites: topaz-](#)
622 [bearing leucogranite in the Eurajoki Rapakivi granite stock, Finland. *Journal of Petrology*](#)
623 [38, 1645-1659.](#)
- 624
- 625 Hanson, G.N., Langmuir, C.H., 1978. Modelling of major elements in mantle-melt systems using
626 trace element approaches. *Geochimica et Cosmochimica Acta* 42, 725 -742.
- 627 Irvine, T. N.,-Baragar, W. R. A., 1971. A guide to the chemical classification of the common
628 volcanic rocks. *Canadian Journal of Earth Sciences* 8, 523-548.
- 629 [Jochum, K.P., Arndt, N.T., Hofmann, A.W., 1991.- Nb-Th-La in komatiites and basalts:](#)
630 [constraints on komatiite petrogenesis and mantle evolution. *Earth and Planetary Science*](#)
631 [Letters 107, 272-291.](#)
- 632
- 633 Jutras, P., McLeod, J., MacRae, R.A., Utting, J., 2015. Complex, interplay of faulting,
634 glacioeustatic variations and halokinesis during deposition of upper Viséan units over thick
635 salt in the western Cumberland Basin of Atlantic Canada. *Basin Research* 2015, 1-24.
- 636 Keppie, J. D., Dostal, J., 1980. Palaeozoic volcanic rocks of Nova Scotia. *International*
637 *Geological Correlation Programme Project 27: Caledonide Orogen. Proceedings of Virginia*
638 *Polytechnic Institute and State University Memoir* 2, 249-256.
- 639 Keppie, J. D., Dostal, J., Murphy, J. B., Cousens, B. L., 1997.-Palaeozoic within-plate
640 volcanic rocks in Nova Scotia (Canada) reinterpretation: isotopic constraints on magmatic
641 source and palaeocontinental reconstructions.-*Geological Magazine* 134, 425-447.
- 642 Keppie, J.D., Murphy, J.B., Nance, R.D., Dostal, J., 2012. Mesoproterozoic Oaxaquia-type
643 basement in peri-Gondwanan terranes of Mexico, the Appalachians and Europe: TDM age
644 constraints on extent and significance. *International Geology Review* 54, 313-324.

Formatted: Indent: Hanging: 0.75
cm, Space After: 0 pt

645 Kooiman, G.J.A., McLeod, M.J., Sinclair, W.D., 1986. Porphyry tungsten-molybdenum ore
646 bodies, polymetallic veins and replacement bodies, and tin-bearing greisen zones in the Fire
647 Tower Zone, Mount Pleasant, New Brunswick. *Economic Geology* 81, 1356-1373.

648 ~~LaFlèche, M.R., Camire, G., Jenner, G.A., 1998. Geochemistry of post Acadian, Carboniferous~~
649 ~~continental intraplate basalts from the Maritimes Basin, Magdalen Islands, Quebec, Canada.~~
650 ~~*Chemical Geology* 148, 115-136.~~

651 Leterrier, J., Maury, R.C., Thoron, P., Girard, D., Marchal, M., 1982. Clinopyroxene
652 composition as a method of identification of the magmatic affinities of paleo-volcanic series.
653 *Earth and Planetary Science Letters* 59, 139-154.

654 Linnen, R.L., Cuney, M., 2005. Granite-related rare-element deposits and experimental
655 constraints on Ta-Nb-W-Sn-Zr-Hf mineralization. In: Linnen, R.L., Samson, I.M. (Eds.)
656 Rare-element geochemistry and mineral deposits: Geological Association of Canada Short
657 Course Notes, v. 17, p. 45-68.

658 Lynch, G., Tremblay, C., 1994. Late Devonian-Carboniferous detachment faulting and
659 extensional tectonics in western Cape Breton Island, Nova Scotia, Canada. *Tectonophysics*
660 238, 55-69.

661 McCutcheon, S.R., 1990. The Late Devonian Mount Pleasant Caldera complex stratigraphy,
662 mineralogy, geochemistry and geological setting of a Sn-W deposit in southwestern New
663 Brunswick. Unpublished Ph.D. thesis, Dalhousie University, Halifax, Nova Scotia, 609 p.

664 McCutcheon, S.R., Anderson, H.E., Robinson, P.T., 1997. Stratigraphy and eruptive history of
665 the Late Devonian Mount Pleasant Caldera Complex, Canadian Appalachians. *Geological*
666 *Magazine* 134, 17-36.

667 McCutcheon, S.R., Sinclair, W.D., McLeod, M.J., Boyd, T., Kooiman, G.J.A., 2010. Mount
668 Pleasant Sn-W-Mo-Bi-In deposit. In: Fyffe, L.R., Thorne, K.G. (Eds.) *Polymetallic Deposits*
669 *of Sisson Brook and Mount Pleasant, New Brunswick, Canada*. New Brunswick Department
670 of Natural Resources; Lands, Minerals and Petroleum Division, Field Guide No. 3, p. 37-68.

671 McGregor, D.C., McCutcheon, S.R. 1988. Implications of spore evidence for Late Devonian
672 age of the Piskahegan Group, southwestern New Brunswick. *Canadian Journal of Earth*
673 *Sciences* 25, 1349-1364.

Formatted: Indent: Left: 0 cm, First line: 0 cm

674 McLeod, M.J., 1990. Geology, Geochemistry, and Related Mineral Deposits of the Saint George
675 Batholith; Charlotte, Queens, and Kings Counties, New Brunswick. New Brunswick
676 Department of Natural Resources and Energy, Mineral Resources, Mineral Resource Report
677 5, 169 p.

678 McLeod, M. J., Smith, E.A., 2010. Uranium. New Brunswick Department of Natural Resources;
679 Lands, Minerals and Petroleum Division, Mineral Commodity Profile No. 6, 7 p.

680 Moore, G.M., Carmichael, I.S.E., 1998. The hydrous phase equilibria (to 3 kbar) of an andesite
681 and basaltic andesite from western Mexico: constraints on water content and conditions of
682 phenocryst growth. *Contributions to Mineralogy and Petrology* 130, 304-319.

683 Murphy, J.B., Dostal, J., Keppie, J.D., 2008. Neoproterozoic–Early Devonian magmatism
684 in the Antigonish Highlands, Avalon terrane, Nova Scotia: tracking the evolution of the
685 mantle and crustal sources during the evolution of the Rheic Ocean. *Tectonophysics*
686 461, 181-201.

687 ~~Murphy, J.B., Dostal, J., Gutierrez-Alonso, G., Keppie, J.D., 2011a. Early Jurassic magmatism~~
688 ~~on the northern margin of CAMP: derivation from a Proterozoic sub-continental lithospheric~~
689 ~~mantle. *Lithos* 123, 158-164.~~

690 Murphy, J.B., Waldron, J.W.F, Kontak, D.J., Pe-Piper, G.P., ~~Piper, David~~ J.W., 2011~~ab~~. Minas
691 fault zone; late Paleozoic history of an intra-continental orogenic transform fault in the
692 Canadian Appalachians. *Journal of Structural Geology* 33, 312-328.

693 ~~Murphy, J.B., Dostal, J., Gutierrez-Alonso, G., Keppie, J.D., 2011b. Early Jurassic magmatism~~
694 ~~on the northern margin of CAMP: derivation from a Proterozoic sub-continental lithospheric~~
695 ~~mantle. *Lithos* 123, 158-164.~~

696

697 Nekvasil, H., Simon, A., Lindsley, D. H., 2000. Crystal fractionation and the evolution of intra-
698 plate hy-normative igneous suites: insights from their feldspars. *Journal of Petrology* 41,
699 1743-1757.

700 Osborn, E. F., 1959. Role of oxygen pressure in the crystallization and differentiation of basaltic
701 magma. *American Journal of Science* 257, 609-647.

702 Pe-Piper, G., Piper, D.J.W., 1998. Geochemical evolution of Devonian-Carboniferous igneous
703 rocks of the Maritimes Basin, Eastern Canada: Pb-and Nd-isotope evidence for mantle and
704 lower crustal sources. *Canadian Journal of Earth Science* 35, 201-221.

705 Pearce, J.A., 2008. Geochemical fingerprinting of oceanic basalts with applications to ophiolite
706 search for Archean oceanic crust. *Lithos* 100, 14-48.

707 Peate, D.W., Hawkesworth, C.J., 1996. Lithosphere to asthenosphere transition in low-Ti
708 from southern Paraná, Brazil. *Chemical Geology* 127, 1-24.

709 Pegram, W.J., 1990. Development of continental lithospheric mantle as reflected in the
710 [Appalachian tholeiites](#). *Earth and Planetary Science Letters* 97, 316-331.

711 Richards, B.C., 2013. Current status of the International Carboniferous Time Scale. In: Lucas, S.
712 G., et al., (Eds.) *The Carboniferous-Permian Transition*. New Mexico Museum of Natural
713 History and Science, Bulletin 60, 348-353.

714 Richards, J.P., 2011. High Sr/Y magmas and porphyry Cu ± Mo ± Au deposits: Just add water.
715 *Economic Geology* 106, 1075-1081.

716 Richardson, D.G., Birkett, T.C., 1996. Peralkaline rock-associated rare metals. In: *The Geology*
717 *of North America*, Geological Society of America, v. P-1, p. 523–540.

718 [Romer, R.L., Kroner, U., 2014. Magmatic tin-tungsten deposits within the Acadian-Variscan-](#)
719 [Alleghanian orogen: from the Gondwana source to the mineralization. Gondwana 15](#)
720 [Conference, Madrid , Abstract Book, p. 151.](#)

721 [Schuiling, R. D., 1967. Tin belts on the continents around the Atlantic Ocean. Economic](#)
722 [Geology 62, 540-550.](#)

723

724 Sinclair, W.D., Kooiman, G.J.A., Martin, D.A., 1988. Geological setting of granites and related
725 tin deposits in the North Zone, Mount Pleasant, New Brunswick. In: *Current Research, Part*
726 *B*, Geological Survey of Canada, Paper 88-1B, pp. 201–208.

727 Sinclair, W.D., Kooiman, G.J.A., Martin, D.A., Kjarsgaard, I.M., 2006. Geology, geochemistry
728 and mineralogy of indium resources at Mount Pleasant, New Brunswick, Canada. *Ore*
729 *Geology Reviews* 28, 123-145.

730 Sisson, T.W., Grove, T.L., 1993. Experimental investigations of the role of H₂O in calc-alkaline
731 differentiation and subduction zone magmatism. *Contributions to Mineralogy and Petrology*
732 113, 143–166.

733 [Smith, E., 2006. Bedrock geology of southwestern New Brunswick \(NTS 21 g. part of 21 B\).](#)
734 [New Brunswick Department of Natural Resources, Minerals, Policy and Planning Division,](#)
735 [Plate NR-5 2nd edition, scale 1:250 000.](#)

736 [Smith, E., Fyffe, L.R., 2006. Bedrock geology of central New Brunswick \(NTS 21J\). New](#)
737 [Brunswick Department of Natural Resources, Minerals, Policy, and Planning Division, Plate](#)
738 [NR-4 2nd edition, scale 1: 250 000.](#)

739 [Strong, D.F., 1980.– Granitoid rocks and associated mineral deposits of eastern Canada and](#)
740 [western Europe. In: D.W. Strangway, D. W. \(Ed.\) *The Continental Crust and its Mineral*](#)
741 [Deposits. Geological Association of Canada Special Paper 20, 742-769.](#)

742
743
744 Sun, S. S., McDonough, W. F., 1989. Chemical and isotopic systematics of oceanic basalts:
745 implications for mantle composition and processes. In: Saunders, A.D., Norry, M.J. (Eds.)
746 *Magmatism in the Ocean Basins: Geological Society London Special Publication 42*, 313-
747 345.

748 Taylor, R.P., 1992. Petrological and geochemical characteristics of the Pleasant Ridge
749 zinwaldite-topaz granite, southern New Brunswick, and comparison with other topaz-
750 bearing felsic rocks. *Canadian Mineralogist* 30, 895-921.

751 Taylor, S.R., McLennan, S.M., 1985. *The continental crust: Its composition and evolution: An*
752 *examination of the geochemical record preserved in sedimentary rocks.* Blackwell Scientific,
753 Oxford, United Kingdom, 312 p.

754 Thorne, K. G., Fyffe, L.R. Creaser, R.A., 2013. Re-Os geochronological constraints on the
755 mineralizing events within the Mount Pleasant Caldera: implications for the timing of
756 subvolcanic magmatism. *Atlantic Geology* 49, 131-150.

757 Tucker, R.D., Bradley, D.C., Ver Straeten, C.A., Harris, A.G., Ebert, J.R., McCutcheon,
758 S.R., 1998. New U-Pb zircon ages and the duration and division of Devonian time: *Earth*
759 *and Planetary Science Letters* 158, 175-186.

Formatted: Indent: Left: 0 cm,
Space After: 0 pt, Line spacing: 1.5

Formatted: Space After: 0 pt, Line
spacing: 1.5 lines

Formatted: Line spacing: 1.5 lines

Formatted: Indent: Left: 0 cm,
Hanging: 0.75 cm, Line spacing: 1.5
lines

760 ~~van Staal, C.R., Whalen, J.B., Valverde Vaquero, P., Zagorevski, A., Rogers, N., 2009. Pre-~~
761 ~~Carboniferous, episodic accretion related, orogenesis along the Laurentian margin of the~~
762 ~~Northern Appalachians. In: Murphy, J.B., Keppie, J.D., Hynes, A.J. (Eds.), Ancient~~
763 ~~Orogens and Modern Analogues. Geological Society, London, Special Publication~~
764 ~~327, 271-316.~~

765 van de Poll, H. W., 1967. Carboniferous volcanic and sedimentary rocks of the Mount Pleasant
766 area, New Brunswick. New Brunswick Department of Natural Resources and Energy,
767 Mineral Resources Branch, Report of Investigations 3. 52 pp.

768 van Staal, C.R., Barr, S.M., 2012. Lithospheric architecture and tectonic evolution of the
769 Canadian Appalachians and associated Atlantic margin. Chapter 2. In: Percival, J.A.,
770 ~~---~~ Cook, F.A., Clowes, R.M. (Eds.), Tectonic Styles in Canada: the LITHOPROBE
771 Perspective. Geological Association of Canada, Special Paper 49, pp. 41–95.

772 Wang, K., Plank, T., Walker, J.D., Smith, E.I., 2002. A mantle melting profile across the Basin
773 and Range. SW USA. Journal of Geophysical Research 107(B1): ECV 5-1–ECV 5-21.

774 Whalen J.B., Fyffe, L.R., Longstaffe, F.J., Jenner, G.A., 1996. The position and nature of the
775 Gander-Avalon boundary, southern New Brunswick, based on geochemical and isotopic
776 data from granitoid rocks. Canadian Journal of Earth Sciences 33, 129-139.

777 Winchester, J.A., Floyd, P.A., 1977. Geochemical discrimination of different magma series and
778 their differentiation products using immobile elements. Chemical Geology 20, 325-343.

779 Wood, D. A., 1980. The application of a Th-Hf-Ta diagram to problems of tectomagmatic
780 classification and to establishing the nature of crustal contamination of basaltic lavas of the
781 British Tertiary Volcanic Province. Earth and Planetary Science Letters 50, 11-30,

782 ~~Yang, X.M., Lentz, R.L., McCutcheon, S.R., 2003. Petrochemical evolution of subvolcanic~~
783 ~~granitoid intrusions within the Late Devonian Mount Pleasant Caldera, southwestern New~~
784 ~~Brunswick, Canada: comparison of Au versus Sn-W-Mo polymetallic mineralization~~
785 ~~systems. Atlantic Geology 39, 97-121.~~

786 Zimmer, M.M., Plank, T., Hauri, E.H., Yogodzinski, G.M., Stealing, P., Larsen, J., Singer, B.,
787 Jicha, B., Mandeville, C., Nye, C., 2010. The role of water in generating the calc-alkaline
788 trend: new volatile data for Aleutian magmas and a new tholeiitic index. Journal of
789 Petrology 51, 2411-2444.

790

791

792 Captions to Figures

793

794 Figure 1. A - Map of a part of Atlantic Canada that shows the western boundary of the Maritimes

795 Basin and the location of the Harvey and Piskahegan groups (black fields).—B - Simplified

796 geological map of the southwestern part of the ~~Marysville~~~~Fredericton~~ sub-basin and its

797 surroundings ([modified from Smith, 2006, and Smith and Fyffe, 2006](#)) showing the location

798 of Figure 2. The insert (map of Canada) shows the location of Figure 1A.

799 Figure 2.—Geology of the Mount Pleasant Caldera Complex [and its surroundings](#) (modified from

800 McCutcheon et al. 2010, ~~and~~~~and~~ Thorne et al., 2013). [Late Devonian caldera complex](#)

801 [includes Late caldera-fill sequence, Subvolcanic intrusive rocks, Intracaldera and](#)

802 [Exocaldera sequences while the Piskahegan Group encompasses Late caldera-fill,](#)

803 [Intracaldera and Exocaldera sequences.](#)

804 Figure 3. ~~The~~-(Ti + Cr) versus Ca (number of cations per six oxygens) discrimination diagram of

805 Leterrier et al. (1982) comparing the composition of clinopyroxenes from the intermediate

806 rocks of the Piskahegan Group with compositional fields for clinopyroxenes from

807 nonorogenic and orogenic rocks. Each value (Table 1) is an average composition of a

808 number of analyzed crystals, and composition of each crystal is an average of 4 analyses

809 (Table 1).

810 Figure 4. Variations of $\text{FeO}_{(\text{tot})}$ ~~and~~ TiO_2 (wt.%) and various element ratios versus SiO_2 (wt.%)

811 in the basaltic and andesitic rocks of the Piskahegan Group. Association 1 - basalt: Carrow

812 Formation (CF), Kleef Formation (KF); Association 2 - andesite: South Oromocto Andesite

813 Formation (SOA); Scoullar Mountain Formation (SMF). In A and B, the vectors show calc-

814 alkaline and tholeiitic trends whereas E and F show vectors for crustal contamination (cc)

815 and fractional crystallization (fc).

816 Figure 5.—~~The~~ Zr/TiO_2 versus Nb/Y discrimination diagram of Winchester and Floyd (1977) for

817 mafic and intermediate rocks of the Piskahegan Group. Alk-Bas - alkali basalt; TrachAnd -

818 trachyandesite. Association 1 - basalt: Carrow Formation (CF), Kleef Formation (KF);

819 Association 2 - andesite: South Oromocto Andesite (SOA); Scoullar Mountain Formation
820 (SMF).

821 Figure 6. AFM diagram ($A = \text{Na}_2\text{O} + \text{K}_2\text{O}$, $F = \text{total Fe as FeO}$, $M = \text{MgO}$) for analyzed
822 mafic and intermediate volcanic rocks from the Piskahegan Group. The solid line is the
823 boundary between tholeiitic and calc-alkaline fields after Irvine and Baragar (1971);
824 Association 1 (basalts): Carrow Formation (CF), Kleef Formation (KF); Association 2
825 (andesites): South Oromocto Andesites (SOA), Scoullar Mountain Formation (SMF).

826 Figure 7. Chondrite-normalized REE patterns for basaltic and andesitic rocks of the Piskahegan
827 Group. A- Range of basalts from the Carrow Formation; B - Range of basalts from the Kleef
828 Formation; C - Range of andesites from the South Oromocto Andesite Formation; D - range
829 of andesites from the Scoullar Mountain Formation. Normalizing values are after Sun and
830 McDonough (1989).

831 Figure 8. Primitive mantle-normalized multielement patterns ~~of~~in basaltic and andesitic rocks of
832 the Piskahegan Group. A - Basalts of the Carrow Formation; B - basalts of the Kleef
833 Formation; C- andesites of the South Oromocto Andesite Formation; D- andesites of the
834 Scoullar Mountain Formation. Normalizing values are after Sun and McDonough (1989).

835 Figure 9. ~~The~~ Th-Hf-Ta tectonic discrimination diagram of Wood (1980) for mafic and
836 intermediate volcanic rocks of the Piskahegan Group. Fields: N-MORB - normal, depleted
837 mid-ocean ridge basalt; E-MORB/WPT - enriched mid-ocean ridge basalt and within-plate
838 tholeiite; Alk WPB - alkaline within-plate basalt; CAB - calc-alkaline volcanic arc basalts;
839 ATB - volcanic arc tholeiites; CC (star) - average continental crust composition of Taylor
840 and McLennan (1985). Note that the trend of the Piskahegan rocks is suggestive of a mixing
841 between basaltic magma and crustal material.

842 Figure 10. $\epsilon_{\text{Nd}(t)}$ versus time plot comparing Sm-Nd isotopic data of the Piskahegan basalts and
843 andesites and the Carboniferous Cumberland Hill trachytes with a compilation of Sm-Nd
844 isotopic data for the Upper Devonian-Lower Carboniferous volcanic rocks of the Maritimes
845 Basin and the Avalon Terrane (Keppie et al., 1997, ~~and~~ Pe-Piper and Piper, 1998). ~~The~~
846 shaded area is the Avalonian basement and the SCLM (after [Murphy et al., 2011b](#), Dostal et
847 al., 2016a5; [Murphy et al., 2011a](#)). ~~The~~ field for Mesoproterozoic rocks is from Murphy et
848 al. (2008). Bars show a range of samples.

849 | Figure 11. ~~The~~ Th/Yb versus Nb/Yb diagram of Pearce (2008) for Piskahegan basalts and
850 | andesites. Vectors indicate the influence of a subduction component (S), within-plate
851 | enrichment (W), crustal contamination (C), and fractional crystallization (FC); N-MORB-
852 | N-type mid-ocean ridge basalt; E-MORB- enriched mid-ocean ridge basalt; OIB-ocean
853 | island basalt (after Sun and McDonough, 1989). The star (CC) is the average of continental
854 | crust (Taylor and McLennan, 1985).

855 | Figure 12. ~~(Tb/Yb)_n~~ versus (La/Sm)_n diagram for the Piskahegan basalts and andesites. The
856 | values are normalized to the primitive mantle after Sun and McDonough (1989). The solid
857 | line separating the range of magmas formed by the melting of spinel peridotite mantle from
858 | that of magmas formed by the melting of garnet peridotite mantle is after Wang et al. (2002).
859 | Vector D indicates an increase of melting depth whereas the vector M depicts an increase in
860 | ~~the~~ degree of partial melting. The limited range of ~~the~~ (Tb/Yb)_n values for the basalts
861 | indicates a similar mantle source. The higher (La/Sm)_n ratios of the calc-alkaline rocks is
862 | more suggestive of crustal contamination than of changes in the magma source region. The
863 | E-MORB (enriched mid-ocean ridge basalt) and OIB (ocean island basalt) are after Sun and
864 | McDonough (1989).

865 | Figure 13. (Nb/Th)_n versus (Th/Yb)_n diagram for the Piskahegan basalts and andesites. The ratios
866 | are normalized to the primitive mantle values of Sun and McDonough (1989). N-MORB and
867 | E-MORB compositions are from Sun and McDonough (1989). CC (star) - average
868 | continental crust (Taylor and McLennan, 1985). Note that the very distinct trend (the solid
869 | curve is a mixing curve) of the Piskahegan rocks is suggestive of a mixing between parental
870 | basaltic magmas and crustal material, indicating that the andesitic magma assimilated
871 | significant amounts of crustal material prior to its emplacement.

872 | Figure 14. Th/La versus $\epsilon_{Nd(T)}$ ~~plot~~ for the Piskahegan basalts and andesites. An increase of the
873 | Th/La ratio accompanied by a decrease of $\epsilon_{Nd(T)}$ is indicative of a crustal contamination of
874 | the basaltic magmas. CC (star) - average continental crust composition (Taylor and
875 | McLennan, 1985). The solid triangles are ~~the~~ data from Anderson (1992) for the
876 | Piskahegan basaltic and andesitic rocks.

877

878

879

880

881

882

883

884

885 **Tables**

886 Table 1. Chemical composition and structural formulas of clinopyroxene in andesites of the
887 Piskahegan Group

888 Table 2. Major and trace element compositions ~~of~~in the mafic and intermediate rocks of the
889 Piskahegan Group

890 Table 3. Sm-Nd isotopic data for volcanic rocks of the Piskahegan Group and Cumberland Hill
891 Formation

892

Figure 1
[Click here to download high resolution image](#)

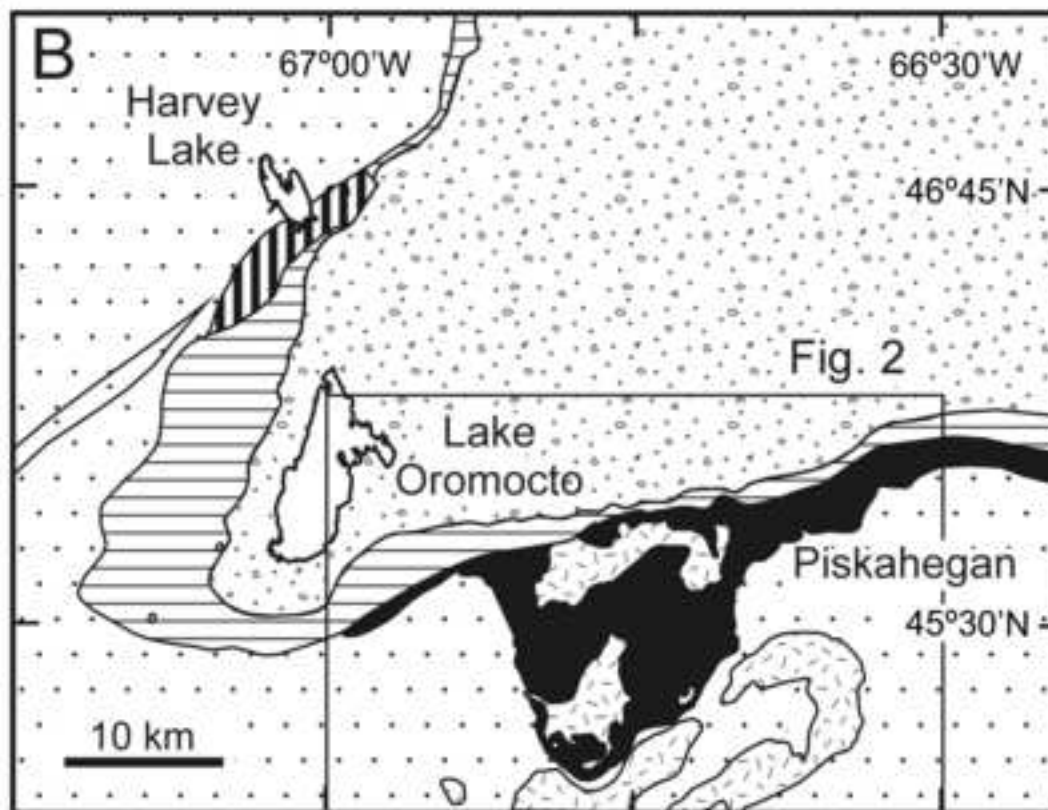
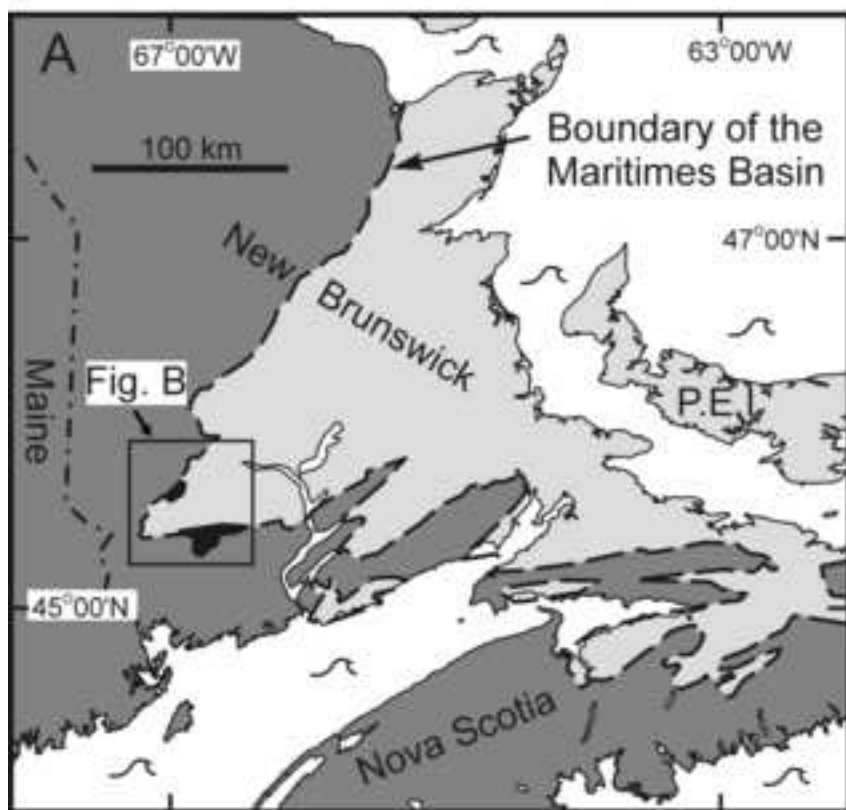
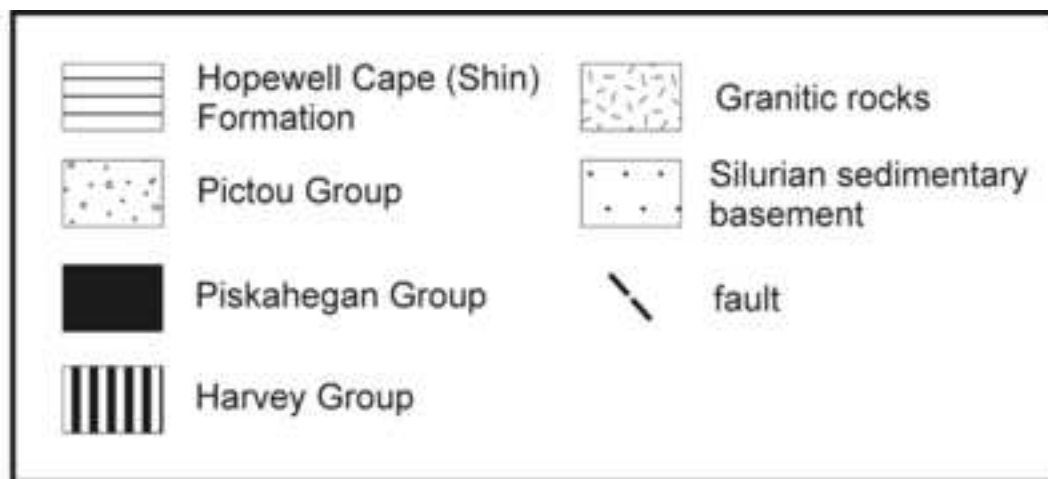
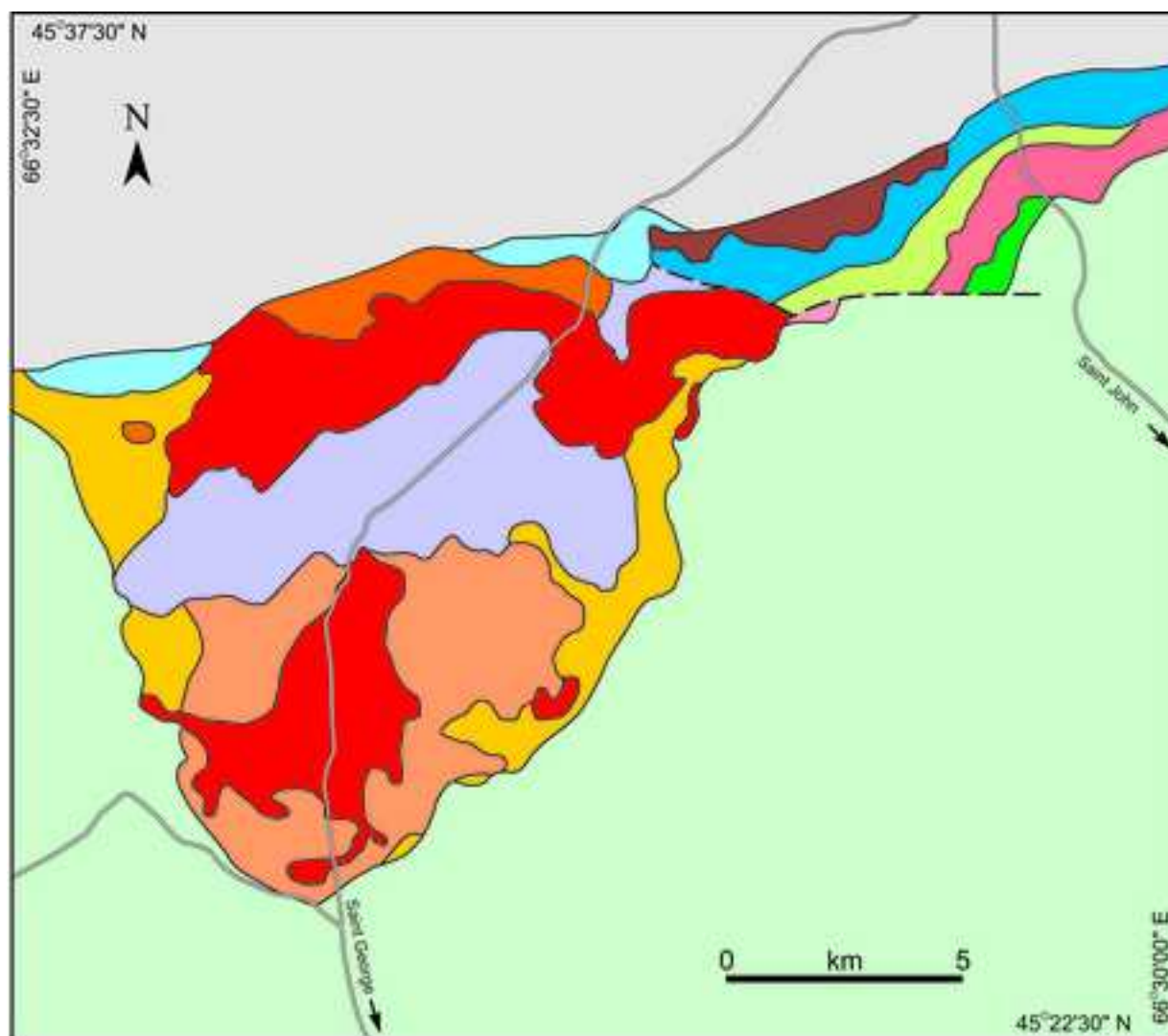


Figure 2

[Click here to download high resolution image](#)



CARBONIFEROUS

 sedimentary rocks

LATE DEVONIAN

Late Caldera - Fill Sequence

 Kleaf Formation

 Big Scott Mountain Formation

Subvolcanic Intrusive Rocks

 McDougall Brook Granite Suite

Intracaldera Sequence

 Seelys Formation

 Little Mount Pleasant Formation

 Scoullar Mountain Formation

Exocaldera Sequence

 Bailey Rock Rhyolite

 Carrow Formation

 South Oromocto Andesite

 Rothea Formation

 Hoyt Station Basalt

ORDOVICIAN - LATE SILURIAN

 Pre-caldera rocks

Figure 3
[Click here to download high resolution image](#)

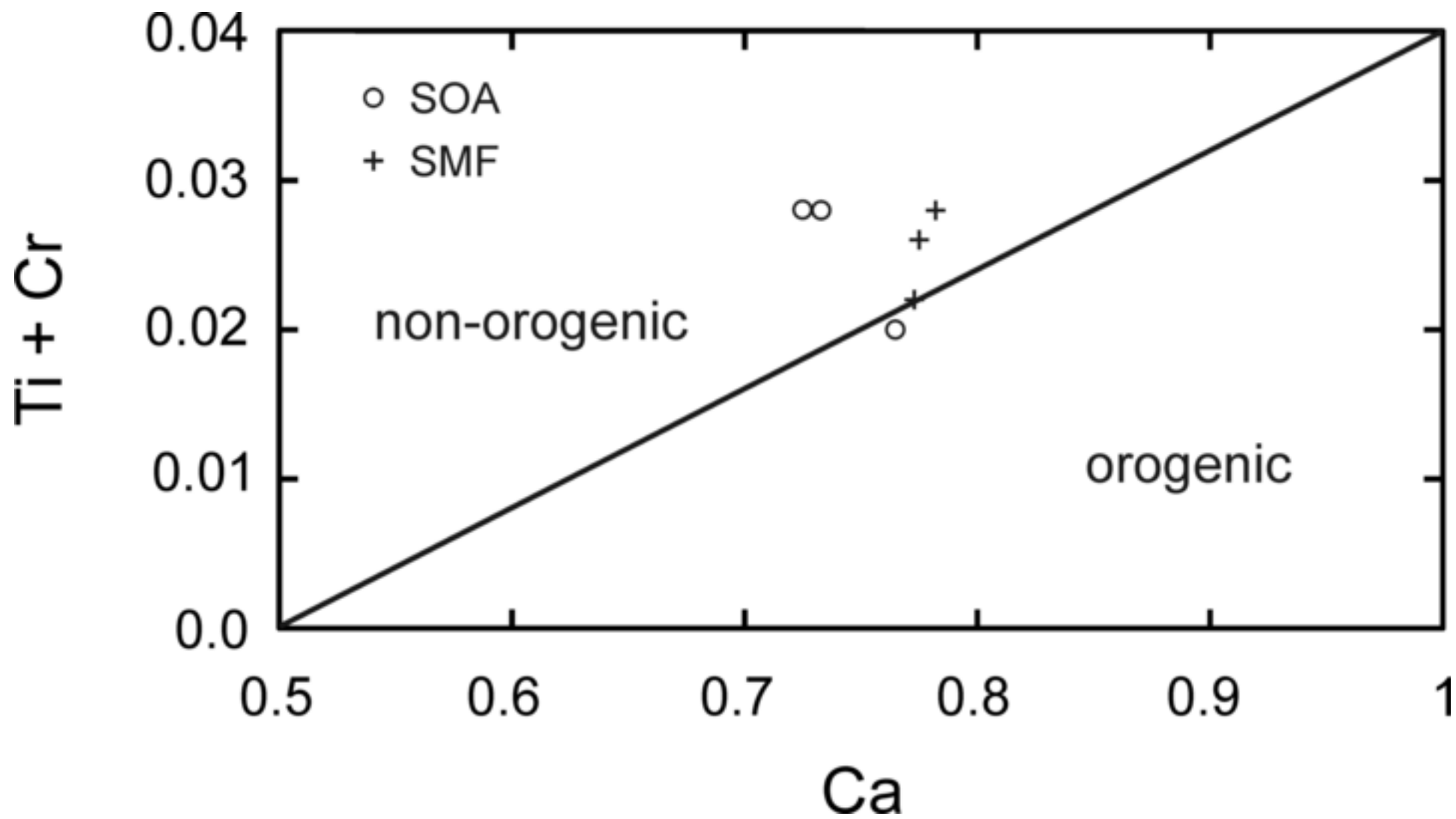


Figure 4
[Click here to download high resolution image](#)

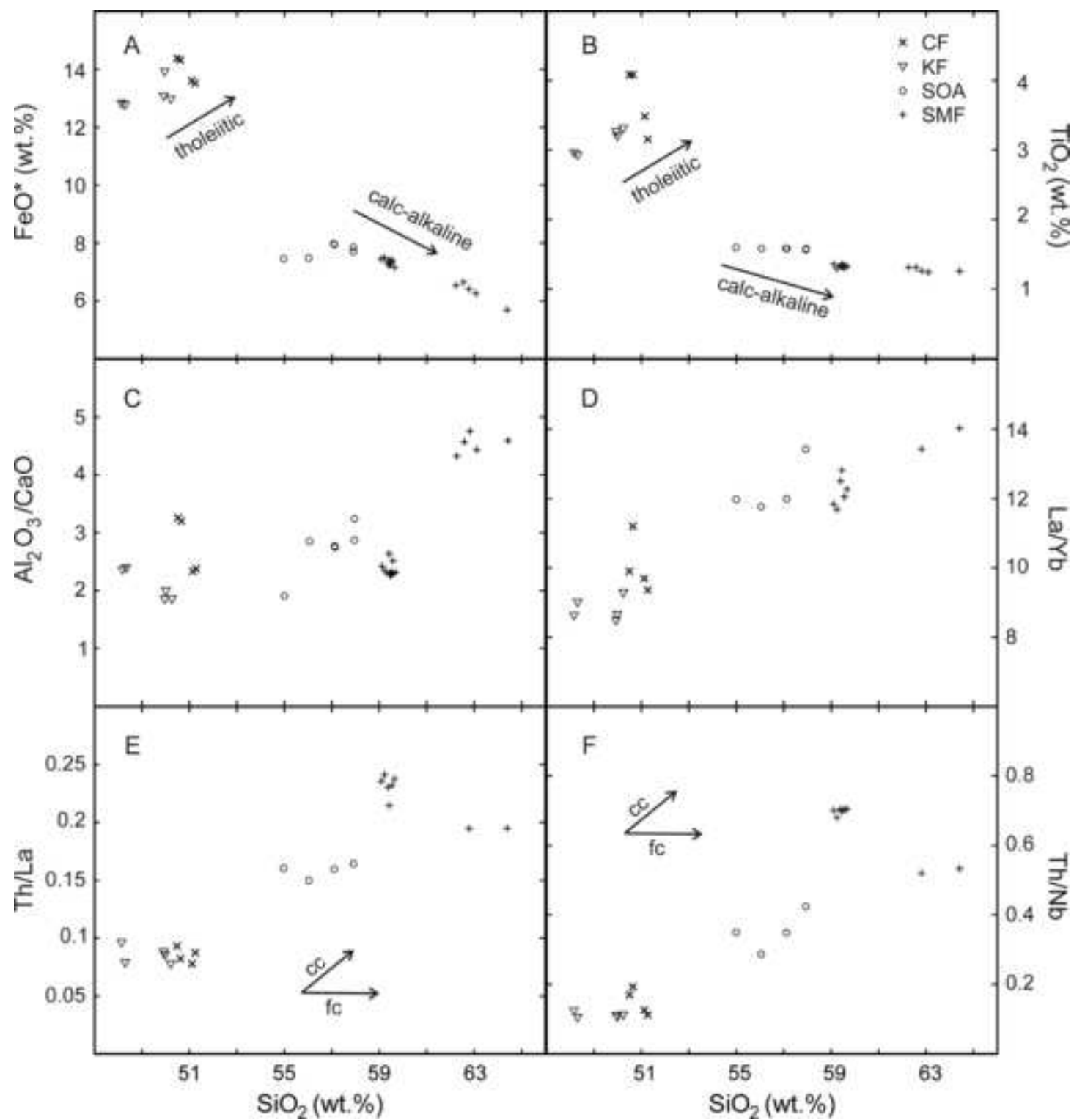


Figure 6
[Click here to download high resolution image](#)

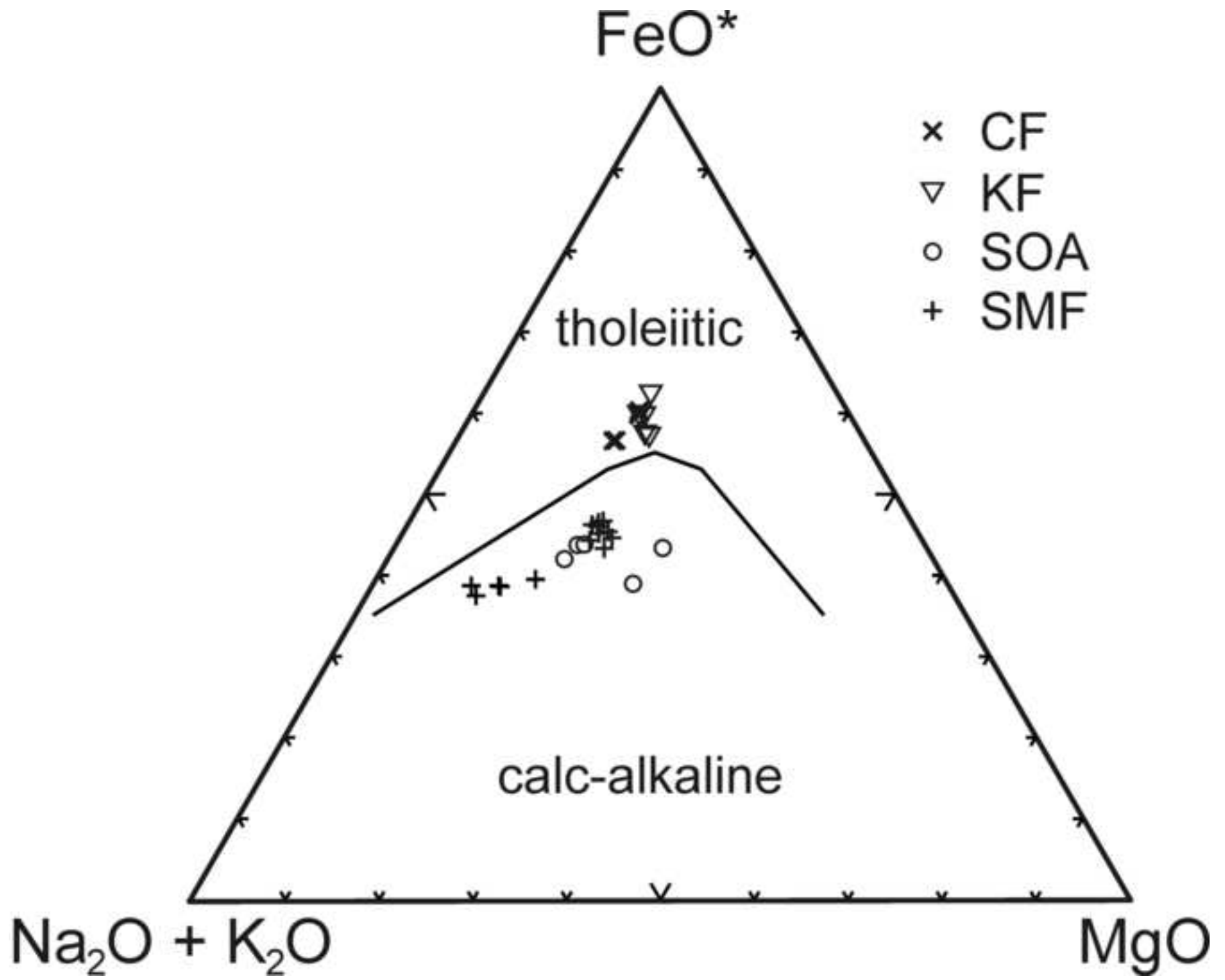


Figure 7
[Click here to download high resolution image](#)

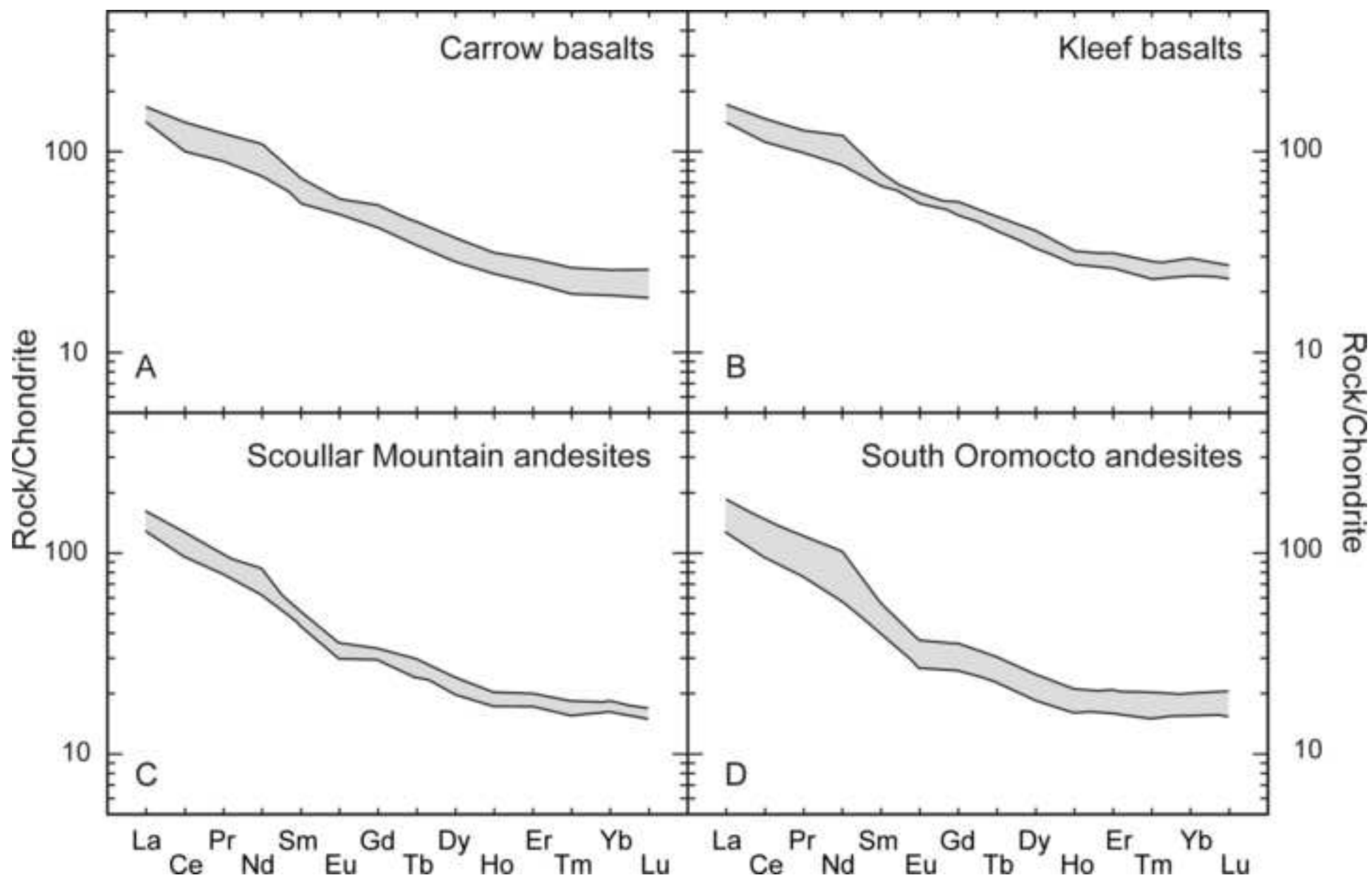


Figure 8
[Click here to download high resolution image](#)

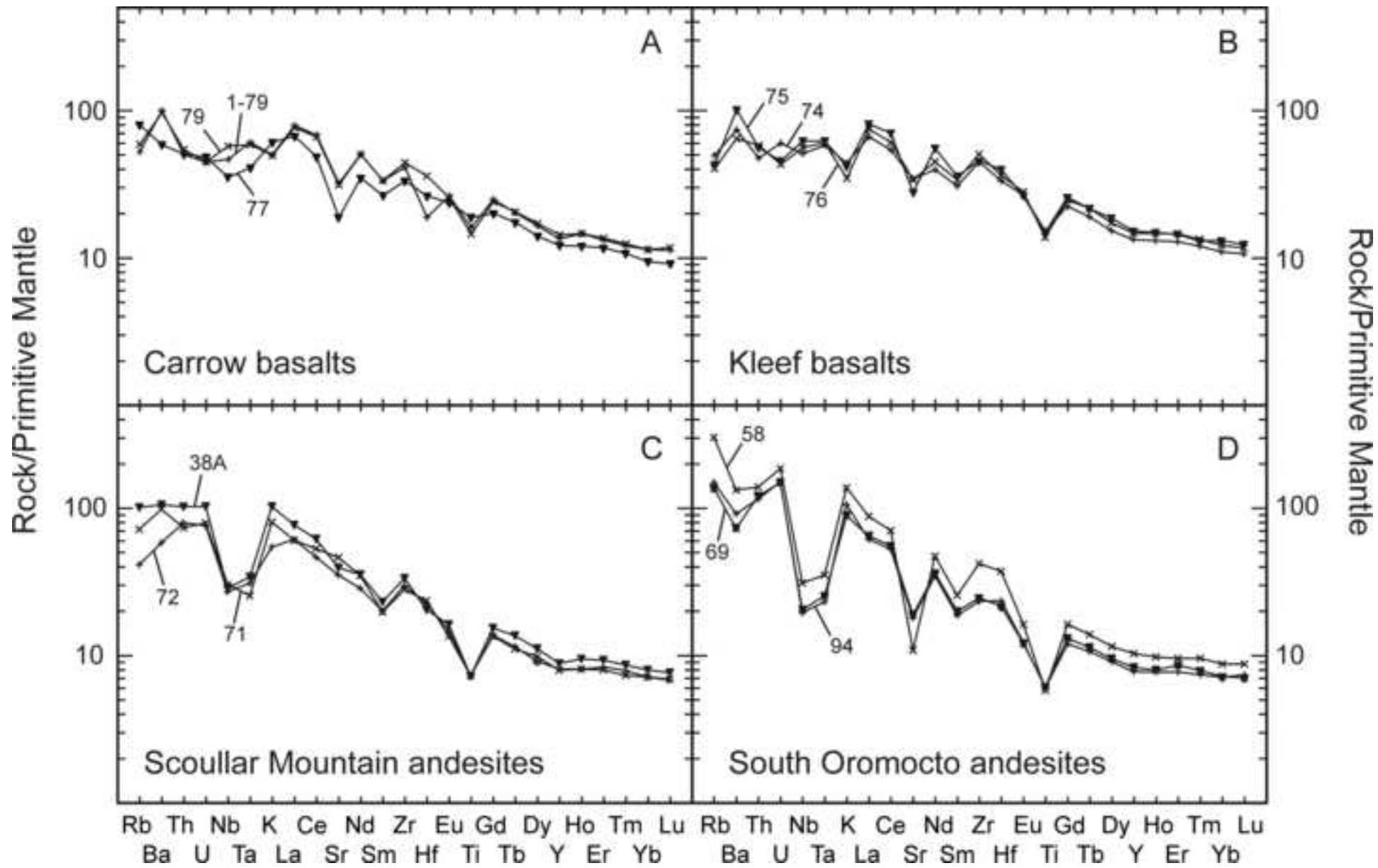


Figure 9
[Click here to download high resolution image](#)

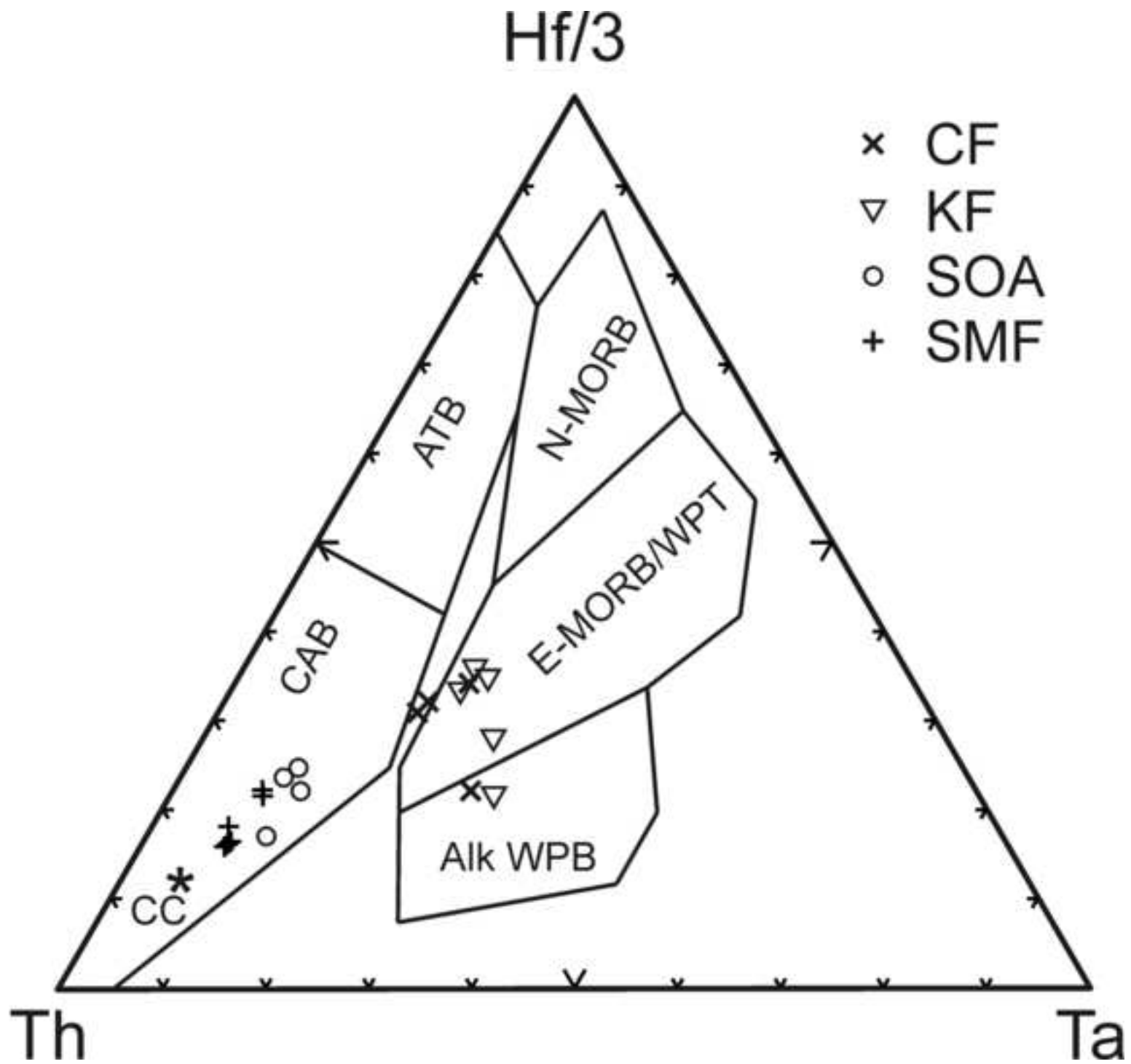


Figure 10
[Click here to download high resolution image](#)

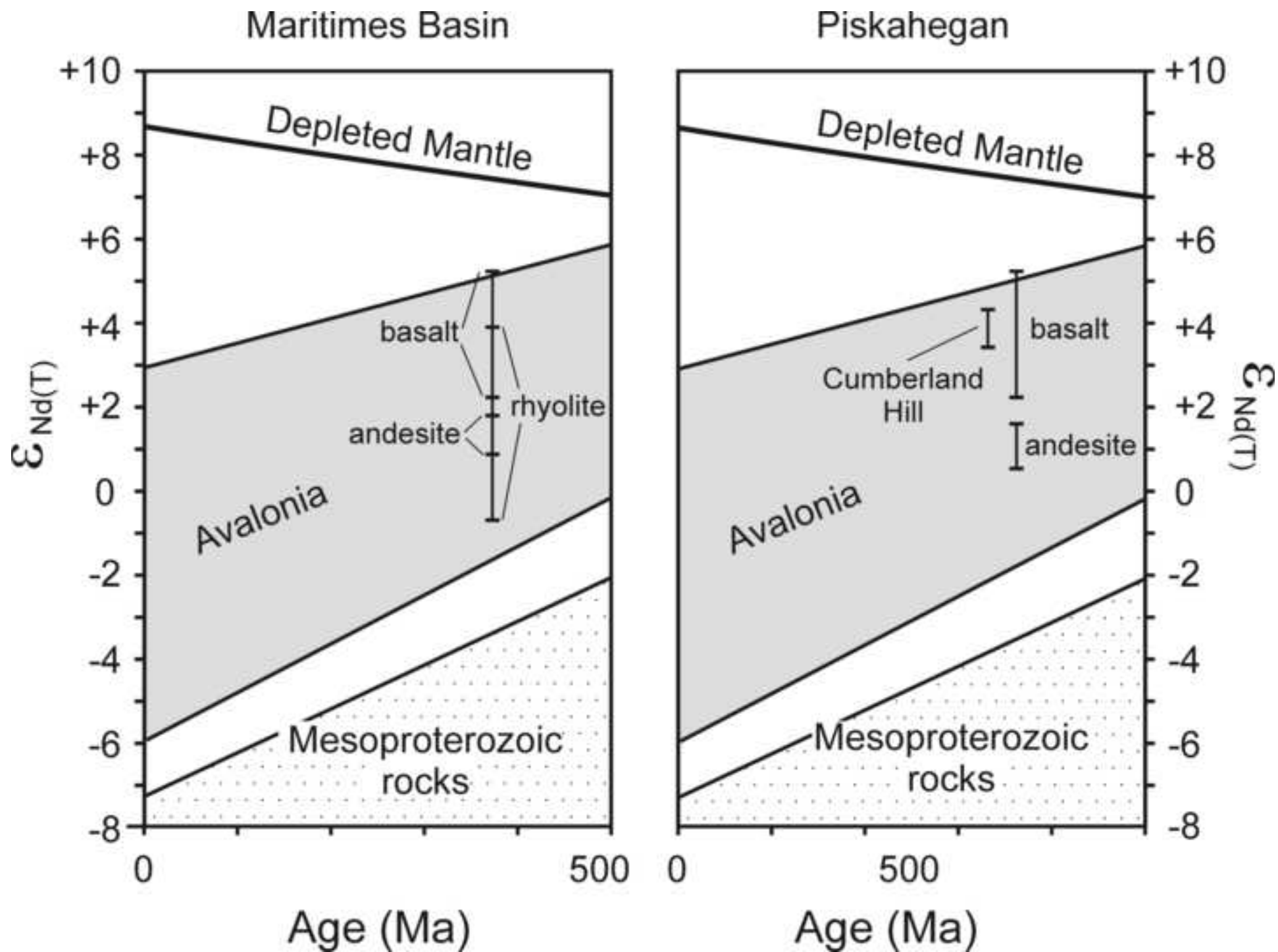


Figure 11
[Click here to download high resolution image](#)

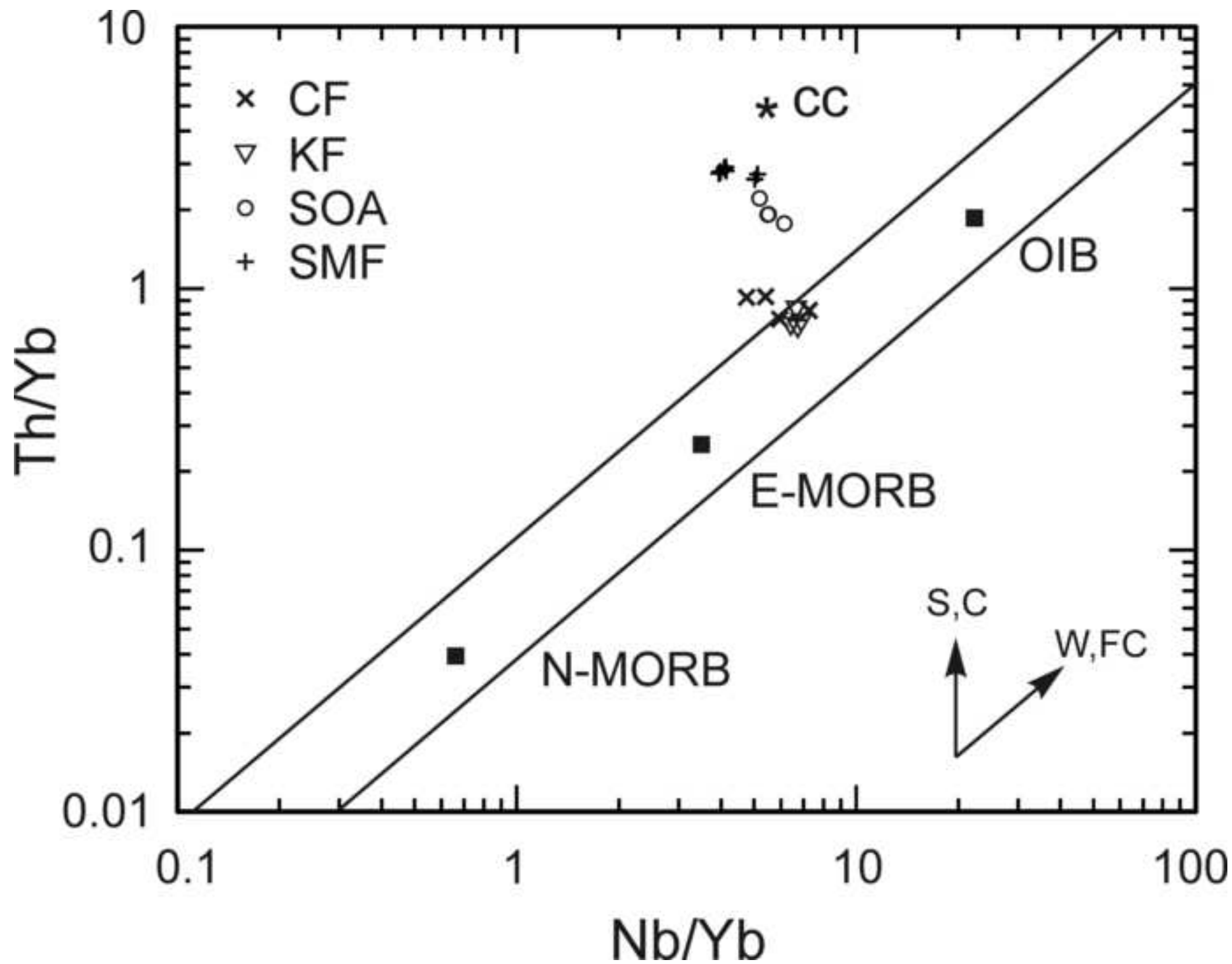


Figure 12
[Click here to download high resolution image](#)

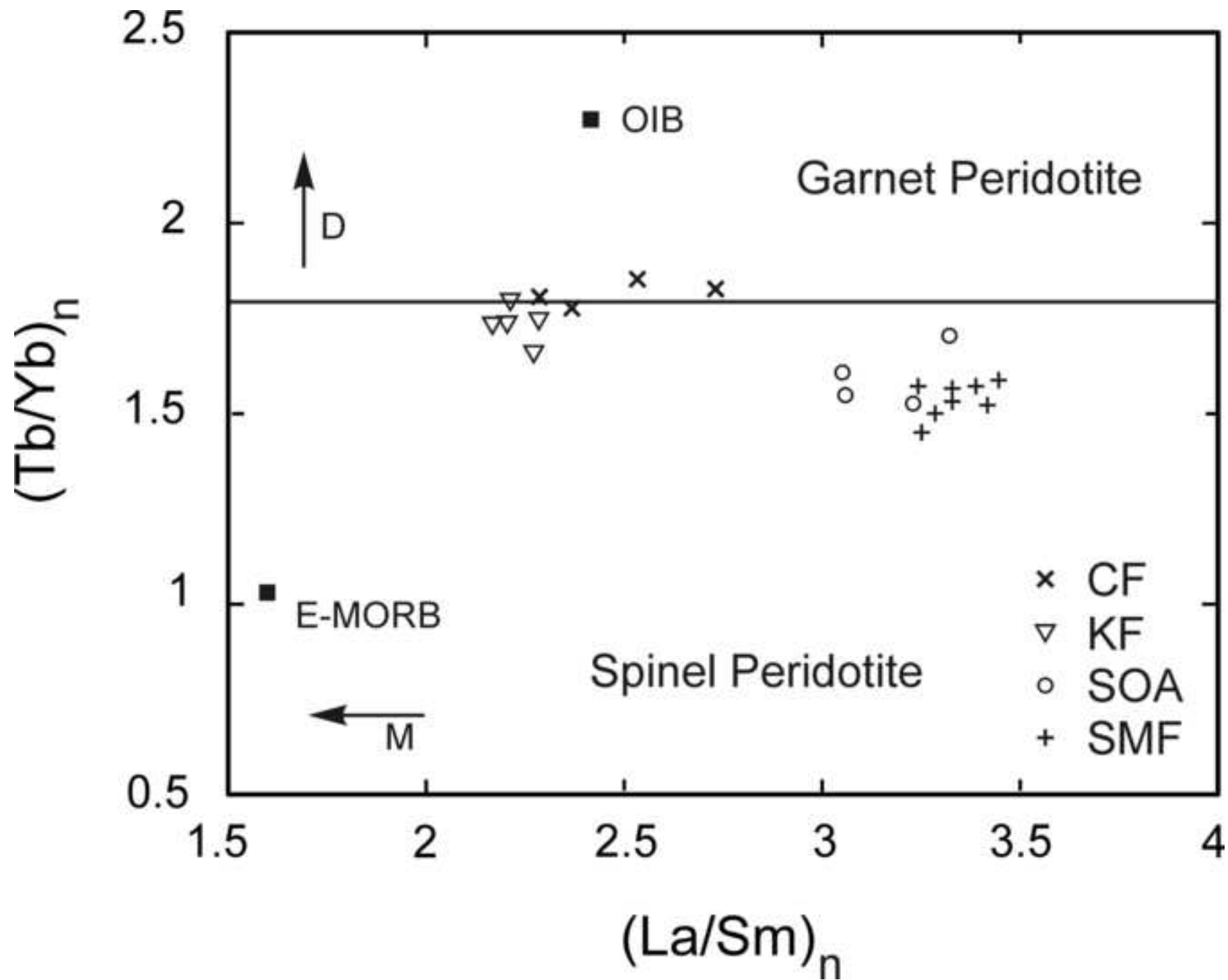


Figure 13
[Click here to download high resolution image](#)

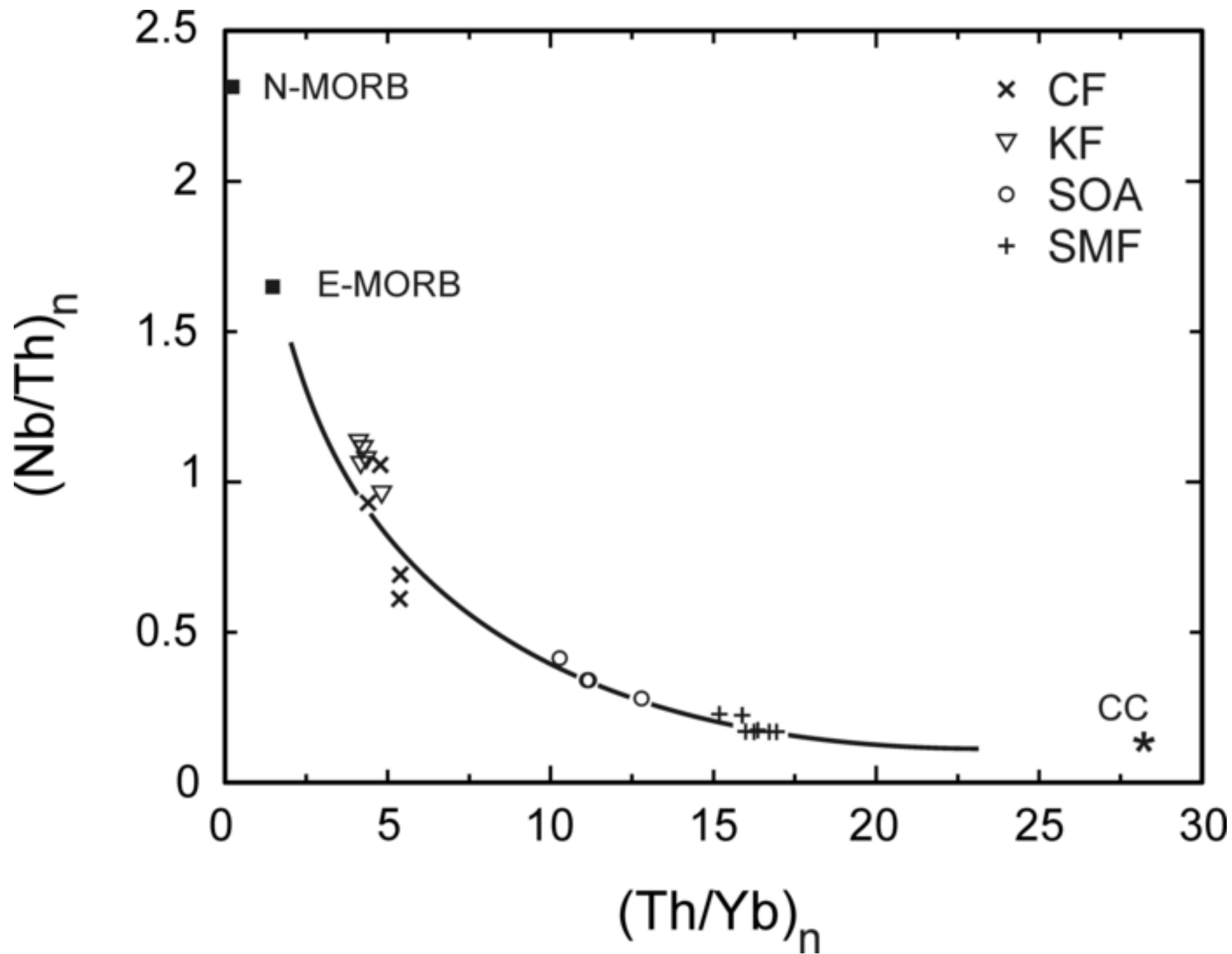


Figure 14
[Click here to download high resolution image](#)

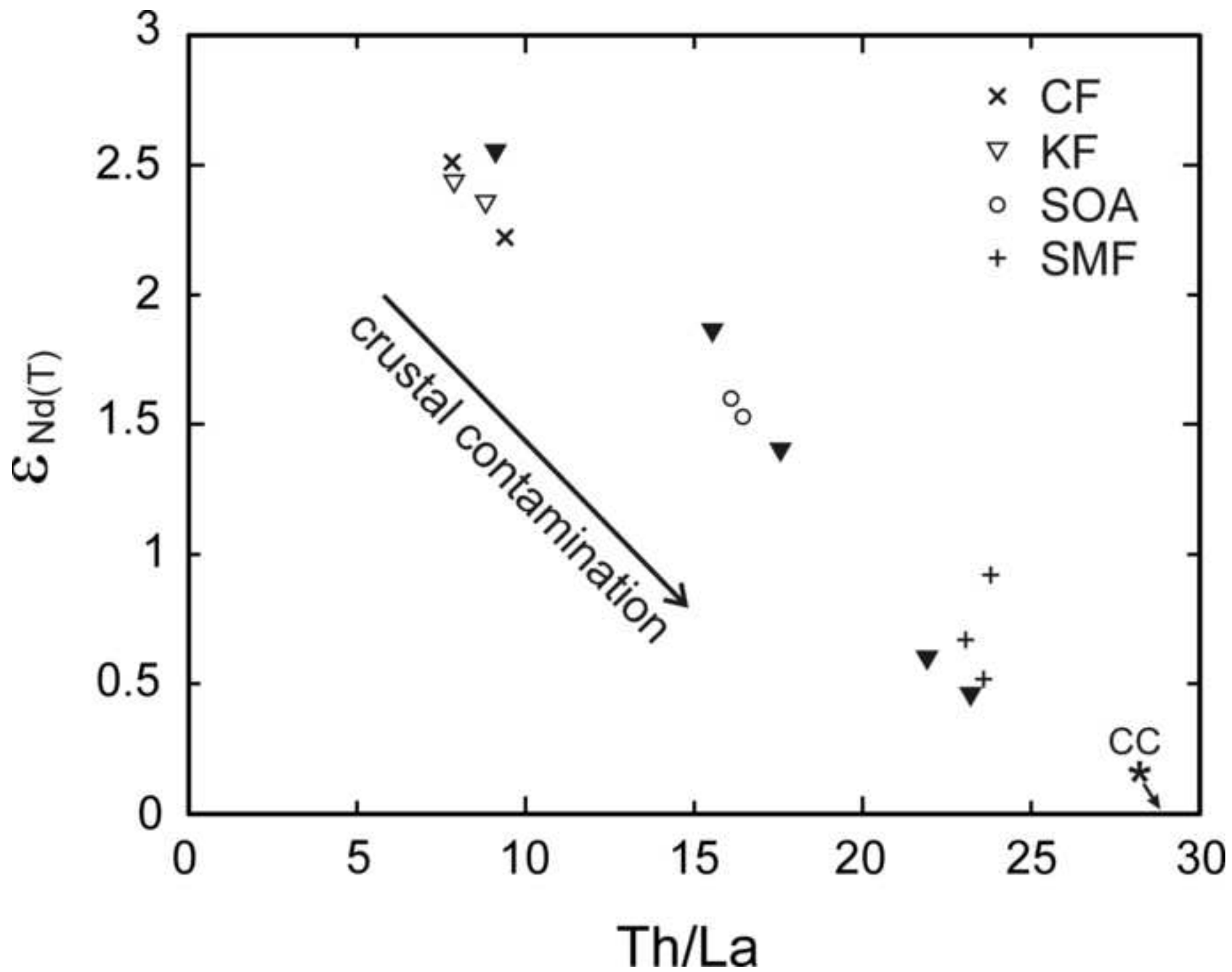


Table 1[Click here to download Table: PKTable 1.xlsx](#)

Table 1. Composition and structural formulas of clinopyroxene from andesites of the Piskahegan Group

(wt.%)	South Oromocto Andesite						Scoullar Mountain Formation					
	38A		38B		38C		68		69		92	
	average	sd	average	s.d.	average	s.d.	average	s.d.	average	s.d.	average	s.d.
SiO ₂	50.40	0.49	50.54	0.50	50.89	1.02	51.02	0.39	51.00	0.32	51.09	0.31
TiO ₂	0.87	0.10	0.65	0.15	0.64	0.22	0.71	0.11	0.70	0.10	0.70	0.15
Al ₂ O ₃	2.79	1.79	3.51	0.26	2.20	1.16	2.04	0.34	2.31	0.42	1.84	0.44
Cr ₂ O ₃	0.09	0.07	0.35	0.24	0.08	0.07	0.21	0.20	0.26	0.15	0.08	0.15
FeO [†]	10.75	1.00	8.08	2.20	9.65	1.32	9.50	1.90	8.62	0.78	10.75	1.69
MnO	0.31	0.02	0.20	0.09	0.30	0.07	0.26	0.06	0.25	0.04	0.29	0.07
MgO	15.05	1.29	15.84	1.02	15.76	0.75	15.87	0.80	16.07	0.51	15.03	1.03
NiO	0.02	0.02	0.03	0.01			0.01	0.01	0.01	0.01	0.03	0.02
CaO	18.01	1.30	19.43	0.91	19.13	0.74	19.40	0.57	19.59	0.22	19.22	0.51
Na ₂ O	0.53	0.52	0.46	0.09	0.39	0.11	0.27	0.02	0.26	0.02	0.27	0.02
K ₂ O	0.05	0.05	0.02	0.01	0.02	0.00	0.02	0.01	0.02	0.01	0.02	0.02
Σ	98.86		99.11		99.06		99.31		99.08		99.32	
n	7		10		11		16		16		21	
Si	1.893		1.877		1.900		1.902		1.901		1.917	
Ti	0.025		0.018		0.018		0.020		0.020		0.020	
Al	0.124		0.154		0.097		0.089		0.101		0.081	
Fe ³⁺	0.079		0.080		0.094		0.081		0.070		0.064	
Cr ³⁺	0.003		0.010		0.002		0.006		0.008		0.002	
Fe ²⁺	0.259		0.172		0.208		0.215		0.199		0.273	
Mn	0.010		0.006		0.010		0.008		0.008		0.009	
Mg	0.843		0.877		0.877		0.882		0.893		0.840	
Ca	0.725		0.773		0.765		0.775		0.782		0.773	
Na	0.039		0.033		0.028		0.020		0.018		0.020	
K	0.002		0.001		0.001		0.001		0.010		0.001	
Σ	4.00		4.00		4.00		4.00		4.01		4.00	
Wo	39.69		42.44		41.37		41.39		41.74		40.97	
En	46.14		48.15		47.40		47.13		47.65		44.55	
Fs	14.17		9.42		11.22		11.48		10.61		14.48	

n = number of crystals; each crystal had four analyses; average is the arithmetic mean; s.d. = standard deviation; formulas based upon 6 oxygens; End-member components: Wo - wollastonite; En - enstatite; Fs - ferrosilite; FeO[†] - total Fe as FeO

Table 2 a

[Click here to download Table: PKTable 2rev.xlsx](#)

Table 2. Major and trace element compositions of mafic and intermediate rocks of the Piskahegan Group

Sample #	Carrow Formation				Kleef Formation				
	77	79	1-77	1-79	74	75	76	1-74	1-76
SiO ₂ (wt.%)	47.64	48.87	47.93	49.08	47.87	47.57	45.45	48.09	45.60
TiO ₂	3.85	3.00	3.86	3.34	3.12	3.04	2.79	3.16	2.76
Al ₂ O ₃	13.77	14.41	13.76	14.36	14.65	14.53	16.49	14.58	16.65
FeO*	13.55	12.88	13.54	13.06	12.51	13.23	12.07	12.39	12.03
MnO	0.16	0.24	0.17	0.24	0.18	0.28	0.26	0.17	0.26
MgO	4.12	3.88	4.01	3.85	3.92	3.82	4.33	3.75	4.17
CaO	4.24	6.08	4.31	6.18	7.99	7.35	7.03	7.95	7.02
Na ₂ O	4.59	3.40	4.62	3.35	3.33	3.03	3.81	3.33	3.81
K ₂ O	1.74	1.43	1.80	1.45	1.26	1.18	0.98	1.31	1.00
P ₂ O ₅	0.68	1.13	0.65	1.09	1.01	1.13	1.14	0.98	1.07
LOI	4.00	3.40	3.50	2.61	2.40	3.50	4.20	2.14	3.79
Σ	98.34	98.72	98.15	98.61	98.24	98.66	98.55	97.86	98.16
Mg #	0.35	0.35	0.35	0.34	0.36	0.34	0.39	0.35	0.38
Cr (ppm)	0	8	30	30	19	6	6	40	30
Ni	16	16	60	60	21	17	18	60	30
Co	50	31	40	27	30	32	29	29	29
V	393	204	421	208	247	205	196	247	192
Pb	34	3	31	12	13	12	30	9	36
Zn	417	160	420	170	146	162	153	160	160
Rb	48	36	42	32	30	26	24	28	23
Ba	386	645	447	670	493	672	422	529	472
Sr	374	630	387	649	691	555	672	714	701
Ga	23	22	24	23	21	21	22	23	26
Ta	1.58	2.30	1.50	2.40	2.27	2.40	2.32	2.30	2.60
Nb	23.7	39.0	19.0	32.0	34.7	42.0	37.4	32.0	37.0
Hf	7.7	10.6	7.5	5.6	9.8	11.6	10.5	6.9	5.4
Zr	352	474	319	443	478	484	531	426	325
Y	52	62	48	59	57	66	63	53	57
Th	4.08	4.40	3.70	4.10	3.85	4.50	4.65	3.60	3.90
U	0.96	0.90	0.90	0.90	1.20	0.90	0.85	1.20	0.90
La	43.5	50.2	44.8	52.4	43.6	52.7	48.3	46.4	49.5
Ce	81.6	112	90.5	116	91.6	118	101	105	112
Pr	11.0	14.7	12.1	15.3	12.1	15.6	13.4	13.8	14.3
Nd	44.7	64.8	50.4	65.5	51.2	71.2	56.9	58.3	60.8
Sm	11.1	14.2	10.6	14.3	13.0	15.0	14.1	13.6	14.0
Eu	3.77	4.11	3.54	4.26	4.29	4.19	4.42	4.03	4.01
Gd	11.3	13.6	10.9	14.3	12.7	14.5	13.8	13.0	13.9
Tb	1.78	2.12	1.60	2.10	1.95	2.21	2.20	1.90	2.10
Dy	9.77	12.1	9.10	11.7	10.7	12.9	11.9	10.8	11.9
Ho	1.86	2.29	1.80	2.30	2.04	2.30	2.25	2.00	2.20
Er	5.31	6.24	4.70	6.10	5.87	6.53	6.54	5.60	6.10
Tm	0.75	0.88	0.65	0.86	0.84	0.91	0.93	0.77	0.87
Yb	4.39	5.36	4.00	5.40	5.14	6.09	5.60	5.00	5.50
Lu	0.64	0.83	0.60	0.80	0.75	0.86	0.81	0.76	0.80

FeO* - total Fe as FeO; LOI - loss on ignition; Mg# = MgO/(MgO+FeO*) mol%; major element oxides are not recalculated to 100%

Table 2 b

[Click here to download Table: PKTable 2rev cont.xlsx](#)

Table 2 cont. Major and trace element compositions of mafic and intermediate rocks of the Piskahegan Group

Sample #	South Oromocto andesite				Scoullar Mountain Formation							
	71	72	38-C	38A	56	58	1-60	61	68	69	94	96
SiO ₂ (wt.%)	53.73	52.37	55.15	55.91	56.65	56.33	56.54	55.60	57.12	56.74	62.51	60.21
TiO ₂	1.52	1.52	1.53	1.51	1.26	1.24	1.28	1.28	1.25	1.27	1.22	1.21
Al ₂ O ₃	15.91	15.94	15.85	15.70	15.02	14.91	15.30	15.06	14.88	15.16	14.76	14.85
FeO*	7.16	7.10	7.67	7.57	6.80	6.99	6.87	7.00	7.22	6.98	5.51	6.15
MnO	0.16	0.17	0.14	0.14	0.13	0.12	0.13	0.12	0.14	0.12	0.11	0.13
MgO	5.12	4.70	3.43	3.46	3.17	3.57	2.95	3.38	3.34	3.64	1.74	2.16
CaO	5.60	8.36	5.78	5.48	6.51	5.95	6.67	6.25	6.40	5.77	3.22	3.13
Na ₂ O	3.84	3.03	3.48	3.24	2.17	2.15	2.06	1.92	3.20	2.98	3.47	3.86
K ₂ O	2.33	1.57	3.01	2.99	2.94	3.00	3.02	3.15	2.57	2.56	4.03	3.73
P ₂ O ₅	0.49	0.49	0.50	0.50	0.30	0.30	0.28	0.31	0.30	0.31	0.47	0.44
LOI	3.20	3.80	3.00	2.70	4.80	4.80	4.51	5.40	2.10	2.80	1.00	2.70
Σ	99.06	99.04	99.54	99.20	99.74	99.37	99.62	99.47	98.51	98.33	98.05	98.56
Mg #	0.56	0.54	0.44	0.45	0.45	0.48	0.43	0.46	0.45	0.48	0.36	0.39
Cr (ppm)	58	61	24	21	75	81	90	70	88	64	19	26
Ni	42	38	20	24	15	15	30	22	28	15	7	8
Co	24	24	26	20	27	24	21	26	25	22	15	13
V	162	163	145	140	163	147	166	161	155	154	91	98
Pb	0	8	4	13	12	17	18	12	12	12	18	17
Zn	95	92	95	95	78	79	80	78	81	79	88	91
Rb	44	25	65	62	79	90	74	100	82	83	187	151
Ba	659	388	751	713	556	606	606	599	476	489	901	899
Sr	936	707	835	805	346	359	356	322	409	381	223	360
Ga	17	19	20	17	17	18	18	20	19	17	17	18
Ta	1.00	1.21	1.10	1.35	0.99	0.90	1.00	1.02	1.01	1.00	1.40	1.40
Nb	20.8	18.4	21.2	19.7	13.3	13.2	13.0	13.4	14.2	13.9	21.5	21.1
Hf	7.0	6.6	8.0	6.1	6.1	6.9	6.1	6.1	6.2	6.4	11.2	10.4
Zr	300	319	348	362	272	248	255	272	282	263	458	434
Y	35	35	39	39	34	34	33	35	36	36	46	45
Th	6.00	6.45	7.40	8.39	9.40	9.30	9.10	9.41	9.68	9.80	11.50	11.00
U	1.60	1.53	1.90	2.08	2.91	3.00	2.80	2.80	2.74	3.00	3.80	3.60
La	39.9	40.1	46.3	51.0	39.5	40.0	42.3	39.9	40.1	42.5	58.9	56.4
Ce	90.4	78.7	101	106	78.2	88.3	90.4	79.1	79.4	94.3	122	122
Pr	10.8	9.65	12.0	12.3	9.42	10.5	10.7	9.36	9.53	11.2	15.3	14.8
Nd	45.4	36.8	50.5	46.5	35.7	44.6	40.4	34.7	35.2	46.8	62.1	60.6
Sm	8.43	8.49	9.26	9.92	7.67	7.87	8.00	7.61	7.97	8.47	11.05	10.95
Eu	2.18	2.36	2.34	2.64	1.97	1.95	2.01	2.11	2.07	1.94	2.66	2.70
Gd	7.74	7.80	8.16	8.84	7.05	6.76	7.00	7.25	7.13	7.48	9.46	9.29
Tb	1.15	1.18	1.29	1.42	1.08	1.09	1.10	1.16	1.09	1.17	1.46	1.44
Dy	6.97	6.42	7.43	7.93	6.15	6.33	6.10	6.82	6.10	6.71	8.26	8.16
Ho	1.27	1.26	1.32	1.50	1.18	1.20	1.20	1.27	1.19	1.25	1.56	1.51
Er	3.68	3.81	3.97	4.31	3.53	3.52	3.40	3.74	3.54	3.94	4.46	4.45
Tm	0.52	0.56	0.56	0.62	0.51	0.52	0.50	0.54	0.53	0.56	0.69	0.65
Yb	3.39	3.35	3.86	3.80	3.22	3.32	3.30	3.37	3.43	3.40	4.20	4.20
Lu	0.49	0.48	0.54	0.55	0.50	0.52	0.51	0.49	0.51	0.50	0.63	0.66

FeO* - total Fe as FeO; LOI - loss on ignition; Mg# = MgO/(MgO+FeO*) mol%; major element oxides are not recalculated to 100%

Table 3

[Click here to download Table: PKTable3 rev.xlsx](#)

Table 3. Sm-Nd isotopic data for volcanic rocks of the Piskahegan Group and Cumberland Hill Formation

Sample	Nd (ppm)	Sm (ppm)	$^{147}\text{Sm}/^{144}\text{Nd}$	$^{143}\text{Nd}/^{144}\text{Nd}_m$	2σ	$^{143}\text{Nd}/^{144}\text{Nd}_i$	$\epsilon_{\text{Nd}(T)}$	T_{DM1} (Ma)	T_{DM2} (Ma)
Carrow Fm (basalts)									
77	48.3	10.4	0.1302	0.512593	6	0.512282	2.22	1016	831
1-79	62.1	13.7	0.1337	0.512616	6	0.512296	2.51	1017	824
Kleef Fm (basalts)									
74	58.5	13.2	0.1368	0.512615	8	0.512288	2.35	1059	857
1-76	60.7	13.4	0.1338	0.512612	7	0.512292	2.43	1025	832
South Oromocto Andesite Fm (andesites)									
72	40.8	8.02	0.1189	0.512534	6	0.512250	1.60	990	827
38A	46.5	9.92	0.1291	0.512556	8	0.512247	1.55	1069	885
Scoullar Mt. Fm (andesites)									
61	39.6	7.63	0.1165	0.512473	6	0.512195	0.52	1061	900
69	46.8	8.47	0.1095	0.512464	8	0.512202	0.67	1004	854
56	39.0	7.48	0.1160	0.512492	6	0.512215	0.92	1026	867
Cumberland Hill Fm (trachytes)									
1-203	104	20.9	0.1210	0.512690	7	0.512425	4.26	757	598
1-208	84.8	16.0	0.1137	0.512630	7	0.512381	3.40	793	644

T_{DM1} -depleted mantle model age calculated using a linear evolution for a mantle separated from the CHUR at 4.55 Ga and having a present day ϵ_{Nd} value of +10; T_{DM2} - depleted mantle model age calculated using the model of DePaolo (1988); $^{143}\text{Nd}/^{144}\text{Nd}_i$ and $\epsilon_{\text{Nd}(T)}$ values were calculated for the respective crystallization ages ($T=365$ Ma, Piskahegan Group; $T=335$ Ma, Cumberland Hill Formation); $^{143}\text{Nd}/^{144}\text{Nd}_m$ – measured values; $^{143}\text{Nd}/^{144}\text{Nd}_i$ – initial, calculated; 2σ – uncertainty in measured $^{143}\text{Nd}/^{144}\text{Nd}$ – the value is the sixth decimal place; estimated precision of $^{147}\text{Sm}/^{144}\text{Nd}$ data is +/- 0.5% (2σ)

Appendix 1

[Click here to download Background dataset for online publication only: PKAppendix1 rev.xls](#)

Appendix 2

[Click here to download Background dataset for online publication only: PKAppend2.xls](#)